WPI

Micro-Aircraft Design for AIAA Design Build Fly Competition

A Major Qualifying Project Report
Submitted to the Faculty of
WORCESTER POLYTECHNIC INSTITUTE
in Partial Fulfillment of the Requirements for the
Degree of Bachelor of Science
in Aerospace Engineering

Submitted By:
Anwar Hughes-Crawford
Alexander Psenicka
David Reynolds
Julian Robles
Sean McMahon
Noah Mester

April 24, 2023

Submitted To and Approved By:
Zhangxian Yuan, Advisor
Professor, Aerospace Engineering Department, WPI

Abstract

The goal of this project was to design, construct, and test a fixed wing remote-controlled micro-aircraft to satisfy the design parameters and mission requirements of the 2023 AIAA Design Build Fly Competition. The project started by creating a sensitivity analysis of the published mission set. These missions and other competition requirements were further analyzed to create functional and design requirements. After comprehensive theoretical analysis and testing in each aspect of the design, the team designed and manufactured an aircraft capable of reaching 45 mph with a wingspan of 70 inches and weighing 7 lbs. The aircraft was able to successfully complete glide, taxi, and hop tests; however, it crashed during the flight test due to a lack of elevator authority.

Acknowledgments

Throughout our project, the authors of this report have put a lot of effort and expertise into this MQP. However, this project could not have been as successful without the help of others. We would like to recognize the following individuals for their contributions in multiple key aspects of the project:

- Professor Zhangxian Yuan for his help and guidance throughout this project.
- The WPI aerospace department for funding and support for this project.
- Professor David Olinger for advice on wind tunnel testing and previous Design Build fly competitions.
- Cameron Best for piloting our plane for our flight tests.
- Randy Holtgrefe for his expertise in remote-controlled aircraft.
- Jordan Jonas for insights into the design process and logistics of the WPI team and MQP that competed in the 2022 Design Build Fly competition.
- The "Design of an RC Aircraft for the 2023 AIAA Design, Build, Fly (DBF) Competition Team 2" MQP, for their collaboration on the competition documents.
- The AIAA Chapter of WPI and the following non-senior members for giving us the ability to qualify for the Design Build Fly competition:
  - Evan Mandel
  - Nathaniel Polus
  - Catalina Mudgett
  - Justin Shen

With the involvement of the above individuals, we were able to overcome various roadblocks during the development of this project. And because of their advice, we were able to engage in the core aspects of the project more effectively. Once again, we would like to acknowledge their assistance and guidance throughout the project and thank them for their time and contributions.

Executive Summary

This MQP project was tasked with the design, manufacturing, and testing of a micro-aircraft for the 2023 AIAA Design Build Fly competition. The design requirements were set using the missions outlined in the competition rules. These included one ground mission where the plane was suspended in the air with a weight suspended from the aircraft to test the structure of the aircraft. Then three aerial missions; the first being a simple circuit flight, then the same mission carrying a payload, and a final mission carrying a simulated jamming antenna. The rules also state that the wings must be removable and interchangeable.

To set performance goals a sensitivity analysis was completed on the scoring of each mission to determine which attributes would be most valuable. From this flight speed was determined to be the most important performance value to raise the overall score. Next most important was antenna length and payload weight. Keeping these goals in mind, a desired top speed of 45 mph was set. Next the airfoil was selected as well as the wing configuration. This allowed the coefficient of drag to be calculated at 0.33 with a lift coefficient of 0.521. Using this the thrust required at cruise was able to be estimated to be 25 newtons. Further analysis revealed that the thrust required at takeoff was 50 Newtons.

Following this, the first prototypes were constructed. Each prototype was largely the same with small differences in scaling and materials. From the first to the second prototype the tail was scaled up and the material was changed from foam to wood. For the second to third prototype the tail material was changed back to foam. For the final prototype the fuselage material was changed from oak ply to birch ply and the motor plate was also moved further back into the fuselage. The final wingspan is 69.5" and weight is 7.08 lbs. Meeting the required build quality proved to be a much greater challenge than expected. The final prototype completed multiple glide tests as well as a hop test. A full flight test was attempted; the plane took off successfully but lacked elevator authority resulting in a controlled crash.

The aircraft was aerodynamically stable and structurally sound. This resulted in a good performance in the ground mission but failure to complete the three flight missions due to a lack of control authority on the pitch axis. To fix this, future projects could increase the size of the elevator and horizontal stabilizer. The tail boom could also be extended to increase the moment arm from the elevator; however, this would also require the creation of an attachment mechanism for the tail so that the aircraft would fit within the required box.

Authorship Table[1]

Section	Author
Abstract	DR, JR, & NM
Acknowledgments	AH & NM
Executive Summary	DR
Introduction	
Our Project	NM & DR
Design Build Fly	SM & NM
Timeline	AP
Team Organization	NM
Mission Requirements Summary	SM & NM
Preliminary Approach	
Functional Requirements	AP & DR
Sensitivity Analysis	NM
Design and Sizing Trades	NM
Considered Concepts	AH, AP, DR, and NM
Preliminary Design and Analysis	
Analysis Methods	JR
Aerodynamic Design and Analysis	DR and JR
Propulsion System Design and Analysis	AH & SM
Control Design and Analysis	DR & SM
Structural Design and Analysis	AP, DR, and NM
Predicted Mission Performance	JR, SM, and NM
Manufacturing Processes	
Laser Cutting	NM
Machining	NM
Assembly Methods	AP, SM, and NM
Subsystem Tests Conducted	
Propulsion System Tests	AH
Aerodynamics Tests	JR
Controls Tests	DR & SM
Structural Tests	NM
Final Design Parameters	
Electronic System Design	SM & DR
Aerodynamic and Control Surface Design	SM & DR
Structural Design	AP, JR, and NM
Performance Results	
Flight Readiness Checklist	SM
Glide Tests	SM & DR
Take-Off & Taxi Tests	JR and SM
Flight Test	JR and SM

---

[1] Blank authorship means all section content is contained in secondary sections. The use of "and" signifies separate authorship, while "&" signifies collaborative authorship. Authorship is written alphabetically by last name.

Table 1: Authorship Table Initials Legend

Initials Legend	
Name	Initials
Anwar Hughes-Crawford	AH
Alexander Psenicka	AP
David Reynolds	DR
Julian Robles	JR
Sean McMahon	SM
Noah Mester	NM

Table of Contents

Table of Figures

Table of Tables

List of Abbreviations

μ	Viscosity
μPa	Micropascals
A	Amperes
AIAA	American Institute of Aeronautics and Astronautics
AOA	Angle of attack
C_D	Coefficient of Drag
C_L	Coefficient of Lift
DBF	Design Build Fly
deg	Degrees
E	Young's Modulus
F	Force
I	Area Moment of Inertia
kg	Kilograms
L	Length
lbf	Pounds (force)
lbs	Pounds (mass)
m	Meters
m/s	Meters per second
mAh	Milliamp hours
mins	Minutes
mm	Millimeters
MPa	Megapascals
mph	Miles per hour
N	Newtons
O.D.	Outer diameter
Q	Dynamic pressure
Re	Reynold's Number
s	Seconds
S	Wing area
THK	Thickness
V	Volts
v_∞	Free stream velocity

1   Introduction

1.1   Our Project

At Worcester Polytechnic Institute, seniors engage in hands-on projects to demonstrate their learned knowledge and skills. Our project, Aircraft Design for American Institute for Aeronautics and Astronautics (AIAA) Design Build Fly Competition, was dedicated to designing, building, and testing the components, subsystems, and final design of a radio-controlled aircraft, meeting the functional and design requirements of the annual Design Build Fly Competition hosted by the AIAA. Through this report the team will describe the analysis methods and processes used to design and manufacture our aircraft.

1.2   Design Build Fly

In September 2022, the official ruleset for the 27th annual Design/Build/Fly Competition in Tucson Arizona was released, to take place in April 2023. The theme of the competition for 2022-2023 was designing an unmanned airplane to be used in electronic warfare applications and stowed in an airline checked baggage compliant shipping box. Due to this theme, along with the base flight challenges, there are additional restrictions to test the aircraft's ability to be used in electronic warfare. In accordance with this theme, several rules and missions were created by the AIAA to showcase the capabilities of this type of aircraft design.

1.3   Timeline

Figure 1: Gantt chart

Figure 1 is a Gantt Chat which show several major project milestones for both the DBF competition and WPI's MQP timeline. This chart served as a rough guide to how the team was going to approach the project and meet hard deadlines put forth by AIAA and WPI. Highlighted

in yellow and annotated with exact date show hard deadlines from both AIAA and WPI. This Gantt chart has been updated through the project to reflect our changing goals and any changes to our milestones. As an example, our initial goal was to have a glide test before the end of December. This goal was meet but due to damage sustained to the plane and lessons learned it was decided that another round of glide testing with a new prototype was needed.

1.4 Team Organization and Budget

To participate in the DBF Competition, our MQP, along with another MQP, formed the Worcester Polytechnic Institute Design Build Fly team. The DBF team was split into two design teams, Design Group 1 and Design Group 2, with each defined by an MQP (Figure 2). Each were also given a budget of $250 per senior member for a total budget of $1750. The DBF Team was additionally joined by six freshmen, sophomores, and juniors to comply with DBF team member requirements. This paper reflects the work of Design Group 1, whose authors make up the senior members of this Design Group. After submitting a shared proposal with Design Group 2 to Design Build Fly, and participating in an intra-WPI flyoff, Design Group 2 was selected to attend the Design Build Fly competition. While this means our MQP did not attend the competition, our project's goals still reflect the goals and restrictions of it.
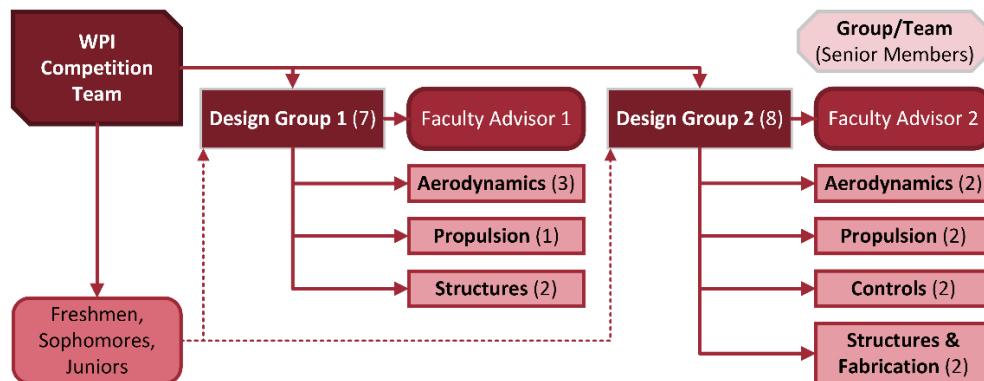
Figure 2: Team Organization Chart

Our group consists of the six authors of this report organized into three subteams (Figure 3). The first is the Structures team, which concentrated on structural analysis, CAD design, and the manufacturing process of the body. The second subteam is the Aerodynamics subteam, focusing on aerodynamic analysis, flight performance, aerodynamic surfaces manufacturing, and electronics systems assembly. The final subteam is Propulsion, focusing on motor performance and testing as well as power system parts selection. Specific additional roles in support of team operations were also assigned. As part of the WPI Aerospace Engineering Department, Professor Zhangxian Yuan acted as our team's DBF advisor in addition to his role as our project advisor. Julian Robles acted in the capacity of team purser, Sean McMahon was the team's safety officer, and Noah Mester was the liaison to the WPI Chapter of the AIAA and the DBF Competition primary contact. The non-senior members of the team did not have specific roles and helped with testing or construction. Only senior members of both design groups were tasked with writing the

Proposal and Design Report documents for the Design Build Fly Competition, the MQP reports, and performing all analysis.
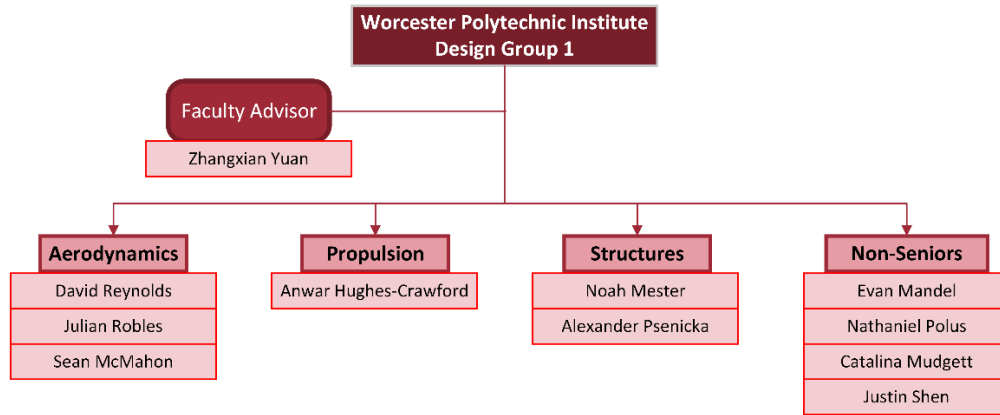
Figure 3: Design Group 1 Organization Chart

1.5   Mission Requirements Summary

1.5.1   Competition Restrictions and Rules

The rules followed, design requirements discussed, and competition descriptions in this section are obtained from the official AIAA Design Build Fly rule sheet [1]. There are a few base requirements for the aircraft that must be applied to the design in general. The primary requirement is that the plane, two wing sets, up to three antennae, and any other plane parts must fit into a box with total linear dimension (length + width + height) of not more than 62", with the package in total weighing less than 50 pounds. Each pair of wings must be removable from the airframe, with the removed pieces accounting for at least 90% of the wingspan. At the beginning of each mission, the left and right wings will be randomly chosen from either of the two wing sets. The process showing the wing selection can be seen below in Table 2.

Table 2: Wing Selection

Coin Flip	Wing Selection
Heads	Left-1 or Right-1
Tails	Left-2 or Right-2

For scoring, each mission has two scoring elements. The first is a static completion bonus score while the second is a variable score. For the variable score, the number of points earned is divided by the highest number of points earned among all teams for that mission. For this year's competition, there are four missions. Three of these are flight missions and one is a ground mission.

The flight course layout is in the shape of a rectangle with half-circle turns on either end. The sides of the rectangle are 1000 feet long, with the radius of the turns being determined by the pilot or day-of flight zone limits. The start and finish line are in the middle of the first 1000-foot straight. During the second 1000-foot stretch the aircraft will deviate from the straight to complete a 360-degree turn, following the same radius requirements as the previous aircraft turns but in the opposite direction of the track turns. The diagram of the track layout can be viewed below in Figure 4.
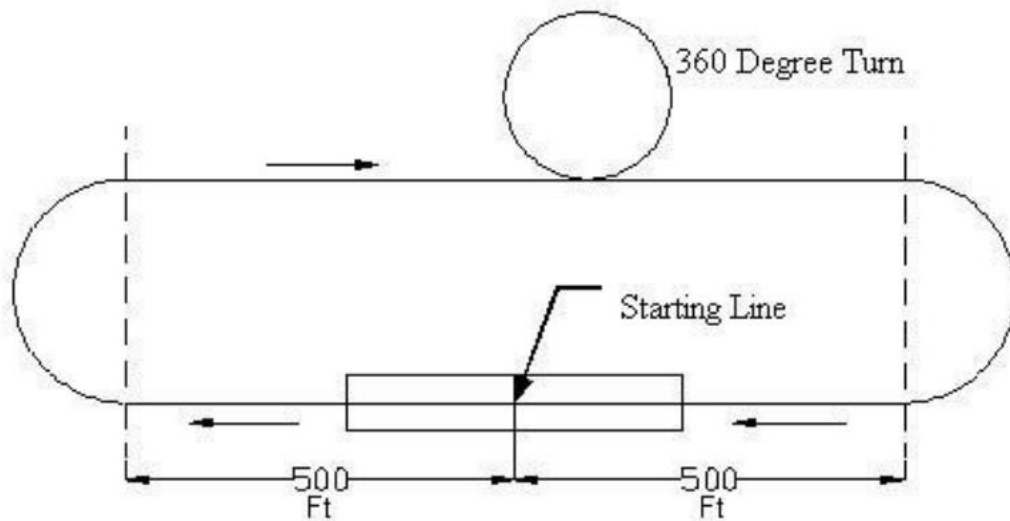
Figure 4: Course Layout

1.5.2 Mission 1

The first mission is the staging flight and is a general flight viability test with a five-minute window. Within this window, the plane must take off within 60 ft and complete three laps of the flight course. The aircraft must then land safely but is not required to do so within the time constraint. If any of these mission requirements are not met, then no score is awarded for this mission. Below is the equation for how the first mission is scored.

$$M1 = 1$$

1.5.3 Mission 2

The second mission shows the first aspect of the electronic warfare theme of the competition with it being a surveillance flight. For this flight the duration is expanded to a 10-minute window with the same takeoff length as the staging flight. For this mission the aircraft is required to hold a simulated electronics package inside the fuselage with a minimum size of 3.00 x 3.00 x 6.00 inches and must weigh a minimum of 30% of the gross lift off weight. Similar to the staging flight, the landing can be attempted after the 10-minute flight window but needs to be successful to earn any points. Unlike Mission 1, Mission 2 has both a completion bonus and variable score. While the completion bonus is the same as Mission 1, the variable score is a function of the payload weight and number of laps completed in the mission window. Below is the equation for how Mission 2 is scored, with 'N' representing our aircraft and 'Max' representing the most points earned of all competing aircraft.

$$M2 = 1 + \frac{N(Payload\ Weight \times Number\ of\ Laps\ Flown)}{Max(Payload\ Weight \times Number\ of\ Laps\ Flown)}$$

1.5.4 Mission 3

The third and final flight mission is also electronic warfare themed, portraying a jamming flight. This mission has the same characteristics as the staging flight with a 5-minute flight window and takeoff length of 60 feet. It also shares the similarity that the aircraft must complete three laps

of the flight course. This mission involves attaching an antenna vertically to one of the wing tips of the plane to model a signal jamming antenna on a full-scale aircraft. It also is important to note that a counterweight can be added to the opposite wing tip if it will make the plane fly smoother, but it is not a necessary addition to the aircraft. Both the antenna, which is made of ½ inch Schedule 40 PVC pipe, and the optional counterweight must be removable from the wings and are installed during the mission staging period along with the wings.

Optional wingtip/counterbalance weight

Jamming Antenna adapter attachment
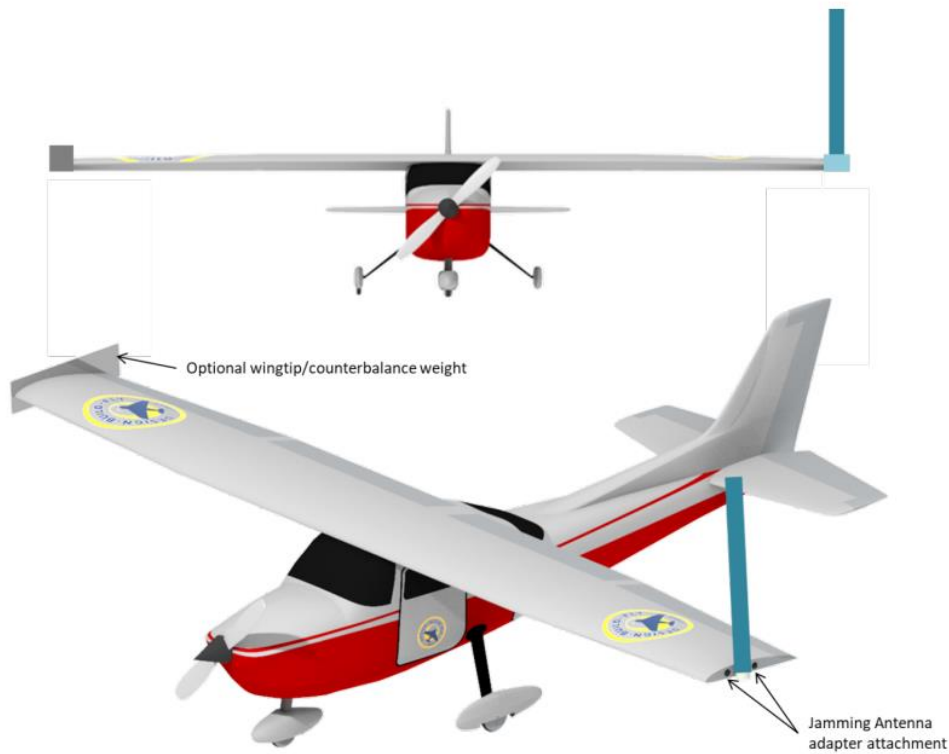
Figure 5: Sample Antenna and Counterweight Configuration Diagram

While this mission has many similarities to Mission 1, this mission has important scoring considerations. The completion bonus is twice that of the previous missions and includes a variable scoring element. In this case, the completion time of the three laps is included in the points calculation, as well as the length of the antenna. Like the other two flight missions, the landing does not need to take place within the flight window, but it does need to be successful to score points. Below is the equation for how Mission 3 is scored. Like Mission 2, 'N' represents the points of our aircraft and 'Max' represents the maximum points earned of all teams' aircraft for this mission.

$$M3 = 2 + \frac{N\left(\frac{Antenna\ Length}{Mission\ Time}\right)}{Max\left(\frac{Antenna\ Length}{Mission\ Time}\right)}$$

1.5.5 Ground Mission

The final mission of the competition is the ground mission and is a structural margin demonstration. For this mission, similarly to the three flight missions, a wing configuration is randomly selected at the beginning of the attempt and then installed onto the aircraft. Then, using the same adapters for the antenna and counterweight as in Mission 2, ground test mounts are installed to hold the aircraft above the ground.

Figure 6: Sample Ground Mission Configuration Diagram

Within a 10-minute window for the mission the wings and ground test mounts must be installed, and test weights applied to the aircraft fuselage. During this experiment the pilot will also prove the flight ability of the craft by controlling the electronic components while loaded. Once the maximum weight desired is applied to the aircraft there will be a 30 second hold period to ensure structural stability and then the flight controls will be tested a final time. The condition of failure for this mission is if there is structural failure at any point or if the flight controls stop functioning, with either of these conditions meaning no points are earned for the mission. Below is the equation for how mission 4 is graded assuming the requirements are all met and as seen in previous missions, 'N' represents our aircrafts performance and 'Max' represents the highest performance of all aircraft in the competition.

$$M4 = \frac{N(\frac{Total\ Test\ Weight}{Max\ Aircraft\ Weight})}{Max(\frac{Total\ Test\ Weight}{Max\ Aircraft\ Weight})}$$

2　Preliminary Approach

2.1　Functional Requirements

The major subsystems, the fuselage, lifting surfaces, and propulsion were preliminarily designed around the completion requirements for each mission. Each of these systems has a significant impact on performance, so to determine which to emphasize the most a sensitivity analysis was conducted. This further identified design requirements for each system.

2.1.1　Fuselage

Our goal when designing the fuselage was to make a fuselage structure strong enough to support a large payload, the battery, and the motor. Due to the ground mission, the fuselage needed to be able to transfer the load from wing to wing well. The fuselage also needed a strong and simple method of attaching the wings so they can be attached within the required time frame. The weight and shape of the fuselage needed to be considered as those can affect the flight characteristics greatly.

2.1.2　Lifting Surfaces

The lifting surfaces must provide the plane with enough lift to allow it to lift the greatest payload possible for Mission 2. Furthermore, the allowable maximum takeoff distance is 60 feet. Therefore, the wings must generate sufficient lift for the aircraft to takeoff within this limit. The wings must be strong and stiff to provide the best results for the ground mission. Mission 2 and 3 are dependent on the speed and endurance of the plane as they are based on the number of laps completed, so the amount of drag produced is an important factor to consider when designing the lifting surfaces. Due to the addition of the antenna in Mission 3 the control surface must be able to keep the plane stable even in an unbalanced condition.

2.1.3　Propulsion

When designing the propulsion system our overall goal was to maximize speed and endurance. We needed plenty of endurance to fly for 10 minutes in Mission 2. The system also needed to be powerful enough to allow for the 60-foot take-off distance and be able to produce enough thrust for the plane to carry a large payload. Similarly, Mission 3 is dependent on speed as well. We compared several different motor and propeller combinations to give the plane the best power to weight ratio.

2.2　Sensitivity Analysis

The sensitivity analysis was split into two parts. The first was an analysis of each mission's parameters and the second was of each independent variables' impact on all missions. Scores for DBF are awarded based on the number of points scored divided by the maximum number of points scored by any one team. As discussed in Section 1.5, this leads to a variable portion of scoring ranging from zero to one for each mission. Therefore, an accurate measure of total score was impossible without knowing other teams' performance estimates. Because of this, our sensitivity analysis was limited to a comparative evaluation of each variable present in scoring.

To accomplish this, a standard distribution model was assumed to nondimensionalize points. Because of the non-dimensional nature of this analysis, reasonable but arbitrary mean performance values could be used (Table 3). The standard deviation was harder to quantify. To create a reasonable spread of points, the standard deviation for each mission was set to the mean point value divided by 1.7. This constant was derived from the standard deviation of variable score components in the 2021-2022 Design Build Fly scores of the teams which completed all missions. As performance variables were varied, points were compared to the standard distribution model for that mission. A score was then assigned based on the cumulative distribution function of the point distribution. This method effectively nondimensionalizes points into a score between zero and one, the same as the competition.

Table 3: Sensitivity Analysis Mean Values

Variable	Assumed Mean
Airspeed	15 m/s
Course Length	775 m
Payload Weight	2.5 kg
Antenna Length	.15 m
Plane Weight	3.5 kg
Added Weight	5 kg

The breakdown of each mission reveals some interesting patterns and visual artifacts. For Mission 2 (Figure 7), the graduated coloring represents laps completed. Because of the number of lap graduations, it can be assumed that the number of laps will be sufficiently large number for the impact of each individual lap to be noticeable, but not all important. For both Mission 2 and Mission 3 (Figure 8), each of their two respective scoring variables are equally impactful. Therefore, when considering each individual mission, each scoring aspect should be considered equally to maximize points for these missions. For the Ground Mission (Figure 9), minimizing the maximum takeoff weight is more important than increasing the maximum weight the wings can support in the loading configuration. However, a conclusion cannot be drawn from these figures alone due to the sharing of scoring variables.
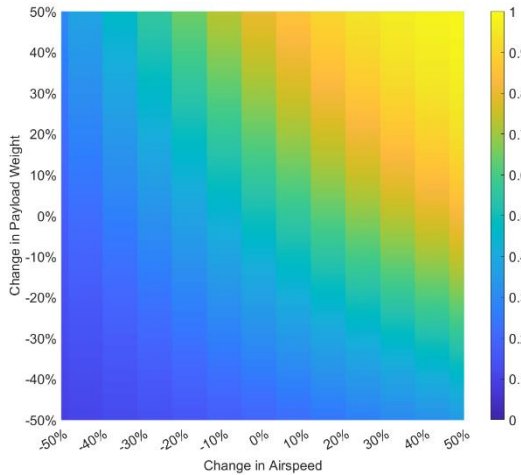
Figure 7: Mission 2 Sensitivity Analysis
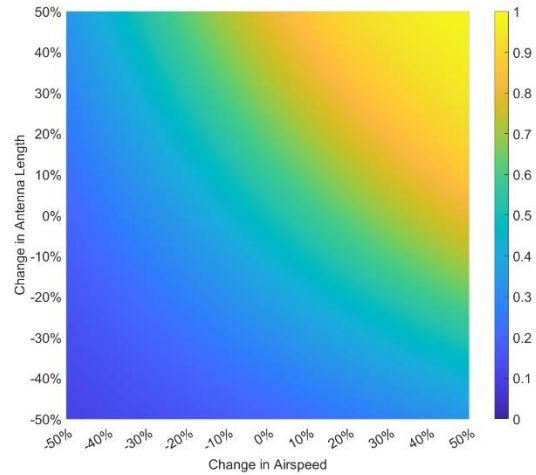
Figure 8: Mission 3 Sensitivity Analysis
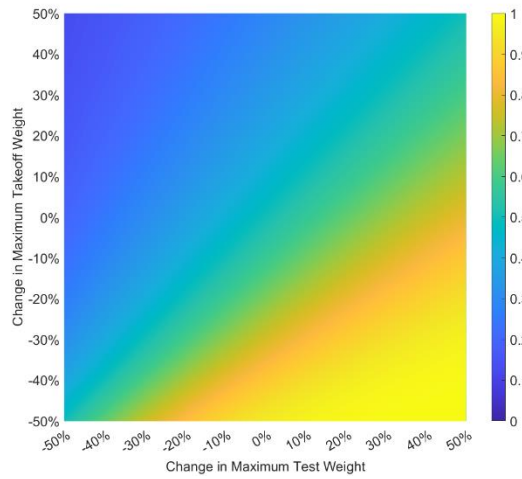
Figure 9: Ground Mission Sensitivity Analysis

Figure 10 displays every aspect of the aircraft that directly impacts scoring while also considering shared variables between missions. The most prominent pattern that emerges is airspeed. While for individual mission its importance was equal to the other scoring criteria, its relevance in both Mission 2 and Mission 3 makes it the most important factor in scoring. The second most important factor in scoring is antenna length. This straightforward conclusion reasonably arrives from its positive impact on Mission 3. Payload, plane, and Ground Mission added weight are the most interesting due to their interconnected nature with each other and the maximum takeoff and Ground Mission total weight. For this analysis, it was assumed the maximum takeoff weight would be in Mission 2 with the payload rather than Mission 3 with the added antenna and optional counterweight. Payload weight is the third most important factor in scoring. While its importance can be understood through its impact on Mission 2 scoring, it slightly negatively impacts the Ground Mission score by increasing the maximum takeoff weight, therefore falling being antenna length. The last two variables, plane weight and the added weight, are the least important factor in scoring. This is because their only positive impact on scoring is shared in

Ground Mission scoring. In conclusion, airspeed, as the primary factor in scoring, should be prioritized, even if at the limited expense of other aspects of the design.
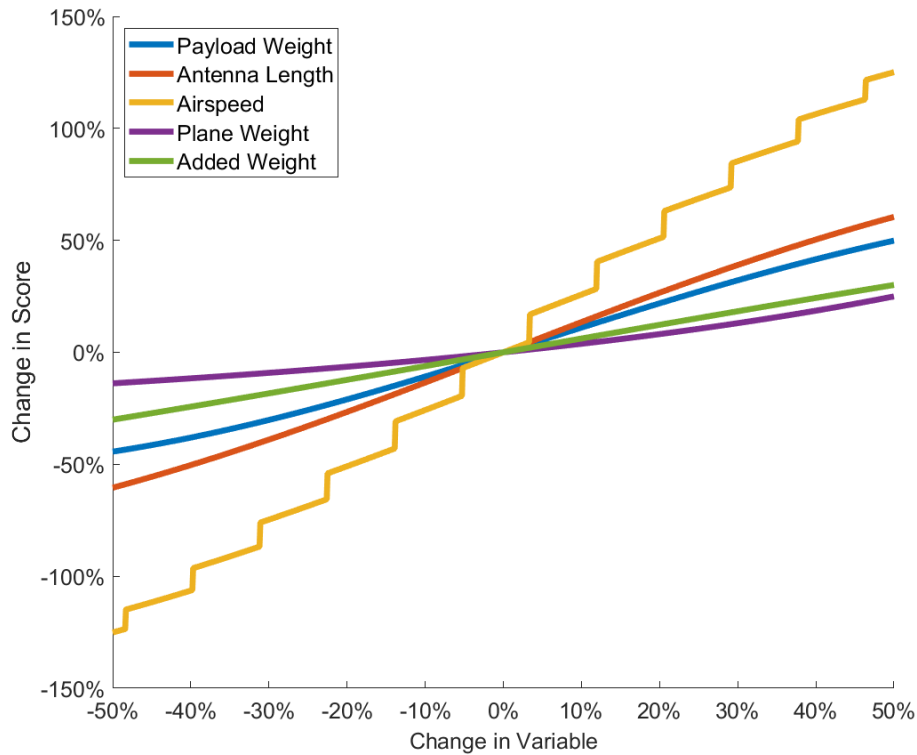
Figure 10: Sensitivity Analysis (Plane Weight Negated)

2.3 Design and Sizing Trades

2.3.1 Package Constraints

Choosing the package for our plane was the first challenge. Limited to 62" total linear dimension, multiple options were considered (Table 4).

Table 4: Package Sizing Options

Option	Length	Width	Height	Total
Option #1	36 in	12 in	10 in	58 in
Option #2	23 in	23 in	16 in	62 in
Option #3	33 in	14 in	14 in	61 in
Option #4	24 in	18 in	18 in	60 in

Because the competition required four wings, wing dimensions were a primary concern. The dimension that would be the most limited would therefore be the wingspan. While a full lift performance analysis was not complete, it was reasoned that Options #2 and #4 would be limiting. In addition, there would be little to no margin for error with Option #2. While the two remaining options were both workable, it was eventually decided that Option #3 would maximize spatial tolerances with the least tradeoffs.

2.4 Considered Concepts

2.4.1 Propulsion System

2.4.1.1 Motor Requirements

Consideration of the motor was based on the raw amount of thrust provided with considerable savings in weight and potentially energy. These requirements were considered due to the sensitivity analysis regarding airspeed of the plane as one of the more important factors in scoring, objectively making it a priority in design choices. Alongside the need for speed in Missions 1 through 3, the payload weight is an important factor in the second mission. In Mission 2 it is important to factor in additional weight as per mission guidelines. Having a powerful motor will aid in the generation of more lift to balance out the drag and additional weight of the payload to score higher. Since takeoff distance is critical for each mission, having a motor with low maximum RPM but capable of outputting approximately 50 Newtons thrust would allow for rapid acceleration in order to takeoff within the required distance. During cruise the expected required thrust is 20 to 25 Newtons; so, the throttle could be reduced during cruise to meet these demands. This also highlights that takeoff performance will be the defining requirement for the motor.

For this year's rules in the competition there was a change that would allow teams to use an Electric Ducted Fan (EDF) instead of the conventional electric motor and propeller set-up. In comparison to the conventional motor and propeller set-up, EDFs have the capability to create much more thrust in comparison but come with their own set of complications. An EDF must be considered as the starting point for building the plane since they take up more space and can't easily be placed at the front of the plane like a motor can. This creates additional complexities when it comes to building the plane itself was seen as a liability in the event of prototyping and repairing the plane. The last comparison drawn between the two is that the EDF thrust is much more linearly directed due to the shroud surrounding the blades. While the thrust that comes from this method is much more powerful, there is less control over where the air passes through which can further complicate the design of the plane to try and account for this aspect. Overall, the conventional method was chosen since EDFs proved to be too unreliable.

2.4.1.2 ESC Requirements

Electronic Speed Controller selection was primarily based on the standard set by the AIAA while also being determined by the continuous current output of the motor. If the ESC could not handle the continuous current output of the motor, then the ESC would overheat and cease to function properly during critical flight operations. This aspect is incredibly important due to the ESC being responsible for more than just the motor itself. The ESC is also responsible for supplying power to the other electronic components of the plane, like the receiver, via the internal Battery Eliminator Circuit. Failure of the ESC would leave a plane unresponsive to pilot input, which is a dangerous situation. Ideally the ESC's continuous current rating is higher than that of the motor's to ensure operations can continue at the motor's full throttle, if necessary, but the ESC max continuous current can also match the motor's continuous current output.

2.4.2 Wing Design

Our wing's design was our first area of consideration due to its influence on general aircraft performance parameters. Some of the design requirements that had to be considered were how the wings were to be attached to the airframe, where would the wings be mounted, and what shape would the wings take? Each of these considerations are impacted by each other, the competition requirements, and our functional requirements in the form of our subsystem design requirements.

2.4.2.1 Wing Attachment

How the wings are attached to the airframe was our primary concern. Our design requirements show that the wings must have a strong structure and the competition requirements told the team that our wings must be modular. Therefore, while the strongest design, a single, removeable wing was not an option. In addition, to prevent a large bending moment on the airframe during the Ground Missions, it was determined that a central attachment system would be necessary. Without a central system connecting both wings together in some way, the full weight of the plane, payload, and Ground Mission test weight would fall onto the wing attachment mechanism and airframe sides, limiting structural margins.

The next task was to design our central spar system. Our first design consisted of a junction block mounted into our airframe that could bear the Ground Mission load. Wing spars would extend past the wings and would interface with the junction block. To accommodate two wings, an ABAB system was drafted, with the wings being secured by four vertical pins going through alternating spars. The main downside of this design was in the needs of the junction block. It would have to be heavy, as it would most likely be made of metal due to strength requirements, and machined. In addition to this primary concern, the right and left wings would have to be manufactured differently to accommodate the ABAB design.

Another considered design would be to extend the spars through the fuselage, into the opposing wing. This design would keep the ABAB system and remove the need for central junction block. It would also increase the strength of each wing due to the spars from the other wing extending into it. However, this design still had several issues. The ABAB spar placement would make the wings uneven, and pins would weaken the spar strength.

While the through-fuselage system would work, drafting it led to our next and final design. Instead of having the spars from the wings extend through the fuselage, the airframe itself would have shorter spars. The wings could then interface onto these central spars using hollow wing spars. To prevent sliding, nuts and bolts would connect the airframe side to the wing ribs. In this way, vertical stresses would be exerted on the central spars, while the smaller horizontal stresses would be taken up by the retaining bolts and airframe sides.

2.4.2.2 Wing Placement

Wing placement was the second consideration. We started by considering a high, mid, or low wing configuration, and each's impact on stability and construction. The first competition requirement that influenced our design was the requirement to have a heavy, removable payload. To prevent a shifting center of gravity with respect to the center of lift, the payload had to be placed

vertically with the wings. This immediately disqualified a mid-wing design due to our central spars. The last two options were a low or high wing design. Of these two options, however, only one was the right choice. With a large, heavy payload, as well as an antenna creating a rolling torque in Mission 3, stability is of great importance. However, a low wing would not be able to provide this. In Mission 2, the payload would cause the aircraft to become inverted or become uncontrollable. Because of this, a high wing design was chosen. A high wing has additional benefits. With the wing attachment mechanism near the top of the fuselage, wing installation becomes more accessible. And although a high wing can block access to the payload bay, the removeable nature of the wing attachment mechanism negates this concern.

2.4.2.3 Wing Shape

The final consideration while developing the wings was their shape. The three designs considered were swept-back wings, trapezoidal wings, and rectangular wings. Because at least 4 wings need to be made, manufacturing feasibility was a primary concern. In addition, the Ground Mission and spar placement were important factors in the strength of the chosen wing options. These concerns narrowed down our final wing shape to be rectangular. Rectangular wings use the same rib shape along their entire span and can more easily accommodate the spars running perpendicular to the fuselage. In a trapezoidal wing, each wing rib would be shaped differently, and our wing spars would need to be closer together if they were to remain colinear throughout the entire wingspan. For a swept-wing configuration, the wing spars would not be able to be perpendicular to the airframe. While this has some implications with manufacturing, the primary concern in this case is Ground Mission performance. Due to the angle of each spar, a central spar system would not be straight.

2.4.3 Structural Design

2.4.3.1 Wing Structure

The wing structure was of critical importance in the ground mission since the entire score is based on how much weight the wings can support. Due to the box requirement and the need to be able to easily attach and detach the wings they had to be made modular. Each individual wing had to be strong on its own. Due to the nature of flying it is also optimal for the wings to be light. Carbon fiber was selected to be the main structural element of the wings since it is a strong lightweight material.

2.4.3.2 Fuselage Structure

The biggest constraint on the fuselage was the dimension requirements of the payload in mission two. The payload had to be at least 3 inches by 3 inches by 6 inches. The payload is only needed for one mission, so the payload box needs to be easily accessible. The need for a quick attachment mechanism for the wings also represented a challenge when doing fuselage construction. The ground mission being supported by the wings meant that the fuselage had to effectively transfer load from one wing to the other. The requirement for the battery to be completely contained lead to the development of a battery box to hold the battery. The need to

keep up with updates to the plane and being able to fix issues quickly led to the development of a modular system for each of the sub assembly contained in the fuselage.

3 Preliminary Design and Analysis

3.1 Analysis Methods

      Simulation and component analysis was the core of preliminary analysis for a majority of the design components of the aircraft. XFLR5, an advanced wind tunnel simulator, as well as SolidWorks were heavily utilized in obtaining initial data needed to begin optimizing the aerodynamic and structural components of the aircraft. Detailed investigation and comparison of different motors as well as electrical power and control components were necessary for ensuring that the aircraft power unit and control system were sufficient for what the initial design and the competition rules would require for each flight mission.

3.2 Aerodynamic Design and Analysis

3.2.1 Airfoil Analysis

      Aerodynamic analysis was completed using XFLR5 simulation software. Plugging in 1.225 kg/m^3 for "ρ" or air density, 13.4 m/s (30 mph) for an average freestream velocity, 18 µPa for an average dynamic viscosity of the atmosphere, as well as the chord length of the aircraft in [m] into the formula below resulted in a Reynold's number of 184,440:

$$Re \; = \; \frac{\rho v_\infty L_{chord}}{\mu}$$

      This number was paired with an estimated Mach number determined from the average 30 mph flight speed to run the batch analysis. Five designs were compared within the analysis: an interpolated NACA 4412/4416, a NACA 4412, NACA 4416, NACA 30815, and finally a NACA 4415. Figure 11 and Figure 12 show side views of the tested designs which are followed by Figure 13, the graphical lift-to-drag results from the simulation analysis of the five selected airfoils mentioned in the preliminary design methodology. Lift-to-drag was prioritized for this selection process as the team wanted to maximize the amount of lift generated while minimizing the drag for the sake of prioritizing top speed, as mentioned in our Sensitivity Analysis. The figure also contains a key, with an additional column containing rough maximum values of each plot:
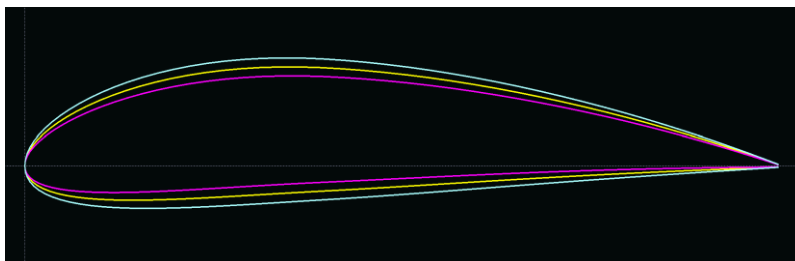
Foil	Color
NACA 4416	
NACA 4412/4416 Interpolation	
NACA 4412	

Figure 11: Foil designs taken from last year's team.
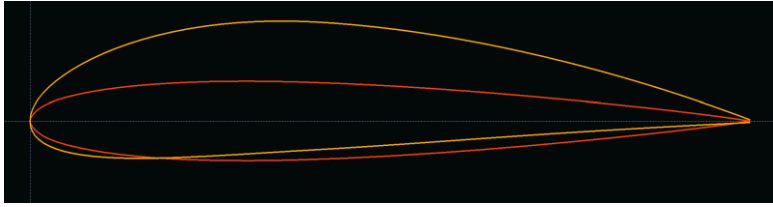
Foil	Color
NACA 4415	
NACA 30815	

Figure 12: Foils designed for this year's aircraft
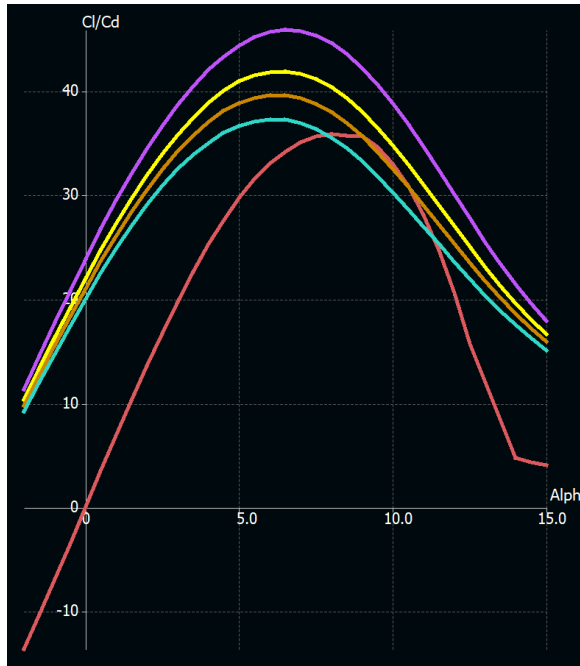
Foil	Color	Max L/D
NACA 4416		37
NACA 4412/4416 Interpolation		43
NACA 4412		46
NACA 4415		40
NACA 30815		37

Figure 13: Lift-to-drag ratio versus AOA for analyzed airfoils, paired with a key containing peak values.

As shown from the maximum values, the NACA 4415 the third largest peak lift-to-drag beneath the NACA 4412 and the interpolated airfoil from last year's team. What set it apart from the other two, apart from wanting to go with a different design, is that it had less of a negative moment coefficient impeding on the airfoil. Last year's foil and the 4415 were printed and ran through an open-ended wind tunnel to validate the simulation's theoretical data (Section 5.2.1).

3.2.2 Wing Configuration Analysis

The overall coefficient of lift and parasitic drag was predicted using XFLR5 analysis and can be seen in table 5. The data from the XFLR5 airfoil analysis was used so that it could be used to analyze the wing configuration. The base wing was modified to match the design specifications and then the vertical stabilizer and horizontal stabilizer were moved and modified to match their position relative to the main wing according to the design. The body was not able to be modeled as XFLR5 cannot accurately predict the flight characteristics of the body of an aircraft. To counter this, historical data from Raymer's Aircraft Design [3] was used to predict the body drag

coefficient of the aircraft. After this was complete, a simulation was run within XFLR5. The resulting graphs can be seen in figure 18 below and the wing configuration can be seen below as well in figure 19 with the pressure coefficient and streamlines visible. The simulation assumed constant airspeed but varied angle of attack. This simulation predicted coefficient of lift, drag, and moment versus angle of attack. It also predicted the neutral point of the wing configuration to be 3.662 inches back from the leading edge of the wing. This simulation was repeated for airspeeds of 10m/s and 8 m/s, the results were identical to the 30 m/s simulation as was expected. The plots seen in Figure 14 were calculated with an airspeed of 30 m/s and is followed by Figure 15 showing the wing configuration with the pressure coefficient overlayed as well as the downwash stream flow.

Table 5: Flight Coefficients and Characteristics

Flight Characteristic	Value
Lift Coefficient	0.521
Drag Coefficient	0.333
Aspect Ratio	8.712
Moment Coefficient at Cruise	-0.195
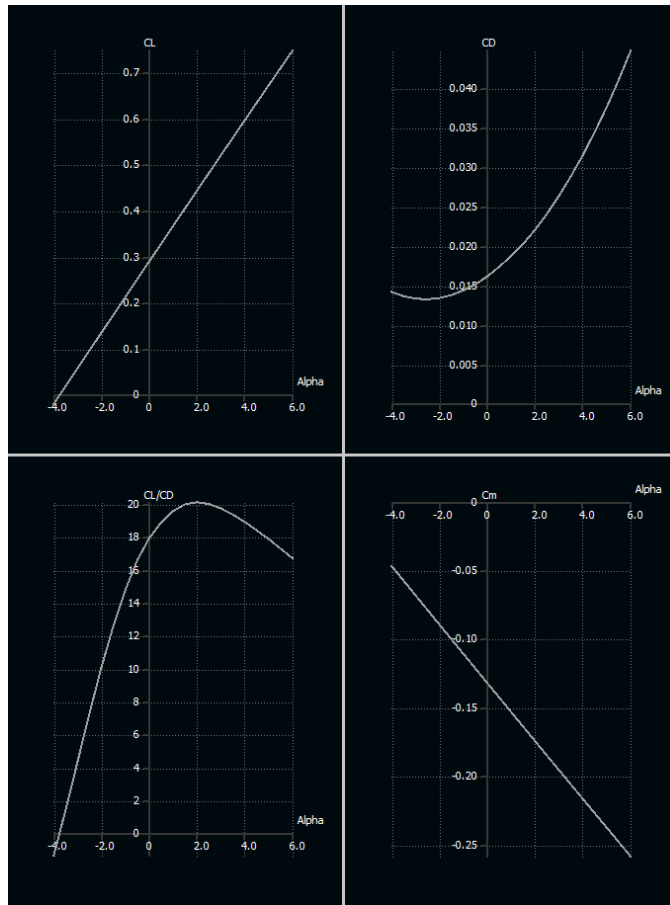
Figure 14: Lift, drag, and moment coefficient as well as lift-to-drag ratio versus AOA
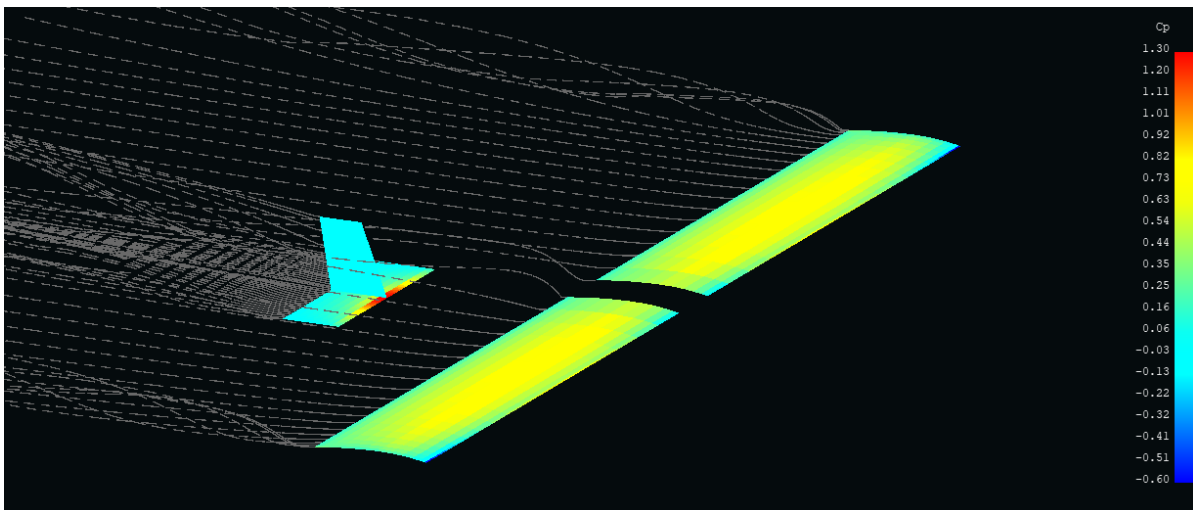
Figure 15: Downwash stream and pressure coefficient on the wing configuration

3.2.3 Thrust Required Analysis

The wind tunnel analysis allowed for the calculation of lift-to-drag ratios across each recorded data point. This ratio was used to determine the angle of attack deg that would be most optimal to the design, and it was discovered that an AOA of 3 deg yielded the highest lift per unit drag. In turn, the ratios at each airspeed at this AOA were recorded and used as an independent variable in a thrust calculation at a set of different aircraft weights ranging from 5 to 25 lbs while also incorporating the 9 lbs empty operating weight and 12 lbs loaded operating weight of the aircraft. The following equation was utilized:

$$T_R = QSC_{D_0} + \frac{KS}{Q}\left(\frac{W}{S}\right)^2$$

With an estimated zero-lift drag coefficient of 0.3, the results were plotted through Excel as follows:
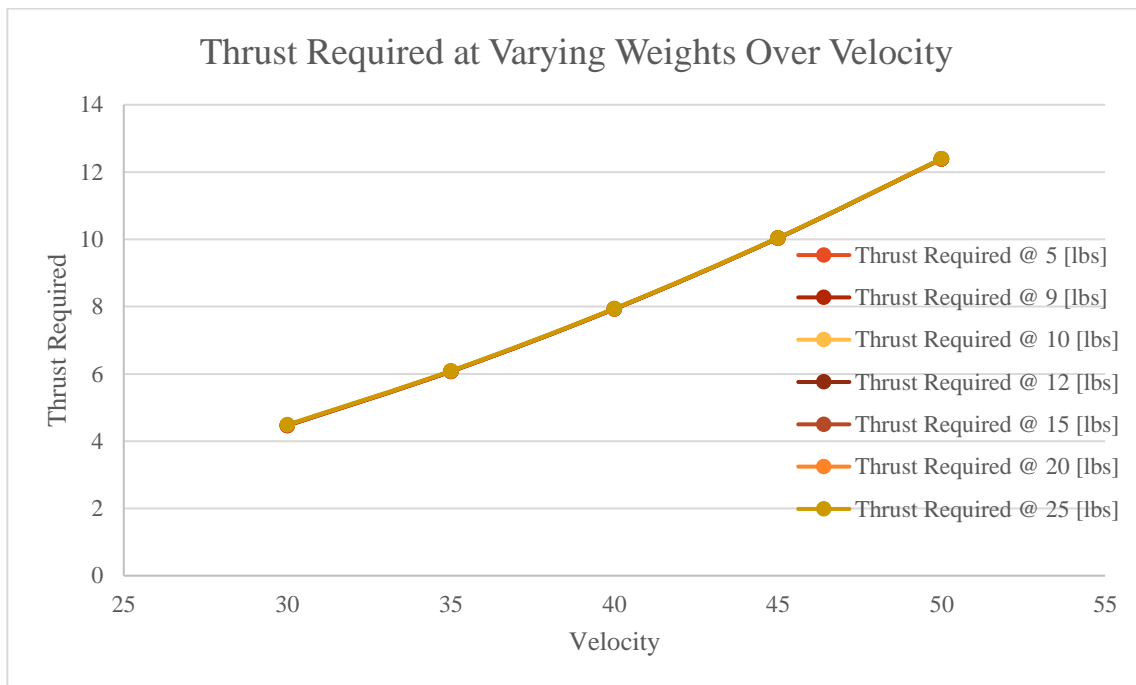
Figure 16: Required thrust(lbf) versus airspeed(mph) for varous airxraft weights

Again, these calculations and plot were generated from the wind tunnel gathered, in which the airfoil was scaled down by half to fit in the tunnel. To maintain the same Reynold's number, the speed of the tunnel was scaled up by half. As shown, the plots are extremely close together, showing that aircraft weight has a near zero impact on thrust.

3.3 Propulsion System Design and Analysis

Propulsion system analysis is comprised of understanding the requirements as specified in section 2.4.1.1 and 2.2, where the main goals were to produce as much thrust as possible while maintaining a reasonable amount of weight to maximize the power-to-weight ratio. The primary concept at play for understanding the output that a motor can produce is the Kv rating, which is the rotations-per-minute (RPM) that a motor will spin at while unloaded at a given input voltage

[2]. The Kv constant itself is given in units of RPM/Volt. By multiplying the Kv constant as specified by the manufacturer the RPMs at maximum voltage supplied can be found and used as an estimate since the motor is loaded with a propeller as shown in this formula[3]:

$$RPM = KV * Input\ Voltage$$

An important thing to note is that Kv only will relate to the speed the motor spins at and does not correlate with the amount of torque that the motor can produce. Higher Kv motors can produce higher maximum speeds with better efficiency and lower Kv motors can produce more torque which will bring the propeller up to top speed quicker. Since motors produce vibration, it must be noted that bringing the propeller up to speed quicker can bypass certain resonance frequencies that could potentially effect signals received by the receiver on the aircraft which is also a very desirable characteristic.

A tertiary analysis point in propulsion systems is the size of the motor. Motor sizing naming schemes follow a diameter-length system usually, if not just the length itself in millimeters. Larger diameter motors operate with more torque and usually have less speed, while longer length motors tend to run at higher speeds with less torque. The size of the motor is standalone from the Kv rating of the motor but if two motors are different sizes with the same Kv the motor that has a larger diameter will have more torque. The additional torque will help the propeller reach optimal speeds quicker while also having more speed at the same RPM. An important thing to note is that larger motors can also run at larger voltages and can also make up for the difference in Kv rating in some cases because of the additional volts supplied.

Propellers also play an important role in the analysis of the propulsion system since they generate the thrust needed for movement based on the motor doing work on the system. Propellers come in multiple shapes and sizes while also having varied amounts of blades. Propellers with more blades end up pushing more air through while also increasing the amount of drag, which affects the efficiency of the propeller.[4] A lower number of blades will produce less thrust with less drag but can be compensated for by using longer blades to mitigate thrust losses by increasing the amount of flux through propeller area. The last thing to note is that with more blades the propeller will vibrate less compared to propellers with less blades, but it is not a primary consideration given the scale of the aircraft.

---

[2] https://directvoltage.com/the-basics-of-drone-motor-kv-rating/
[3]   https://www.astroflight.com/explanation-of-motor-terminology.html#:~:text=The%20Kv%20rating%20designates%20the,in%20units%20of%20RPM%2FVolt.
[4] https://airplaneacademy.com/whats-the-difference-between-2-3-and-4-bladed-propellers/

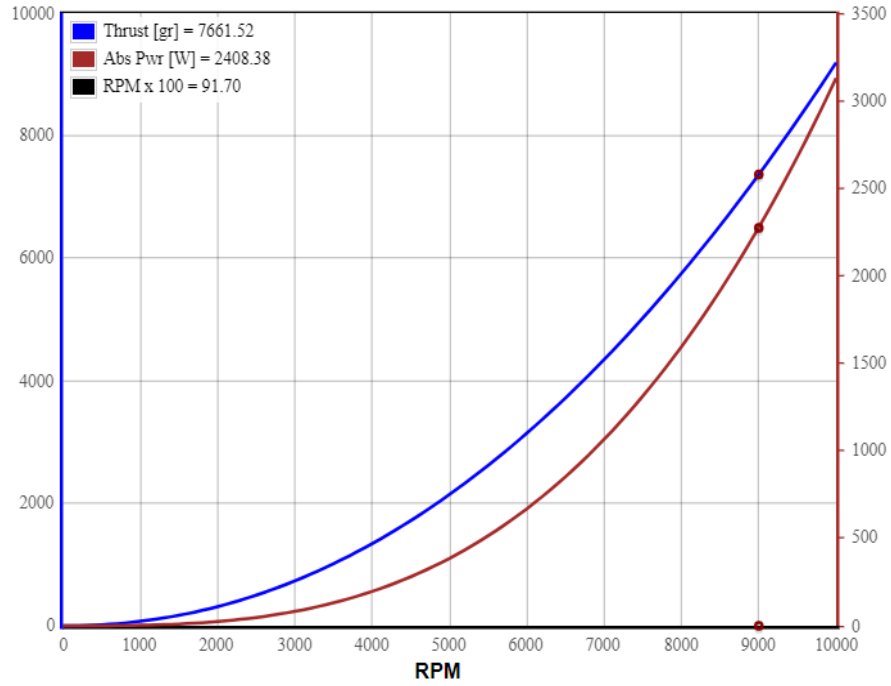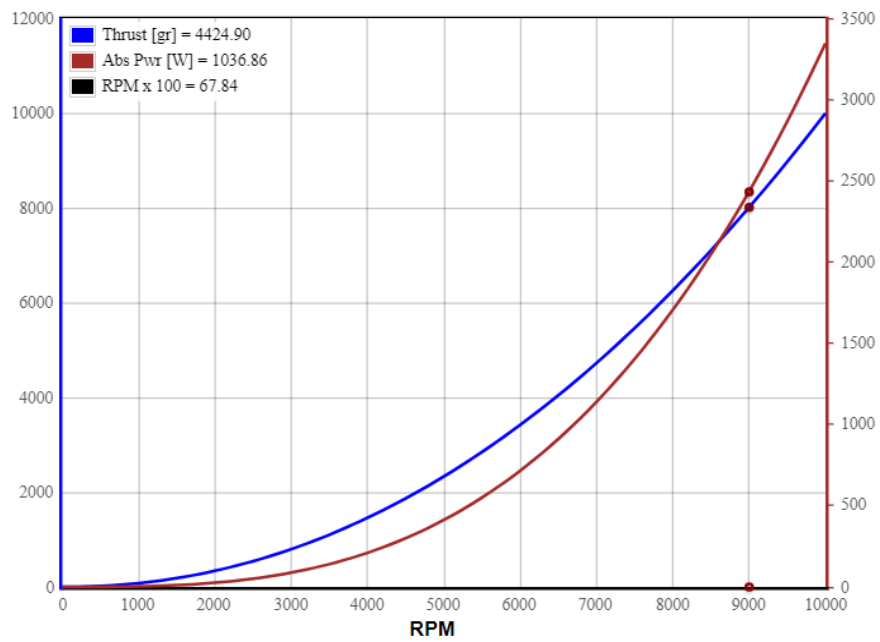*Figure 17: Estimation of 15x7" Tri-Blade Propeller Thrust Performance at 150 ft and 1 bar[5]*

Figure 18: Estimation of 16x8" Dual-Blade Propeller Thrust Performance at 150 ft and 1 bar[5]

---

[5] https://rcplanes.online/calc_thrust.htm

The above figures were used to calculate thrust at estimated conditions for flight give a baseline for the differences in propeller characteristics, and when paired with the motor spinning at a certain number of RPMs gives an idea of thrust outputs. It is to be noted that the amount of thrust produced peaks at the RPM the motor is capable of, determined by the motor's Kv constant. Therefore, thrust will not trend towards infinity since it will have a physical limitation enforced upon it. Another factor to note is that the pitch angle of the blades themselves determines how hard the air is redirected and will also have a large impact on the thrust produced according to the Figures. The graphs themselves are estimates, so other factors like propeller rigidity and wind speed will decrease the amount of thrust produced.

3.3.1 Battery

The battery is one of the most critical components of the plane, and it is one of the components that has the most variety in terms of selection options. The first step in the battery selection process was looking at the rules prescribed by the AIAA for the Design/Build/Fly Competition 2023. The initial restriction given is that there must only be one battery pack and it needs to be either Nickel Cadmium/Nickel Metal Hydride (NiCad/NiMH) or Lithium Polymer (LiPo) batteries [1]. Our team elected to use a LiPo battery pack due to the high energy density and discharge rate, which would generate more power and a more consistent power level throughout the flight. This does increase the price of the battery, but the benefits of this high power and consistency are more than worth the higher price point. Using the LiPo battery pack it comes with the constraint that the maximum continuous discharge cannot exceed 100 amps [1].

The next major decision that had to be made was how many cells were required for the battery pack. This is important as the battery is the heaviest component on the aircraft. This means minimizing the weight of the battery can help maintain a good center of gravity and allow for better performance but could also reduce the power output and available time of flight. The 6-cell LiPo batteries are the largest option that can be used which have a high voltage of over 22.2 V and over a 6000 mAh capacity; however, this option was too heavy as seen in the two options that were considered, the Gens Ace Advanced 6800mAh 6S1P 22.8V 100C HardCase LiPo Battery Pack has a weight of around 955 grams[6] and the Zeee 6S 22.2V 100C 6000mAh LiPo Battery has a weight of 855 grams[7]. Due to this high weight and larger voltage than necessary for our aircraft it was determined that a 4-cell LiPo battery pack would provide the optimal balance of voltage and weight. This led to the decision to use the DXF 14.8V 4S 6500mAh 100C LiPo Battery which has a notably lower weight than the 6-cell options at 575 grams[8]. This type of battery will help make placement in the fuselage easier and will allow for faster flight speeds due to the reduced weight.

Another factor that needed to be considered was the physical size of the battery, since it is a competition safety requirement that the battery have a quarter inch firewall surrounding it in order to protect the other components of the aircraft. Now that the battery is selected, the

---

[6] https://genstattu.com/gens-ace-advanced-6800mah-22-8-v-100c-6s1p-hardcase-lipo-battery-pack-61-with-ec5-plug/
[7] https://www.aliexpress.com/i/2255801081650329.html?gatewayAdapt=4itemAdapt
[8] https://dxf-hobby.store/collections/frontpage/products/dxf-lipo-battery-4s-14-8v-6500mah-100c-goldseries-graphene-lipo-hardc-1

dimensions can be found to be 5.44 x 1.85 x 1.93 inches[3], and with this a shell can be designed around this to ensure that no other component gets within a quarter inch of the battery. With the battery selected then the other electronic components can be selected and added around it.

Figure 19: DXF 14.8V 4S 6500mAh 100C LiPo Battery

3.3.2 Motor

The second critical component needed for the aircraft is the motor, this is because you need to ensure the balance of power and weight. For motor selection it was between many options that were inherited through previous Design/Build/Fly Competitions and other WPI aircraft. With this there was a variety of choices when it came to size, the smallest of which being a Turnigy Park480 Brushless Outrunner 1320kv which only weighed 80 grams[9] which was determined to be much smaller than needed. The four major options considered for the final aircraft motor were the Hacker A40-12L V4 14 Pole[10], the AXI 2820/12 Gold Line[11], the E-flite Power 32BL 770Kv Motor[12], and the Scorpion SII-4020-630kv motors[13]. Of these four choices, the team decided elected to use the Scorpion SII-4020-630kv motor, this motor is the heaviest of the three options at 288 grams[7], however it has significantly more power than the other options. This is important for the design as it was determined in the sensitivity analysis of the missions that having a faster aircraft was the most important factor in gaining the most competition points. So, the higher power motor was selected to generate faster speeds for the competition and the heavier motor is also beneficial as it helps to counteract the weight of the battery which is the heaviest component on the aircraft.

---

[9] https://hobbyking.com/en_us/turnigy-park480-brushless-outrunner-1320kv.html
[10] https://hackermotorusa.com/shop/hacker-brushless-motors/outrunners/a40-12l-v2-14-pole/
[11] https://www.modelmotors.cz/product/detail/223/
[12] https://www.greathobbies.com/productinfo/?prod_id=EFLM4032A
[13] https://www.scorpionsystem.com/catalog/aeroplane/motors_1/sii-40/SII_4020-630/

Figure 20: Scorpion SII-4020-630kv Motor

3.4 Control Design and Analysis

3.4.1 Electronic Components Selection

The electronic components and how they interact with the structure of the aircraft is one of the most critical parts of the design process. This is due to the many different necessary parts, and the precise placement of each part to ensure that the aircraft remains stable. In this section the decision process and part selection will be discussed and how each part impacted on the overall design of the aircraft.

3.4.1.1 Electronic Speed Controller

Another important component to have on a remote-controlled aircraft, especially when using high power LiPo batteries, is an electronic speed controller (ESC). This part is critical as it takes the power from the battery and safely distributes it to other sources, notably the motor and the receiver to control all the functions on the aircraft. This is why it is important to select an ESC that is capable of withstanding the power from the battery and will distribute it at the correct rate. After doing research into different options, it was determined the best option was the E-Flite 100-Amp Pro Switch-Mode BEC Brushless ESC[14]. This is because it was easily made compatible with the battery and motor on the aircraft and the maximum continuous discharge is 100 Amps which is the maximum allowed by the Design/Build/Fly Competition rules [1]. This will prevent the need for ever obtaining a new ESC throughout the design and testing process as even though other parts around it could change, the ESC is already capable of covering all maximum needed continuous discharge.

---

[14]   https://www.e-fliterc.com/product/100-amp-pro-switch-mode-bec-brushless-esc-with-270mm-lead-ec5/EFLA10100AEC5.html

Figure 21: E-Flite 100-Amp Pro Switch-Mode BEC Brushless ESC

3.4.1.2 Servo Motors

Control surfaces such as the elevator, rudder and ailerons are vital to the stable and controllable flight of the aircraft as they allow the orientation of the aircraft to be controlled in flight. For an aircraft of this scale, the control surfaces are maneuvered with servo motors that have 180 degrees of free rotation. That is enough to turn the control surfaces in order to provide controlled steering during flight. Initially HobbyKing HXT900 Micro Servos were considered, they had a low weight of 9.8 grams but only had a torque of 1.6 kg-cm[15]. With the high speeds the aircraft was going to reach, this low torque would not have been enough to move the control surfaces while they were under the aerodynamic loads expected at cruise. This led to the decision to use the Hitec HS-425BB Pro Ball Bearing Servo which is heavier at 45.5 grams but makes up for the weight with a torque of 4.1 kg-cm[16].

Figure 22: Hitec HS-425BB Pro Ball Bearing Servo

3.4.1.3 Radio and Receiver

While the battery, motor and ESC are the three largest electronic components for the aircraft, they need a few other smaller components to function and ensure competition safety requirements. One of these parts is the remote control and receiver, from previous WPI aircraft there is an accumulation of remote controllers, and this led to the use of the Spektrum DX6i[17] being used as our main remote controller. Since a Spektrum brand remote control is used, the

---

[15] https://hobbyking.com/en_us/hxt900-micro-servo-1-6kg-0-12sec-9-8g.html
[16] https://hitecrcd.com/products/servos/analog/sport-2/hs-425bb/product
[17] https://www.spektrumrc.com/product/dx6i-6-channel-full-range-w-o-servos-md2/SPM6600.html

LICHIFIT Fast Speed RC Receiver for Spektrum AR8000 8CH[18] was acquired as it has easy connectivity with all Spektrum remote controls. This is also an 8-channel receiver which allows for control of the throttle, ailerons, elevator, and rudder with room for other ports if there are additional servos for flaps or electronic components that need to be added.

Figure 23: Spektrum DX6i Radio Remote Controller

Figure 24: LICHIFIT Fast Speed RC Receiver

3.4.1.4 Safety Components

One of the most important factors on a remote-controlled plane of this scale is ensuring the safety of the people and surroundings near the plane when it is being tested and flown. Due to this, there are multiple safety measures taken to ensure a controlled flight and emergency stopping. The first precaution comes right after the battery is plugged into the ESC which powers the rest of the components on the plane. Between these joints there is a physical switch that is always in the off position until the wiring is checked during each pre-flight assessment. This ensures that even with the battery plugged in the system, none of the components receive power until the easily accessible switch on the plane, mounted far from the motor and propellor is flipped to the on position. For this step the Heavy-Duty Toggle Switch 20/15A 125/227V[19] is used. This type of switch was also selected for the significant force required to flip it to the on position, preventing any accidental activation of the plane. A fuse 100-amp fuse is also soldered in between the battery and ESC in order to prevent any damage to the components downstream of the battery while the aircraft is active. The next safety measure comes when the plane is already in the air; while it is being controlled from the ground it is important to have a way to shut off the plane remotely if something were to go wrong. For this the Spektrum DX6i remote controller has the safety measure that if the power on the controller is shut off mid-flight, the control surfaces will return to their equilibrium positions and most importantly, the motor will stop spinning. This will cause the plane to descend in a glide but will at least prevent more damage to the plane or its surroundings.

---

[18] https://www.spektrumrc.com/product/ar8000-8-channel-dsmx-receiver/SPMAR8000.html
[19] https://meekoutlet.com/products/heavy-duty-toggle-switch-20-15a-125-277v-2-hp-with-waterproof-rubber-boot-ul-cul-certified

3.4.2 Control Surfaces

Control surfaces on an aircraft is what allows for both the fine-tuned and major maneuvering of the aircraft during flight. Due to this, it is incredibly important to ensure a well-designed system of controls that allows the aircraft to do all the necessary maneuvers for the challenges outlined earlier in the report. The simplest remote control (RC) planes only require the use of a rudder and elevator on the tail to have enough control for the aircraft. However, since this aircraft is larger than the standard RC plane and more fine tune control ailerons are also used to give even more extensive flight control. There are also unimplemented plans for the addition of flaps alongside the ailerons on the wing to give even more control during takeoff and landing. However, this aircraft never got to the stage where these would be attached to the wing.

The control surfaces for our plane were optimized for the high flight speeds, so they are smaller than most remote-controlled plane control surfaces. Due to this the size of the surfaces only ranges from 15 to 20 percent of the total elevator, rudder, or aileron surface area which gives greater fine-tuned control of the aircraft while it is at higher speeds, but less control at slower velocities. The ailerons are also positioned at the far edges of the wings away from the fuselage to maximize the torque produced by the same surface area. It was found that an aileron positioned in the last third of the wing like it is currently in our design generates at least 1.5 times more torque than that of an aileron of the same surface area that spans the entire wing. Each of these control surfaces also have at least 40 degrees of rotation, with the elevator and rudder over 45 degrees, about their pivot point in either direction of their equilibrium which is parallel with their respective surfaces. These surfaces are controlled by the servos placed within the wing for the ailerons and at the back end of the fuselage for the elevator and rudder which connect to the surfaces via rigid steel push rods to ensure fine control of the aircraft.

Initially, the control surfaces were made of 1/8-inch plywood like the rest of the planes interior and mounted using ¼" thick wooden dowels. They were attached to their respective servos simply through bent metal wire connected by adhesive. This initial design brought about a few immediate issues. The dowels would slide slightly parallel to the wingspan, and the plywood composition was heavy which made fine-tuned control with the servos more challenging. To correct these issues, their composition was switched to foam to improve the weight and allow for the embedding of reinforced flat hinges at the edges for wing and tail mounting. Finally, the control surfaces were fitted with control horns and thicker control rods for stiffer, more responsive control when the servos were activated. The elevator and rudder were also adjusted later in the construction process so that the rudder would attach to a pivoting tail wheel. This allowed greater directional control of the aircraft while it was taxiing before takeoff.

Figure 25: Photos of the initial wooden elevator, rudder, and aileron control surface setup

3.5 Structural Design and Analysis

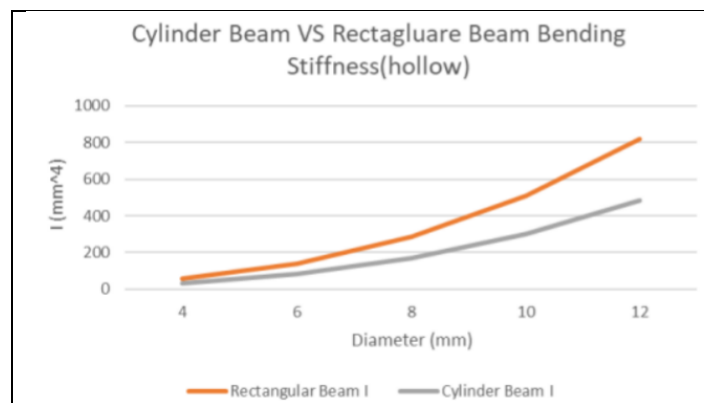### 3.5.1 Wing Structure Selection

Figure 26: Square vs. Round Carbon Fiber Rod Stiffness

Before the team could begin the initial construction of the wings some simple simulations had to be done to determine the best course of action regarding the structure of the wing. Carbon fiber comes in two main forms: round and square rods. To determine which rods should be used a analysis was performed comparing the rods of the same diameter and thickness to determine which was better. The bending stiffness of each rod was compared. To produce Figure 26 Young's Modulus constant held constant and the theoretical bending stiffness of each type rod was plotted varying the diameter of each hollow rod. When Young's Modulus is held constant the bending stiffness becomes solely based on geometry through the second moment of inertia. Due to the better characteristic of square carbon fiber, it was used to span the length of the wings. At the diameter that was purchased; the square carbon fiber rods were theoretically 28 percent stiffer compared to their round counterparts.

3.5.2 Antenna Mount Design

Creating a preliminary design to mount our antenna is an important step of this mission criterion. The Design Build Fly rules stipulate that the mount must have two anchor points to the wing and allow for a Schedule 40 .5" PVC tube to be mounted to it vertically. Figure 27 shows the initial approach to the mount design. The large central hole is for the PVC tube and the two projections engage with the wing's carbon fiber spars. No anchoring mechanism was yet incorporated.
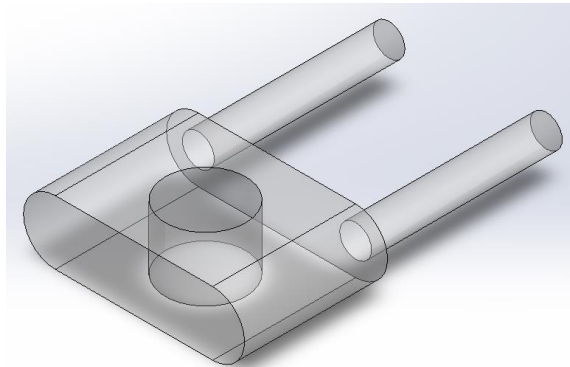
Figure 27: Antenna Mount Initial Sketch

The next step in the antenna mounting design was incorporating a securing mechanism. As an initial design, it was important to only incorporate simple elements. Therefore, a modification of our existing ribs was used, with holes cut for .25" bolts and one going through the PVC tube hole. The projections were replaced with carbon fiber rods to complete the initial design (Figure 28).
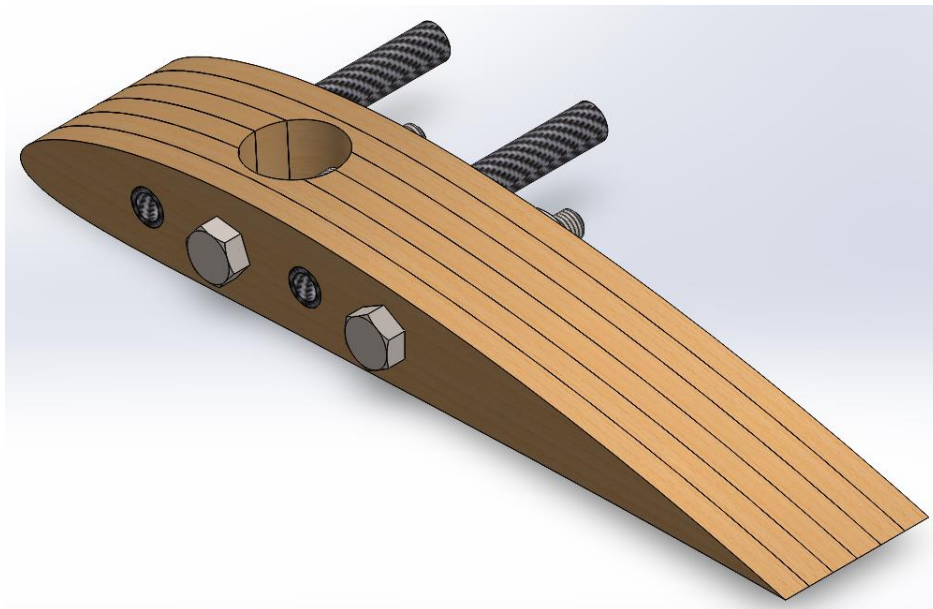

Figure 28: Antenna Mount Model

3.5.3 Finite Element Analysis

Finite Element Analysis (FEA) was completed using a simplified model of our plane in SolidWorks Simulations. The simplified model included only the wing sections and central spars due to this being the subsystem experiencing the highest mechanical stresses. For all simulations, the simulation mode was set to "Auto".

3.5.3.1 Simulations Model

The SolidWorks assembly used for FEA was a simplified version of our plane, concentrating on the wing and spar assemblies (Figure 29). Just like the final revision of the plane (Section 2.4.3.1), two square carbon fiber rods made up the spars of each wing, attached by ¼" wood ribs. While the final wing attachment mechanism is slightly more sophisticated (6.3.2), the model used for simulations utilizes two round carbon fiber rods fused to each wing. The material properties of each material used are described in Table 6.

Table 6: Simulation Material Properties

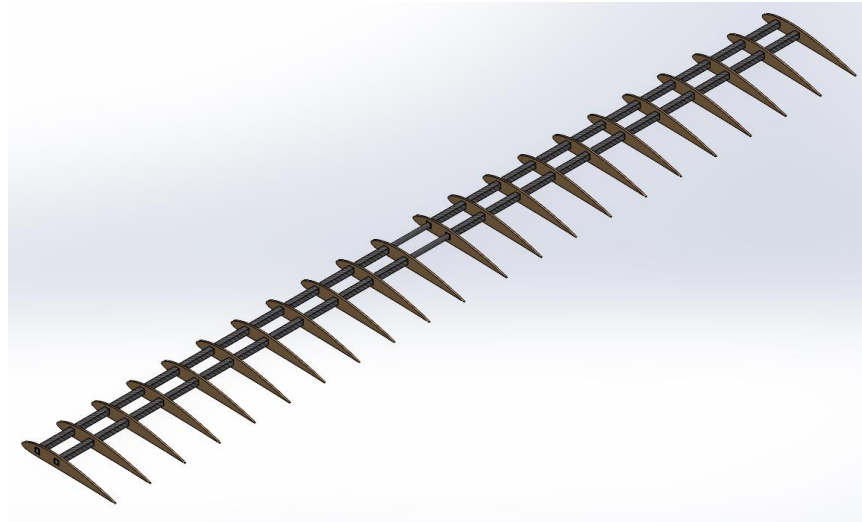| Material	Dimensions (in)	Young's Modulus (MPa)	Yield Strength (MPa)
Wood (Balsa)	.125 (THK)	3,000	20
Round Carbon Fiber Rods	.315 (O.D.)	134,000	1,650
Square Carbon Fiber Rods	.394 (O.D.) x .335 (I.D.)	134,000	1,650

Figure 29: FEA Wing Model

3.5.3.2 Ground Mission Load Analysis

For the fuselage loading as in the Ground Mission, the wing spars at the wing tips were fixed longitudinally and vertically, while all other parts were fused. The only load applied to the wing structure was a vertical force pointing downwards along the interior segment of the round

carbon fiber rods. Gravity was not applied. A Static Study was made with these settings (Figure 30). To find the maximum load while maintaining a minimum factor of safety of 1.25, a Design Study was conducted on the Static Study, maximizing load force while setting the minimum factor of safety.
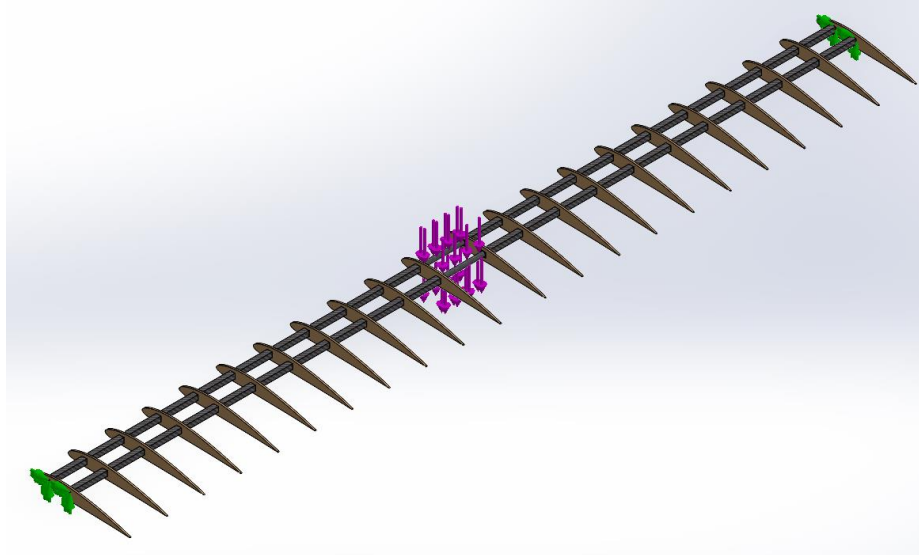
Figure 30: Wing Static Study Setup (Fixtures in green, forces in purple)

SolidWorks solved the simulation using the "Intel Sparse" solver. As shown in Figure 31, the maximum deflection of 2.79 inches is in the middle of the wing. SolidWorks Design Insight (Figure 32) also points to the areas of highest stress concentration: those being the central segment of the round carbon fiber rods, as well as the area where the round carbon fiber rods end. This is reasonable, as the loading force is being applied to the central spars, while also being the furthest body from the fixed geometry.
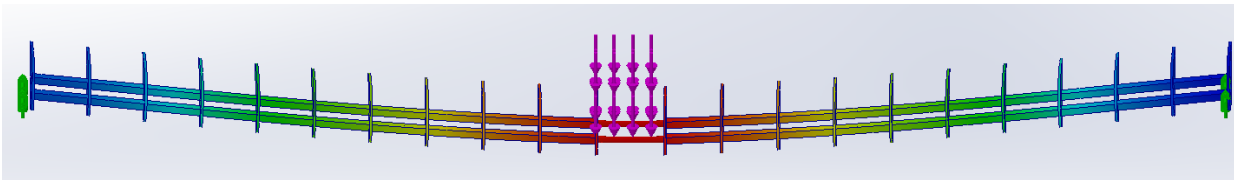
Figure 31: Wing Displacement, 1:1 (Red to blue is maximum to minimum displacement)

Figure 32: Design Insight – Wing Stress Concentration

3.5.3.3 Antenna Mount Analysis

To verify the strength of the antenna mounting mechanism (Section 3.5.2), a static study was created. An arbitrary load of 20 pounds was applied longitudinally to the top of the .5"

Schedule 40 PVC tube antenna to simulate a liberal drag estimate as shown in Figure 33. Hex nuts on the mounting screws were used as fixed geometry points in this analysis, taking the place of the threaded anchors in the wing. The length of the analyzed PVC tube above the attachment mechanism was about 7 inches, with a total length of 8 inches. These values are meant to represent a conservative estimate of antenna choice and structural impact of the antenna mount, not a wholistic analysis of antenna length or aerodynamic consequences.
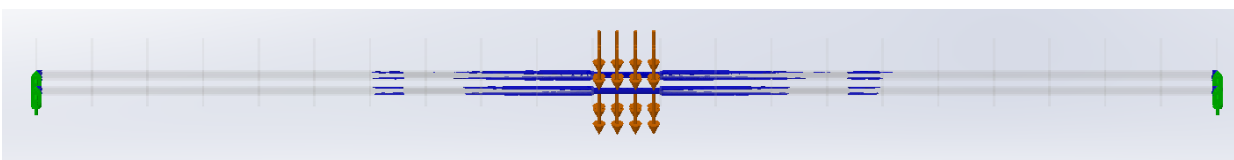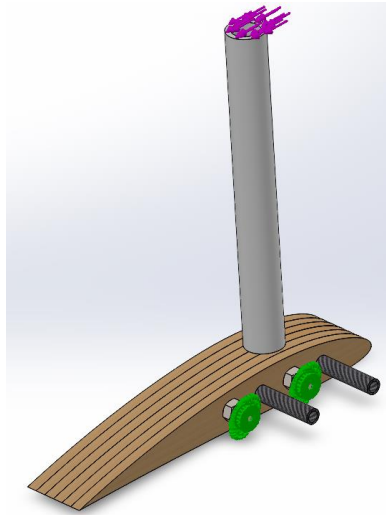

Figure 33: Antenna Mount Static Study Setup (Fixtures in green, forces in purple)

The analysis was run, with SolidWorks utilizing the "Iterative" solver. As shown in Figure 34, the largest displacement is experienced by the PVC tube itself with a magnitude of 0.450 inches. While this does make sense due to the large moment arm, this does not equate to stress concentrations. An analysis of stress concentrations through SolidWorks Design Insight however does reveal the most stress occurring in the PVC tube. However, in the antenna mount itself, stress is concentrated in the area around the PVC tube, as well as in the anchoring sections (Figure 35).
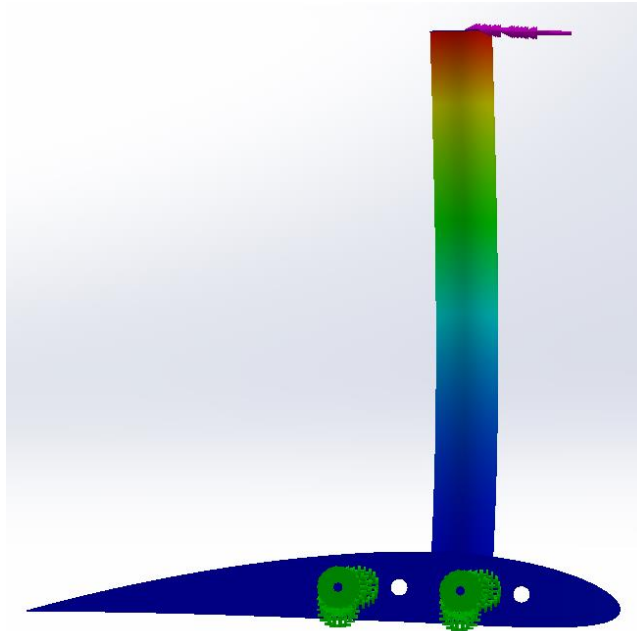
Figure 34: Antenna Mount Displacement, 1:1 (Red to blue is maximum to minimum displacement)
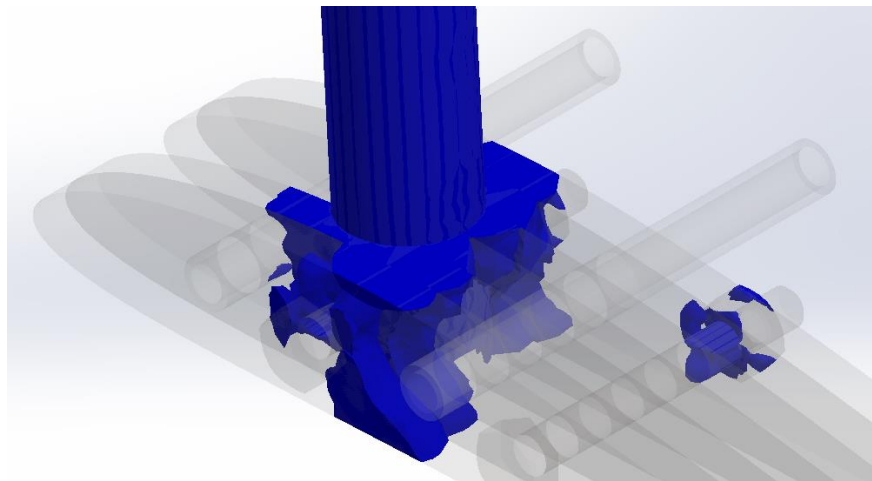
Figure 35: Design Insight – Antenna Mount Stress Concentration

One major concern with this analysis is the factor of safety. While the load is most likely above that to be expected, there are many areas with a factor of safety only slightly above one (Figure 36).
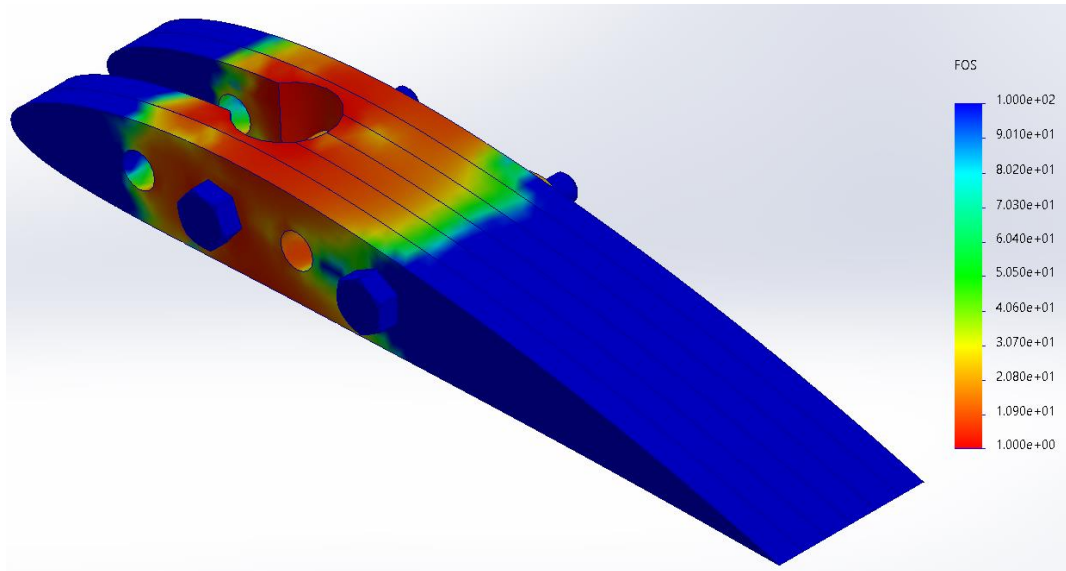
Figure 36: Antenna Mount Factor of Safety Plot

The analysis of the antenna mounting mechanism shows that while the design is practical in holding the antenna, balsa is too weak to be used in the rib arrangement. The biggest change that needs to be made to this design is the choice of a stronger rib material. In addition, the trailing edge section of the stacked ribs are not necessary for structural security. And while the competition rules are ambiguous, an airfoil shape may also not be permissible.

3.5.3.4 Mission 3 Load Analysis

While the design for the antenna mount is viable (Section 3.5.3.3), it will also load the wing in a manner unlike Section 3.5.3.2. Therefore, a separate Static Study of the wing, under a load representative of that expected for Mission 3.

For this analysis, the fixed points will be the same as those in the Ground Mission analysis (Section 3.5.3.2), while the loads will be the same as those in the antenna mount analysis (Section 3.5.3.3). However, this analysis will also include a gravitational force, to account for the weight of the antenna mount and PVC tube mounted on the wingtip. For this analysis, SolidWorks utilized the "Iterative" solver.
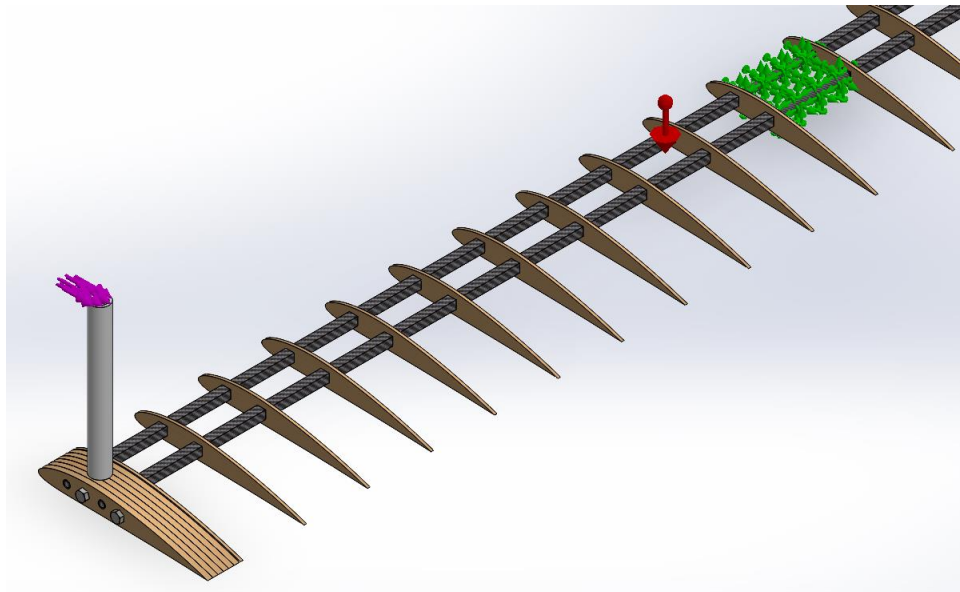
Figure 37: Mission 3 Load Setup (Fixtures in green, forces in red/purple)

The displacement of the wing and antenna shows a similar response to that of the antenna on just the antenna mount. Figure 38 shows the displacement of the wing. As in the antenna mount analysis, the most prominent deflection is at the top of the PVC antenna, with a maximum of 0.380 inches. This is inconsistent with the results of Section 3.5.3.3, whose maximum displacement is .450 inches. However, this inconsistency could be caused by the different fixturing. One trend that does appear is the similarity between displacement in both square carbon fiber rods. This is confirmed in Figure 39, which shows similar stress concentrations along each spar. Another expected area of stress concentration is the ribs. Stress concentrations near the central carbon fiber rods were unexpected. However, these may be due to the surface-to-surface bonding model used in this analysis.
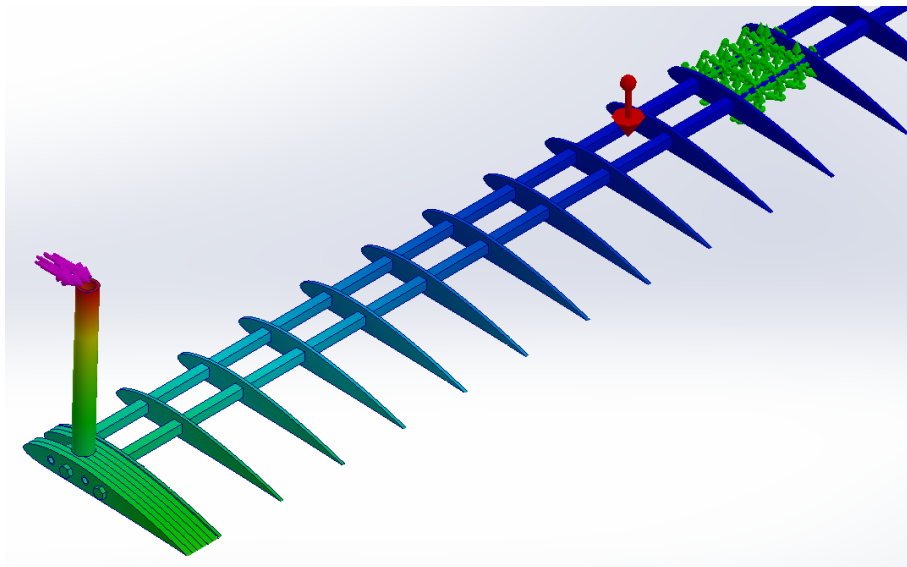
Figure 38: Mission 3 Wing Displacement, 1:1 (Red to blue is maximum to minimum displacement)
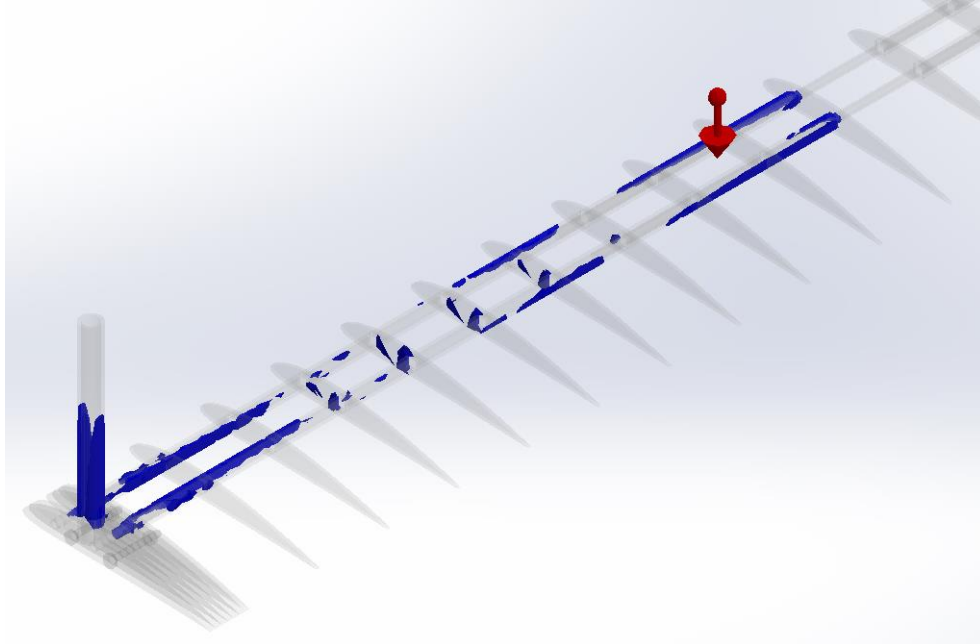
Figure 39: Design Insight – Mission 3 Antenna and Wing Stress Concentration

A factor of safety plot (Figure 40) reveals more clearly that the area of concern are the ribs. However, these ribs still maintain a minimum factor of safety of 3.4. Therefore, it is safe to conclude that the wing is capable of drag loading on the antenna as well as the weight of the antenna mount.
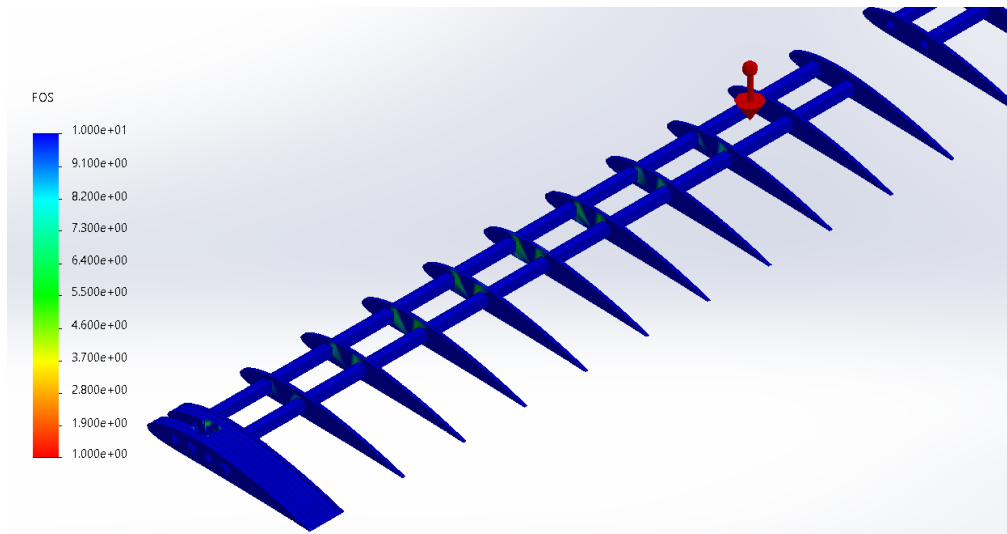
Figure 40: Mission 3 Factor of Safety Plot

3.6 Predicted Mission Performance

3.6.1 Mission 1

With the wings rated to the design and typical flight conditions the aircraft will experience, and the assumption of perfect operation and flight conditions, the maximum velocity of the aircraft was first determined through the following equation:

$$V_{max} = \sqrt{\frac{\left(\frac{T}{W}\right)\left(\frac{W}{S}\right) \pm \left(\frac{W}{S}\right)\sqrt{\left(\frac{T}{W}\right)^2 - 4C_{D_0}K}}{\rho C_{D_0}}}$$

The following parameters needed to be calculated in addition to be plugged into the maximum velocity equation in tandem with known sizing and power parameters of the aircraft, ensuring these parameters are converted into metric units for calculation purposes (note that surface area and zero lift drag coefficient are larger in order to accommodate the entirety of the aircraft as accurately as possible in order to have a more accurate maximum velocity prediction):

Table 7: Mission 1 predicted performance parameters.

| Parameter	Value
C_{D_0}	0.33
T	45 N
ρ	1.225 kg/m^3
W	3.62874 kg
S$_{plane}$	0.60021 m^2
e	0.86
b	1.7653 m
c	0.2032 m

$$S_{wing} = b * c$$

$$AR = \frac{b^2}{S_{wing}}$$

$$K = \frac{W^2}{\pi AR e}$$

Solving these preliminary calculations, and plugging them into the maximum velocity equation results in a top speed of roughly 43 mph. This can be applied to determine timing along the straight sections of the competition course, but as for a 180 deg. turn time the following equation must be used with an aerodynamic safety factor of 1.06 (a standard):

$$t_{180\ turn} = \cfrac{1}{\cfrac{9.81\sqrt{(1.06)^2 - 1}}{V_{max}}}$$

The resultant turn time is approximately 5.6 s. These calculated values along with the course dimensions outlined in Figure 4 are plugged into the following equation for determining the Mission 1 predicted completion time:

$$t_{Mission}[s] = (number\ laps\ required) * (\frac{total\ straight\ distance\ [ft]}{top\ speed\ \left[\frac{ft}{s}\right]}) + (number\ 180\ turns * turn\ time\ [s]))$$

After plugging in the necessary numbers in their correct units, the resultant predicted mission time is approximately 162 s.

3.6.2 Mission 2

While keeping same conditions, assumptions, and calculation process as Mission 1 prediction, the only adjustment to the parameters is increasing the weight by 30% to accommodate for the payload requirement. The result is a new weight of 10.4 lbs, which results in a little to no change in the original 43 mph top speed and 5.6 s turn time. Manipulating the mission completion time calculation to be set equal to the number of laps, substituting 10 min. or 600 s into the mission completion time, it is predicted that the aircraft will be able to complete 11 full laps of the course.

3.6.3 Mission 3

For mission three, it is heavily reliant on the length of the antenna attachment placed on the end of the wing tip. To account for this, a MATLAB script was run to determine the drag on the antenna while flying at a velocity of 45 mph. The carbon fiber beams were determined to have a torque that can withstand a moment of around 20 N. From this it is seen that the maximum length of the antenna could be if it was taking the entirety of this force is roughly 14 in. A plot of how the drag exponentially increases as antenna length increases can be seen earlier in Figure 41: Plot of how the drag on the antenna increases as total antenna length increases. However, since stress on the plane due to standard flight needs to be accounted for and a factor of safety must be present, the length of the antenna is set to be 7 in. in length and applies 2.5 Nn of torque on the wing tip. Due to this, the expect that the performance of the plane will be like that of the previous flights due to a smaller antenna causing a smaller torque, and the plane should be able to correct for this with only the ailerons. Keeping a small antenna also helps to increase the speed of the aircraft, which is the most important quality of our plane as seen in the sensitivity analysis.
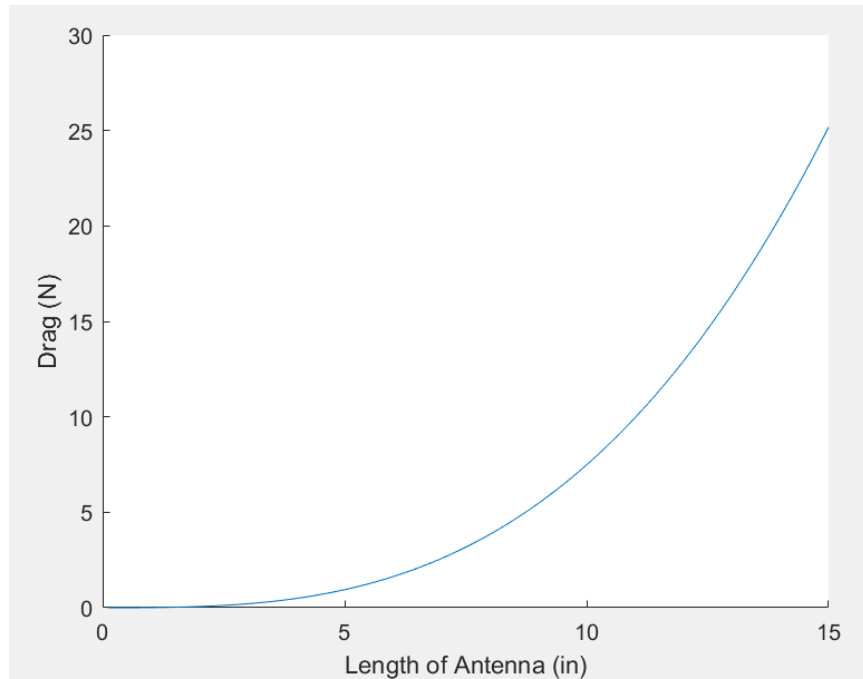
Figure 41: Plot of how the drag on the antenna increases as total antenna length increases

3.6.4 Ground Mission

The most important figure for the Ground Missions is the plane's maximum supported weight. According to SolidWorks analysis (3.5.3.2), the plane can hold a maximum of 30 pounds while maintaining a factor of safety. Early CAD estimates place the plane's weight at 8 pounds, leaving 22 pounds of added weight. While the score from this section can vary depending on the maximum take-off weight of the plane in Mission 2 and Mission 3, the maximum number of points predicted for our design is 2.75. By finding the maximum supported take-off weight of our plane to find a minimum score of 3.55. However, from our sensitivity analysis in Section 2.2, it was concluded that our payload weight impacts our mission score more positively than Ground Mission test weights. Therefore, an estimate closer to the minimum is more likely. Like all prior predicted performance metrics however, these scores are near impossible to compare without other scores to compare to.

4 Manufacturing Processes

4.1 Laser Cutting

Laser cutting was the primary method used for consistent manufacturing of the aircraft. For the wings, ribs were first exported from XFLR5, and imported into SolidWorks, where they were resized. These rib parts, used for the full plane CAD model, were exported to .svg files. A Full Spectrum P-Series 36"x24" Laser Cutter was used for the majority of laser cut parts, with the occasional use of a Full Spectrum P-Series 24"x18" Laser Cutter. For airframe components such as the airframe sides, battery and payload box, and motor mounting plate, designs were exported from SolidWorks and converted into .svg files, which were then laser cut. For these parts, .25" plywood was used. Some control surfaces were cut from .125" thick basswood, with a similar method to the airframe and wing ribs.

Figure 42: Full Spectrum P-Series 24"x18" Laser Cutter   *Figure 43: Full-Spectrum P-Series 36"x24" Laser Cutter*

4.2 Machining

Because of expense and time, CNC machining was used very sparingly during our project. This was also due to the lack of metal components and the lack of need for precisely machined parts. However, machining was used to create holders for the cantilever beam tests in Section 5.4.2. A 3-flute high speed steel, .25" bit was used to prepare two holders: one for the .397" square carbon fiber rods and one for the .315" round carbon fiber rods. These holders allowed for a cantilever beam test to verify ultimate bending strength and Young's Modulus of each carbon fiber rod variety utilized in the wing design. The holder parts were designed, and the CNC program made, in Fusion 360 with machining taking place on a Haas Mini Mill. The holder for the square carbon fiber rod can be seen in Figure 44, with both holders and their respectivive carbon fiber rods in Figure 45.

Figure 44: Cantilever Beam Test Holder

Figure 45: Holder with Rods

4.3 Assembly Methods

4.3.1 Wings

For wing construction, it was started with laser cutting ¼" birch plywood into 22 of the chosen airfoil shape discussed in chapter 4.1. These lasers cut shapes had two parallel square holes cut in order to attach to the support spars. After laser cutting, the spars also had a circular hole drilled between the square holes so that the wires for the aileron servos could be fed through. The last detail for these is that four of the airfoils had the trailing edges cut off to leave space for the ailerons to be inset into the wing itself. Then two carbon fiber spars with a square cross section were taken and marked every 2.72 inches until there were 11 marks on each spar. The laser cut airfoils are then taken and at these markings adhered to the carbon fiber spars using epoxy. The airfoil closest to the fuselage had two laser cut pieces epoxied together for extra structural support at that point. Lastly using balsa wood, a spar is placed on the trailing edges of the cut airfoil shapes that the ailerons will be attached to. This was repeated for the other wing to end up with a full wing set. The wings then have a thin layer of plywood added to the leading edge for structural stability and coated in a layer of Monokote to create an airtight seal.

4.3.1.1 Ailerons

The final ailerons were constructed out of foam as discussed in previous sections. To construct them the wing assembly was taken and the holes where the ailerons would go were traced onto foam board. Then using a heated wire foam cutter, the rough shape of the ailerons was cut out. Then, using sandpaper that progressively got finer, the foam was sanded down until it matched the desired shape of the wing trailing edge and had a smooth leading edge to not impede any of the wing aerodynamics when it was in the neutral position on the wing. After the ailerons were coated in Monokote, a small box cutting knife was used to cut slits into the leading edge of the

aileron and then into the balsa on the wing. With these slits cut, four hinges were inserted and epoxied into the aileron and then into the wing. Then, on the top of the aileron a small hole was punctured, and the control horn was attached using epoxy. The ailerons also used a thin, but rigid 0.6 mm wire connector to attach the control horn to the servo on each wing.

4.3.1.2 Antenna Mount Anchor

The antenna mounting mechanism requires two anchor points to the wing, of which the right wing was chosen. Holes were drilled in the double-thick ribs to match the placement of the antenna mount screws. Epoxy resin was used to fill the holes, and threaded wood anchors hammered into place as the epoxy dried.

4.3.2 Airframe

The Airframe was constructed out of ¼ inch plywood. The sides of the airframe are a single piece on each side with several subassemblies sandwiched between them. The subassemblies in order from front to back of the plane are: motor plate, landing gear plate, battery box, payload box, and finally the tail attachment. See Figure 46 for reference. Each piece of the subassemblies that connects to the air frame have holes and notches and the airframe side pieces have holes and notches opposite of the sub-assemblies. This allows each piece to fit snuggly together. The notches are then glued with wood glue. Each subassembly is assembled and glued together separately and then is slotted and glued into both airframe side pieces.
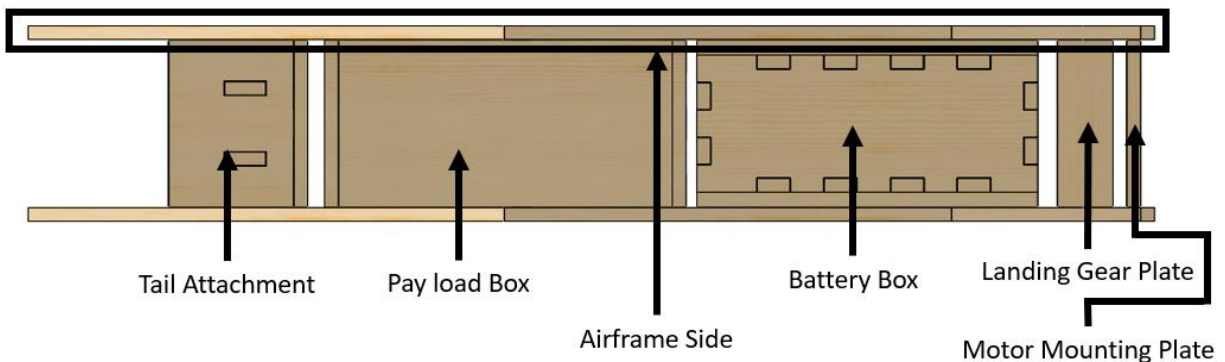
Figure 46: Fuselage with Labeled Subassemblies

4.3.2.1 Airframe Side

The air frame side pieces were designed to accommodate all the structural subassemblies that needed to be contained in the fuselage of the plane. In our testing it was found that the side needed to be as strong as possible so the only cut out are those required for assembly of the plane. The air frame is 4.6 inches tall and 22.25 inches long. The airframe has holes and notches in several spots to allow for each side to interlock with each subassembly to create a strong structure. The airframe side has a line of 0.335 inches diameter holes that are spaced 0.825 inches apart along the top to allow for mounting of the wings. There are several extra holes in the row to allow the wings to be moved if needed. See Figure 47 for refrence.
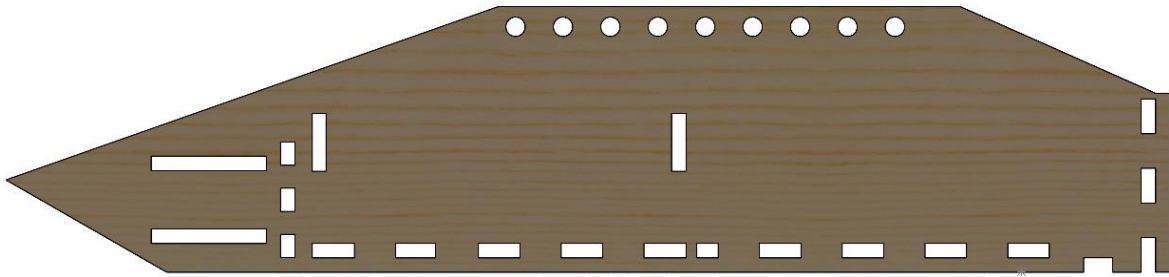
Figure 47: Airframe Side

4.3.2.2 Motor Plate

The motor plate is a rectangle of ¼ plywood that is 3 inches tall by 3.5 inches wide. The extra 0.5 inches allow for 5.4 inch by ¼ inch notches on either end to affix it to the airframe side. In the middle of the plate is a 0.5 diameter hole to allow for the shaft of the motor to not contact any piece of the structure. The plate is set back ¼ of an inch from the front of the air frame so the force produced by the motor can be transferred better. We found that adhesive alone was an insufficient mounting mechanism. See Figure 48 for reference.
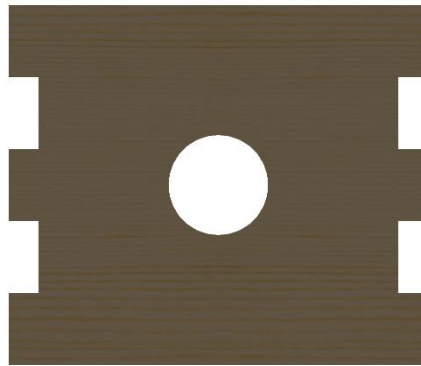
Figure 48: Motor Mount Plate

4.3.2.3 Landing Gear Plate

The landing gear plate is a 3.5 by 1 inch plywood plate with notches on either side to affix it to the airframe. The plate is reinforced by a metal band that extends under and up the sides of the airframe to accommodate the shock that occurs during landing. The plate exists to allow the use of a nut and bolt system to affix our landing gear to the plane. See Figure 49 for reference.

Figure 49: Landing Gear Plate

4.3.2.4 Battery Box

The battery box is made up of 4 pieces: one 3.5 inch by 6.13-inch bottom which affixes it to the airframe, two 2.38 inch by 5.63-inch side pieces, and two 2.38 inch by 2.45-inch pieces and one 2.45 inch by 6.13-inch top piece. The battery box bottom has holes that each of the side pieces slide into. Each side is then glued to the bottom pieces and each other. The top piece is not glued but is held in by friction and a Velcro band. See Figure 50 for reference.
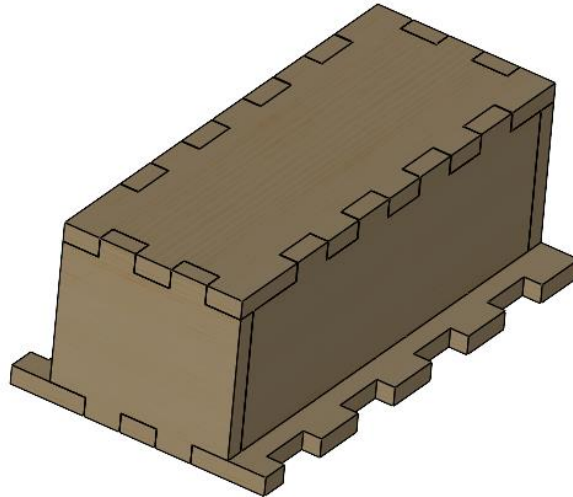
Figure 50: Battery Box

4.3.2.5 Payload Box

The payload box is constructed with two 3.5 inch by 3.5-inch pieces of plywood and one 6.5 inch by 3.5-inch bottom piece. The sides of the payload box have notches that fit into holes in the airframe side pieces on the sides and notches that fit into the bottom piece of the payload box. See Figure 51 for reference.
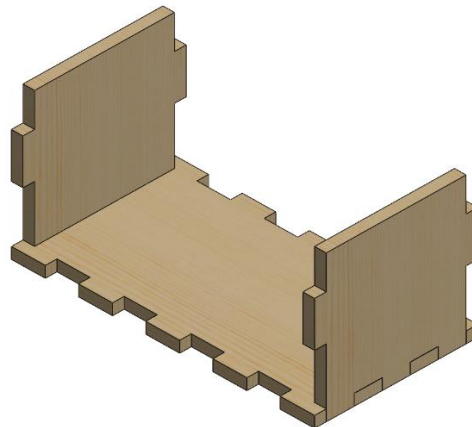
Figure 51: Payload Box

4.3.2.6 Tail Attachment

The tail attachment is designed to attach the tail rod to the main fuselage of the plane. The tail rod that was used is a 1-inch diameter square carbon fiber rod. The tail attachment is 5 pieces:

1 plate and 4 sides of a box referred to as the tail box. The tail attachment is a box that allows the rod to slip into it and then be glued using epoxy in order to make a secure connection between the fuselage and the tail. The tail attachment plate has several holes that allow each side of the box to slip into it and the plate is notched on two sides to allow it to be glued to the airframe side pieces. The top and bottom piece of the tail box are also 3.5 inches allowing them to be glued to the sides of the airframe as well as to provide extra stability and strength to the tail box to up and downward motion. Each side of the tail box also has holes and notches to allow them to interlock in order to create the strongest box possible. See Figure 52 for reference.
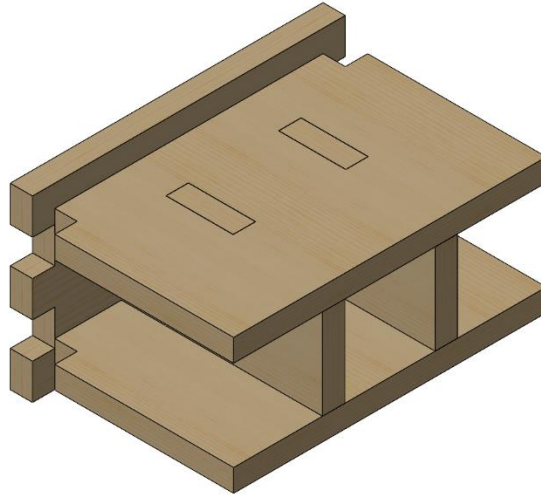
Figure 52: Tail Attachment

4.3.3 Antenna Mount

The antenna mounting mechanism was constructed to attach a Schedule 40 .5" PVC tube vertically to the wingtip of our plane. After the completed structural analysis of a placeholder antenna holder, the final design was manufactured to match the contours of the wing. Eight ribs were cut by laser cutter and epoxied together. Four holes were left, running laterally through the ribs. Two were for round carbon fiber rods. These would provide rigidity and interface with the square rods of the wing. The other two holes were for the .25" mounting bolts, satisfying the requirement for the DBF competition that the antenna should have two mounting points to the wing. The carbon fiber rods were epoxied in place, while the bolts were removeable. Anchors were hammered into the left wing and epoxied for the bolts. To create a hold for the antenna, a 7/8" bit was used to drill a vertical hole through the attachment mechanism. One of the securing screws also passes through the PVC tube to secure it.

Figure 53: Antenna Mount

4.3.4 Tail

The tail was constructed in a very similar way to how the ailerons were, as described in Section 4.3.1.1. The tail, rudder and elevator were made out of foam components that were traced onto large foam board and then cut to the general tail shape using the heated wire foam cutter. Sandpaper was again used to ensure the tail components were all flat and had a smooth aerodynamic shape and leading edge. For the main tail body, the vertical tail frame then had three holes drilled in the base and had three 0.15-inch diameter wooden dowels epoxied in so that the two main tail pieces could connect. Corresponding holes were then drilled in the horizontal tail piece and the two components were epoxied together with a square against one side to ensure they were perpendicular to each other. All the components were also coated with Monokote for better aerodynamic properties and then the elevator and rudder were added to the trailing edge of the tail using the same hinge technique as the ailerons. Control horns were also then added in the same manner as the ailerons and more rigid, 2 mm, push rods were used to connect these control horns to the servos that were located on the back of the fuselage. The tail was then attached to the carbon fiber tail spar by drilling holes into it, then using washers and epoxy to adhere the dowels to the spar. The tail wheel is also epoxied to the back of the spar and then a dowel is epoxied into the bottom of the rudder that runs down the aircraft to the tail wheel for control when the plane is taxiing.
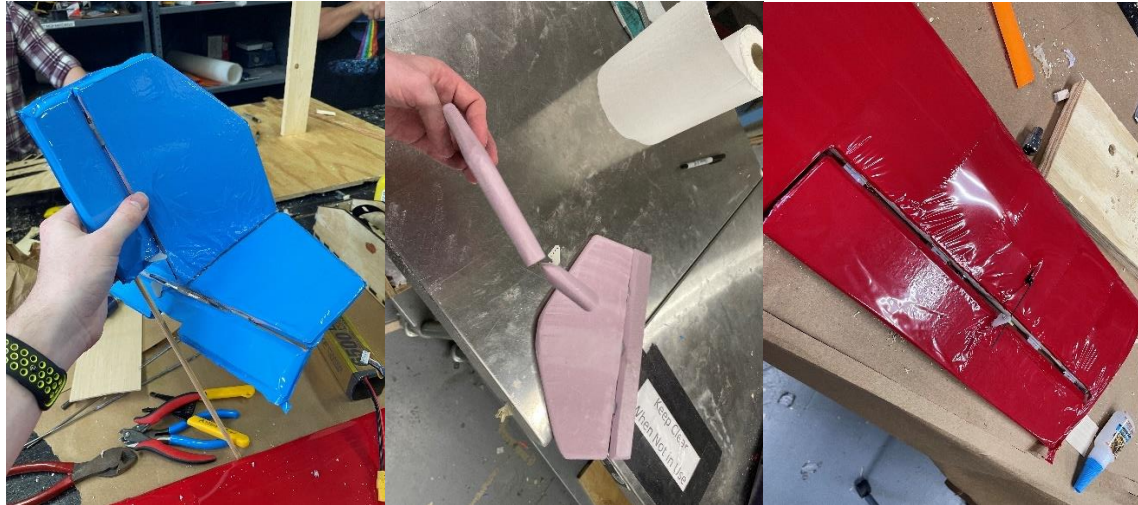
Figure 54: Photos of the final foam elevator, rudder and aileron control surfaces

4.3.5 Electronics

Electronics are some of the last components to be added to the aircraft with only a few exceptions. One exception is the two ailerons' servos, which are attached in between the carbon fiber wing spars using hot glue and the wire is fed through the wings to the wing tip closest to the fuselage. This is done before the Monokote is added in order to ensure as smooth of a coating over the wing as possible. Next the rudder and elevator servos are hot glued to the very back of the fuselage, so they are as close to the tail as possible, this way the push rods do not need to be extended. The battery is then temporarily placed into its box within the structure and the ESC is then attached to the top of the battery box using electrical tape. After the motor is mounted to the front plate on the fuselage, it is then wired to the ESC and the connections are covered with electrical tape to avoid the possibility of a short circuit. The connector from the ESC to the battery is then zip-tied to the inside wall of the fuselage using a hole that is drilled where it is to be secured. This same method is conducted to attach the fuse, and then the switch. The switch is zip-tied to the back of the fuselage to ensure it is far from the motor. The receiver is then attached using Velcro to the back of the aircraft and the extender on the tail spar so it is far from interference from other electronic components and will have a direct way to connect to the remote control from any angle. The servos and ESC are then wired to the receiver and the wires are taped down to ensure a neat and contained wiring setup in the fuselage.

5 Subsystem Tests Conducted

5.1 Propulsion System Tests

5.1.1 Motor Comparisons

Motor comparisons were performed via a thrust stand indoors (as shown in figure 49) at first to find the amount of static thrust produced initially, then once the raw thrust output data was gathered to compare the thrust levels produced a motor was selected.
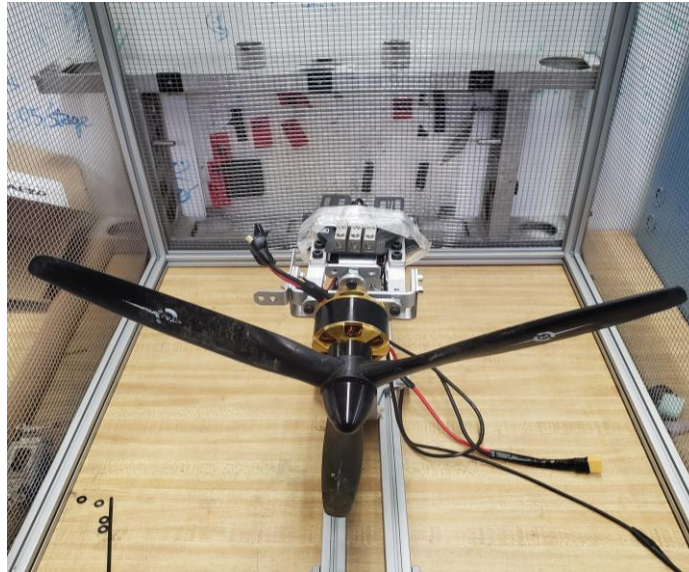

Figure 55: Thrust Stand Apparatus for Testing

To simplify the process, the motors were tested to only 50% thrust to consider continuous current safety limitations set by the ESC on the thrust stand, while also accounting for the power output on a smaller scale indoors. As specified earlier, the motor that could properly generate sufficient thrust while also having extra in reserve would allow for higher scoring in missions involving flight time and speed while also allowing for minimal takeoff distance for the chance to participate in the mission. Full power testing on the thrust stand was mainly completed outside while a test was conducted indoors to properly keep track of the RPM's and current draw that the motor produced. Due to insufficient size, other motors like the Turningy Park motor were excluded from testing since the anticipated output of thrust would not reach the required parameters. As a result, the only motors compared were the E-flite Power 32BL 770Kv and the Scorpion SII-4020-630Kv. These motors would be paired with a 15x7" tri-blade propeller[20] and a 16x8" dual-blade propeller[21] for testing to ascertain the ideal combination.

---

[20] https://www.masterairscrew.com/products/3-blade-15x7-propeller
[21] https://www.masterairscrew.com/products/k-series-16x8-propeller?_pos=3&_psq=16&_ss=e&_v=1.0
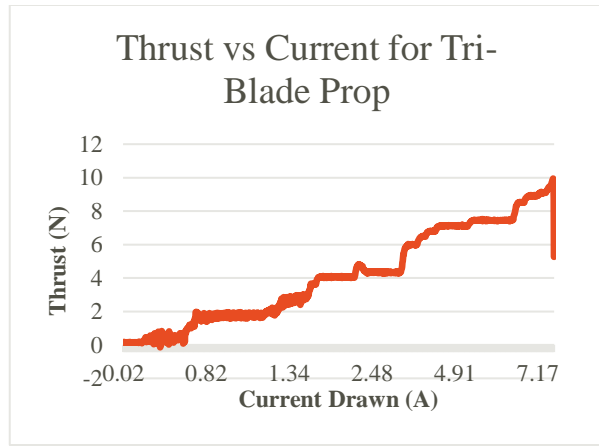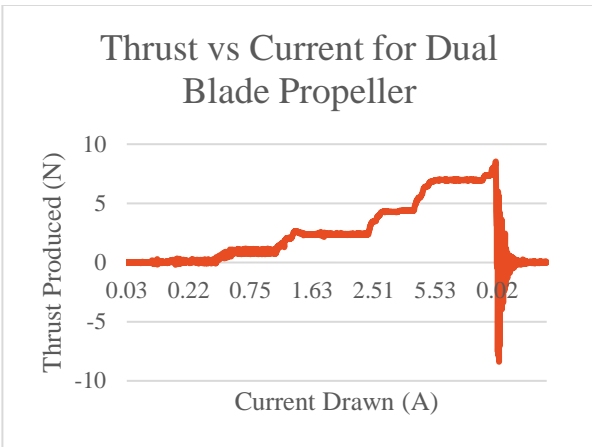
Figure 56: 16x8" Dual-Blade vs. 15x7" Tri-Blade Propellor Performance on E-flite Power 32BL 770Kv Motor
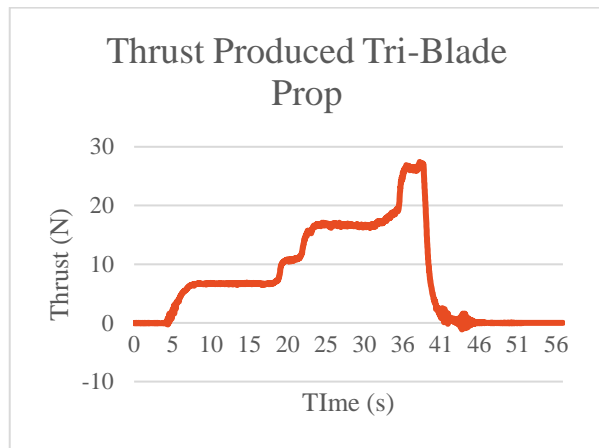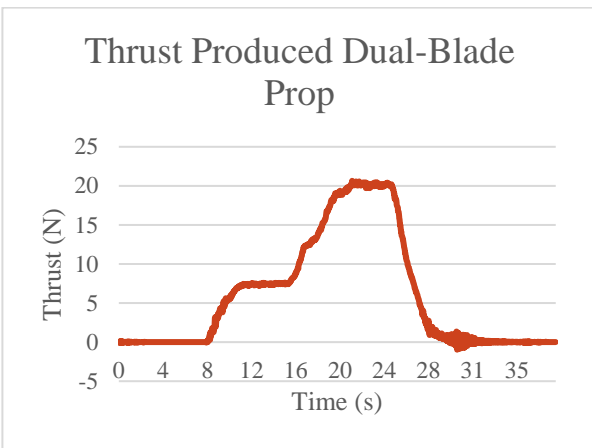
Figure 57:16x8" Dual-Blade vs. 15x7" Tri-Blade Propellor Performance on Scorpion SII-4020-630Kv Motor

From the results of the figures above the motor that was determined to have more thrust is the Scorpion motor, while the propeller that generated the most thrust is the 15x7" tri-blade propeller overall. The cut-offs in thrust on the graph represent the control input of throttle being dropped to 0% as the motor begins to spin at less RPM than before. The tri-blade propeller generates more thrust as indicated by assumptions made in the propulsion analysis section but testing and selection of the dual-blade propeller continued due to higher efficiency. In the event more thrust is needed, the tri-blade propeller remained a viable option if the weather or other factors were present.
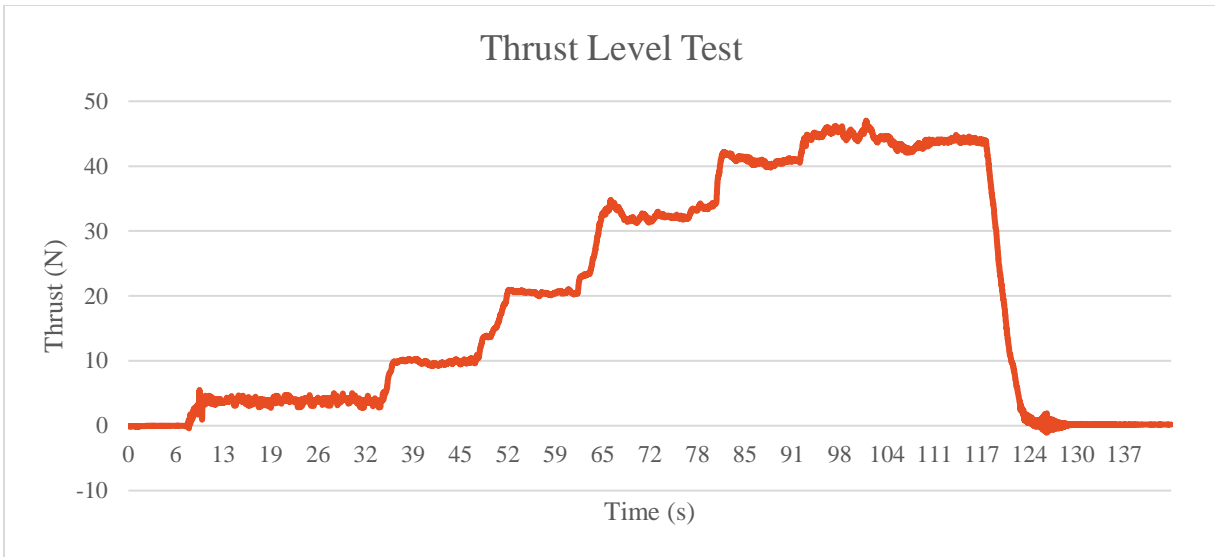
Figure 58: Dual Blade Propellor Thrust on Scorpion SII-4020-630Kv Motor

After selection between the two motors with sizing and Kv's compatible for the plane concluded, a full thrust spectrum needed to be developed to properly understand how much thrust could be produced. Each of the leveled off areas represent the six throttle tick markers on the controller, which can be used to scale certain throttle inputs and associate the throttle levels with a level of thrust. This test ended up garnering ~45 N of thrust for 100% throttle, ~40 N for 83.3% throttle, ~32 N for 66.7% throttle, ~20 N for 50% throttle, ~10 N for 33.3% throttle, and ~4 N for 16.7% throttle. With consideration for the test being outdoors and having more wind to work with, the numbers were different compared to the indoors test which is more confined and has less area for air to flow. The RPM's, however, should remain consistent as a benchmark for the amp draw so motor endurance can be calculated.

5.1.2 Motor Endurance

Figure 59: Maximum Thrust Endurance Test on Scorpion SII-4020-630Kv Motor

A maximum thrust endurance test was conducted in order to see how long the plane could be flown at max speed if necessary. The test was conducted on the same day as the thrust level test with a secondary charged battery to properly ascertain how long the thrust could be produced. It was determined that the max throttle could be used for a total of about 170 s until the thrust tapers off gradually.
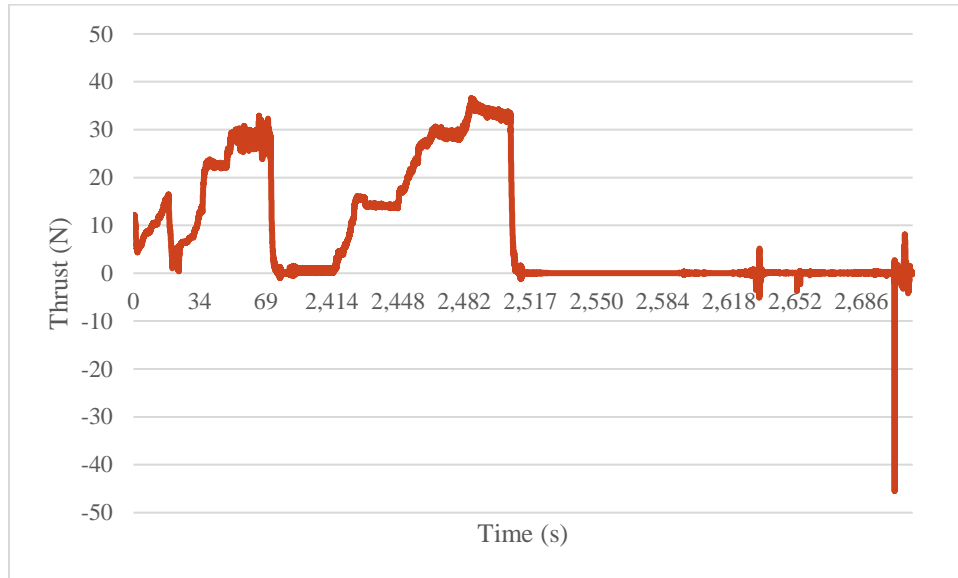
Figure 60: Endurance Thrust for Power Draw on Scorpion SII-4020-630Kv Motor

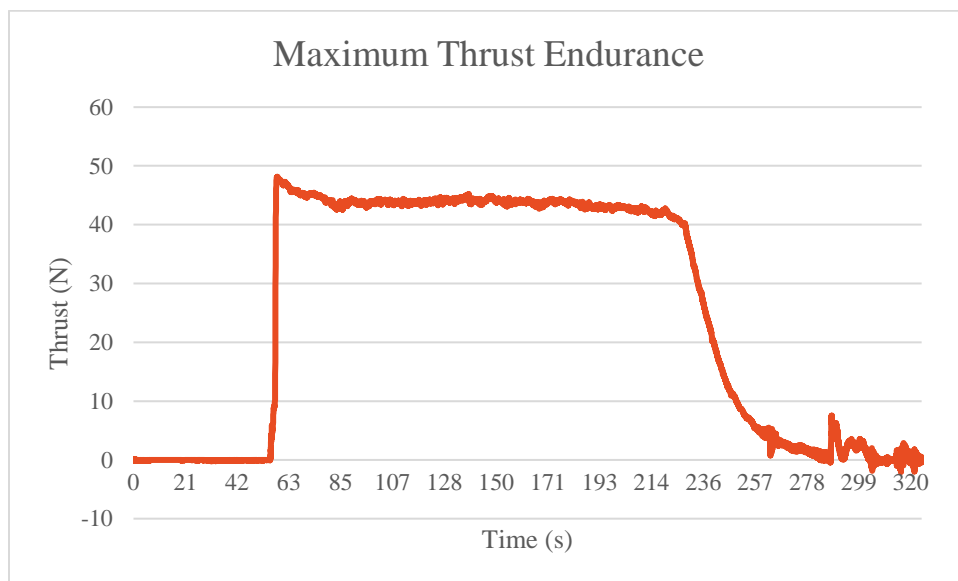Further indoor testing provided the current draw at 50%, 83.3%, and 100% throttle to find the current draw at each of the levels. The corresponding current draws were 12 A, 39 A, and 52 A respectively. Using the capacity of the battery (6500 mAh) the amount of time that the motor can be run at is as follows for each level: 32.5 mins, 10 mins, and 7.5 mins. These serve as estimates, but the maximum thrust endurance test determines that at 100% throttle it would only last about 2.83 mins, so more testing will be needed to confirm the calculations. There is also a spike in the time measurement, which could indicate error in the software that skewed some measurements.

5.1.3 Conclusions Based on Thrust Required

With the consideration of the results from the thrust required curve, the motor output is suitable for achieving the high amounts of speed necessary to accomplish our goals. The propeller choice didn't matter as much as originally anticipated considering that both propellers were able to reach the benchmark needed, so both remained an option that could be picked based on the conditions for flight. However, due to ground clearance issues the propeller that that was used for future testing ended up being the tri-blade propeller.

5.2 Aerodynamics Tests

5.2.1 Airfoil Tests

To compare the theoretical airfoil data generated by the simulation software, wind tunnel testing was conducted for both the NACA 4412/4416 (interpolated) and 4415 designs. The test

was conducted through 3D printing each foil to half scale, thus requiring the speeds of the wind tunnel to be twice as fast as the speed it was designed to receive data for the same Reynold's number. Starting at 60 mph, the normal and axial force, along with the pitching moment on the airfoil were recorded at a range of AOA data points ranging from -2 to 15 deg. The same was done at 70, 80, 90, and 100 mph for each foil. This data was used to compute lift, drag, and quarter-chord moment at each data stamp through the implementing the following formulas into Excel for each data point:

$$L = N\cos(\alpha) - A\sin(\alpha)$$

$$D = N\sin(\alpha) + A\cos(\alpha)$$

$$M_{c/4} = M - (c * N)$$

Their coefficients were determined using the following formulas:

$$C_L = \frac{L}{\frac{1}{2}\rho v_\infty^2 S}$$

$$C_D = \frac{D}{\frac{1}{2}\rho v_\infty^2 S}$$

$$C_{M_{\frac{c}{4}}} = \frac{M_{\frac{c}{4}}}{\frac{1}{2}\rho v_\infty^2 S c}$$

Once these calculations were implemented into Excel, the lift-to-drag ratio was computed by dividing the lift coefficients by their corresponding drag coefficients. The ratio results were plotted to yield the following graphs:
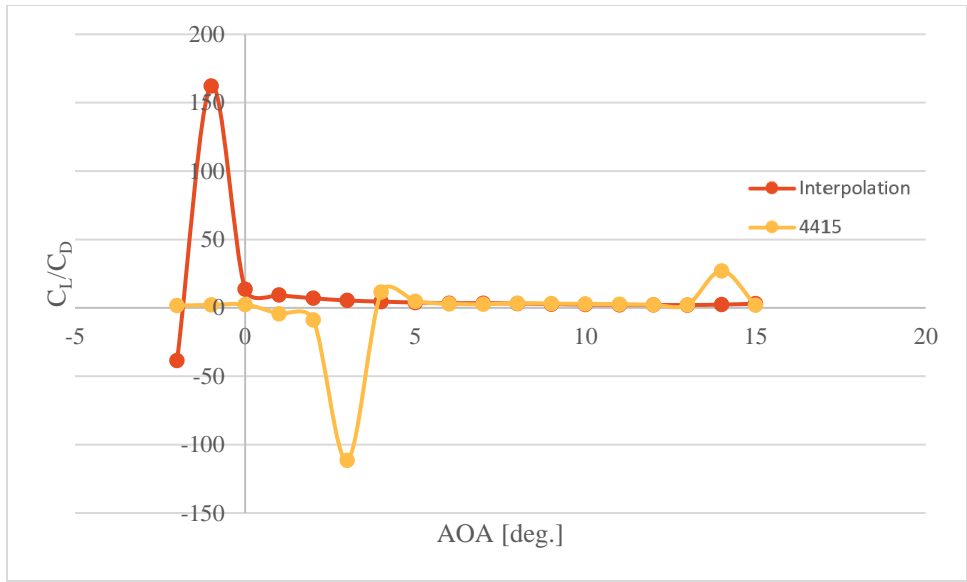
Figure 61: Lift-to-drag versus AOA at 60 mph.
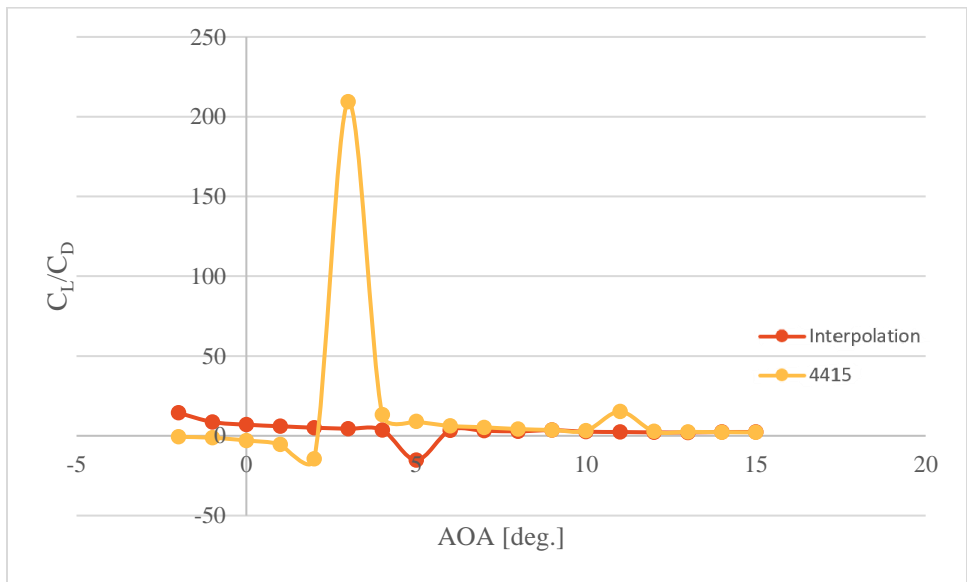
Figure 62: Lift-to-drag versus AOA at 70 mph.
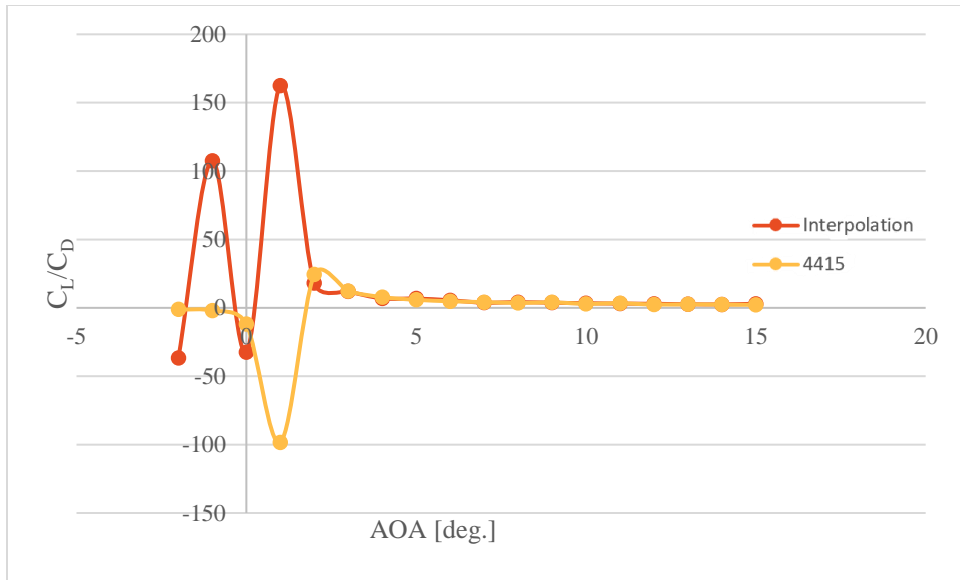
Figure 63: Lift-to-drag versus AOA at 80 mph.
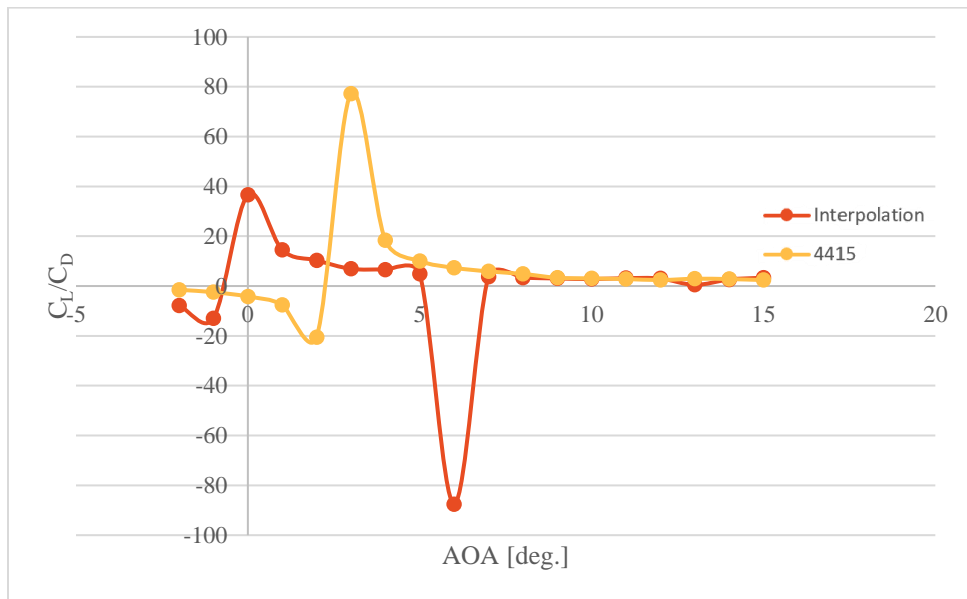
Figure 64: Lift-to-drag versus AOA at 90 mph.

.
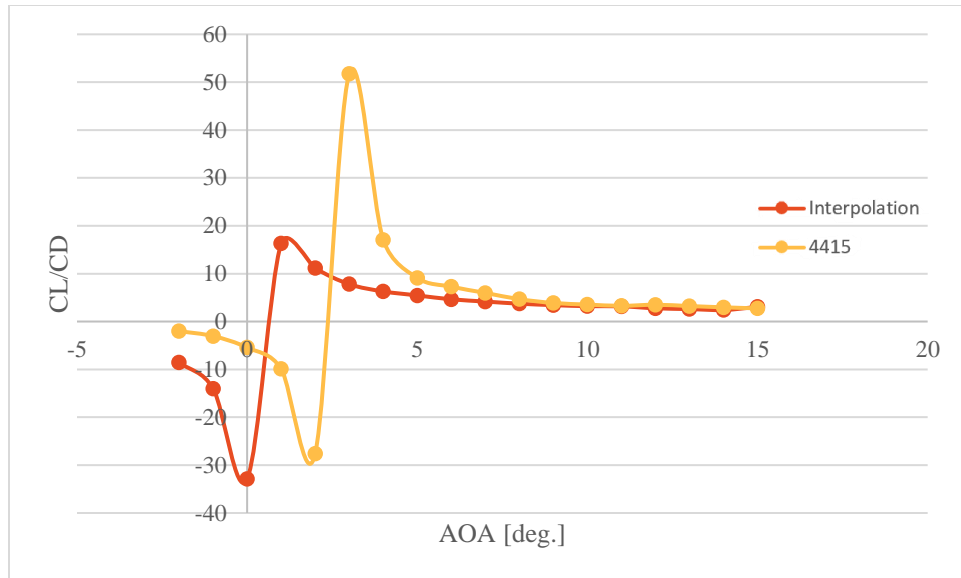
Figure 65: Lift-to-drag versus AOA at 100 mph.

It is important to note that the sporadic behavior of the plots is due to inconsistencies found in the measuring equipment utilized, as well as the method that was used to record the data. The measurements were taken manually, while the readings on the measurement device (shown on the bottom right of Figure 66) continuously fluctuated:

Figure 66: Wind tunnel testing apparatus.

According to the plotted data, the 4415 seemed to have a greater overall lift-drag ratio than the interpolated foil at a majority of AOA's, specifically at 3 deg. and at mid to high speed. Hence, knowing the team had intended to implement more speed into the design, it was decided to use the

NACA 4415 at an AOA of 3 deg. For more wind tunnel data, including quarter-chord moment data, please reference Appendix B – Excess Aerodynamic Data.

5.2.2 Stability Tests

Before real world testing began a static stability analysis was conducted. Using the neutral point found in the aerodynamic analysis the neutral point sits 2.186 inches back from the center of mass. This gives a static margin of 27% which suggests that the aircraft should be stable. This is corroborated by the negative slope of the moment coefficient versus angle of attack graph also found in the aerodynamic analysis section. Based off of these analyses it was determined that our design was statically stable and real-world tests began to verify this.

A glide test was conducted with a full-scale model of the aircraft constructed with the same materials to simulate and accurate weight estimate comparable to the final aircraft model. A total of five individuals were used to conduct the test: one to launch the model, and two sets of two individuals to hold blankets that would safely catch the model after each test. Four tests were conducted: two on level ground at different distances, one on slightly elevated ground, and a final one launching the model off a balcony at a significant height off the ground. The level ground tests showed promise for the next two, as the model glided quite well, and sank to the ground without pitching any one way. The third test showed similar results, with some slight pitching down towards the end due to lack of thrust. The final test the aircraft glided quite well until it lost thrust and began to pitch down toward the ground.

These results indicate that the aircraft is ever so slightly front heavy, which was corrected incrementally with stickable counterweights on the rear boom until the center of gravity was corrected. At the end of the flight tests, it was confirmed that the neutral point sat just over 10 inches from the front of the aircraft as anticipated by the digital model.

The dynamic stability of the aircraft was also challenging to test during this glide, as the models created anticipate that the plane should be perfectly balanced. With the elevator control of the aircraft active, the plot below in Figure 67: How angle of attack recovers with elevator control of the aircraft shows the dynamic stability of the aircraft over the course of a few seconds in flight. It can be seen that it should be able to correct its trajectory quickly due to the small size and weight of the aircraft. It may also have not followed this model as accurately in the tests as the speed of the glide was significantly less than the modeled airspeed of the plane, causing a slower recovery time.

Static stability tests were also conducted when the landing gear was added to find how well it would hold itself up. It was found that it has a static safety factor of 1.2 which is within the expected range of values, as for an RC aircraft, the static stability factor is expected to be over 1 and under 1.5.
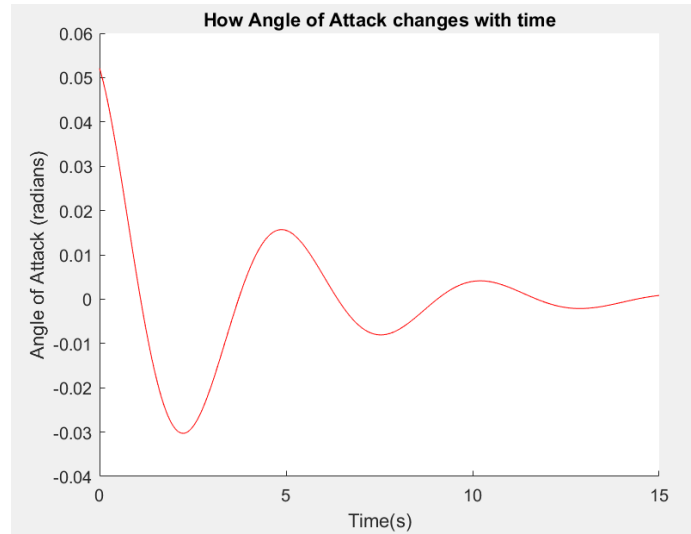
Figure 67: How angle of attack recovers with elevator control of the aircraft

5.3 Controls Tests

5.3.1 Electronic Assessments

A major test that was conducted to ensure the functionality of the electronic systems was setting up the circuit fully outside the plane. This test was completed each time a new part was added. During these tests the motor, without the propellor, would be clamped securely down to ensure lab safety, then the battery would be incorporated into the system. Then using the remote control, tested the responses of all the electronic components. This test was first conducted with just the battery, ESC, receiver, and motor to ensure the remote control would bind effectively and then the motor could be controlled by the correct stick on the remote. This test was then repeated whenever a number of servos were added to the system, ensuring they had full range of motion. It was also repeated when a new item, such as the switch or fuse, was soldered into the circuit to make certain the wiring connections were not broken. All these tests proved that the electronics would function as expected when it was integrated into the plane. The only minor adjustments that were necessary were programming the remote control to ensure the servos rotated far enough and would move the control surfaces in the right directions. Below in Figure 68, an example of an electronics test can be seen, assessing the functionality of a servo setup with ailerons, elevator, rudder, and flaps.

Figure 68: Example of an electronics controls test

5.3.2 Control Surface Testing

Similar to the electronics testing, control surface testing was conducted by attaching the control surfaces to the plane and testing their range of motion and stability. These tests were mostly done to ensure that the surfaces have the correct range of motion, and that the surfaces are well fitted to the wings or tail. They showed that the elevator, with every iteration, always had a 45-degree range of motion in either direction from neutral. The ailerons have a slightly lower range of motion but still had 40 degrees of movement in every iteration. Below in Figure 69 is an early prototype aileron control surface test. For this prototype the controls were made of wood. All control surface tests were conducted in this manner.

Figure 69: Example of a control surface functionality test

5.4   Structural Tests

5.4.1   Full Wing Failure Load Test

While the strength of the wing had been predicted in SolidWorks in Section 3.5.3.2, a more accurate test to failure would allow for a better maximum mission performance prediction and would verify our analytical solutions. While the limit conditions are different from the FEA analysis, the test setup in Figure 70 is a more accurate depiction of the Ground Mission.
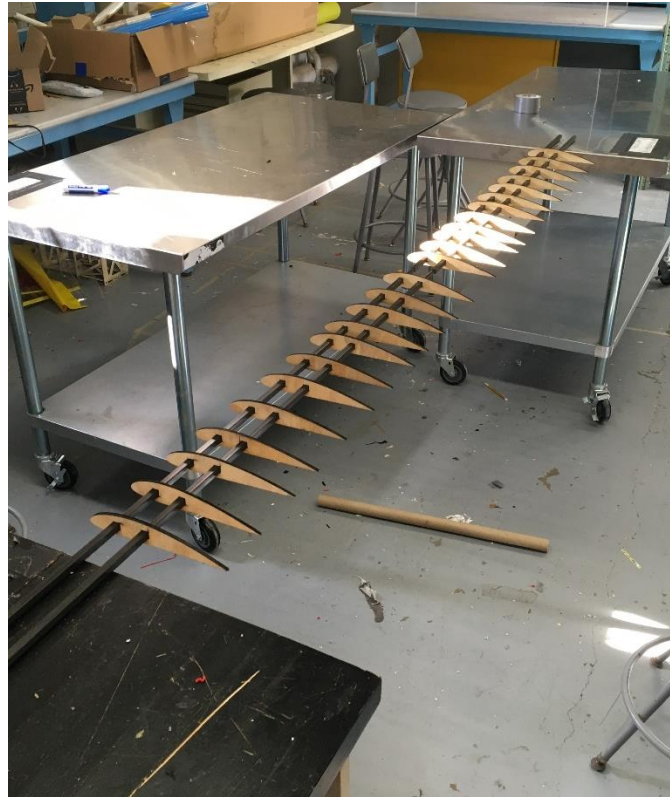
Figure 70: Wing Failure Load Test Setup

As FEA found that the wing could hold 30 lbs, testing was started at 20 pounds. While the wing did hold, its deflection was 4 in. The next increment available with the weights used was 27 lbs. However, this cause failure almost immediately. While the wing could still support twice the predicted weight of the plane, this was much lower than the FEA analysis.

5.4.2   Carbon Fiber Rod Cantilever Beam Test

Because of the low results of the wing loading test (Section 5.4.1), the assumptions for the analysis had to be rethought. Therefore, the purpose of this test was to verify the manufacturer's strength data for the round carbon fiber rods and find the strength and Young's modulus for the square carbon fiber rods. Mounts for the two types of carbon fiber rods were machined as described in Section 4.2. The assembly was then mounted in a vise to form a cantilever beam, shown in Figure 71.

Figure 71: Cantilever Beam Test Setup

Weights were then applied to the end in roughly 50-gram increments, with the total deflection measured using a ruler. The following equation was used to calculate Young's modulus:

$$\Delta x = \frac{FL^3}{3EI}$$

Length and area moment are known from the form of the carbon fiber rod being tested. The first and most important beam to test was the square one, due to the lack of manufacturer's data. Measuring 10 mm square, with an interior 8.5 mm circle, its total area moment I is equal to 577 mm^4. The length of rod used for the cantilever beam test was 44 inches. Data collected for deflection with various weights applied is shown in Figure 72. A highly linear relation develops, which can be gathered from the deflection equation. To solve for Young's Modulus, the deflection equation can be written as the equation below.

$$E = \frac{FL^3}{3I\Delta x}$$
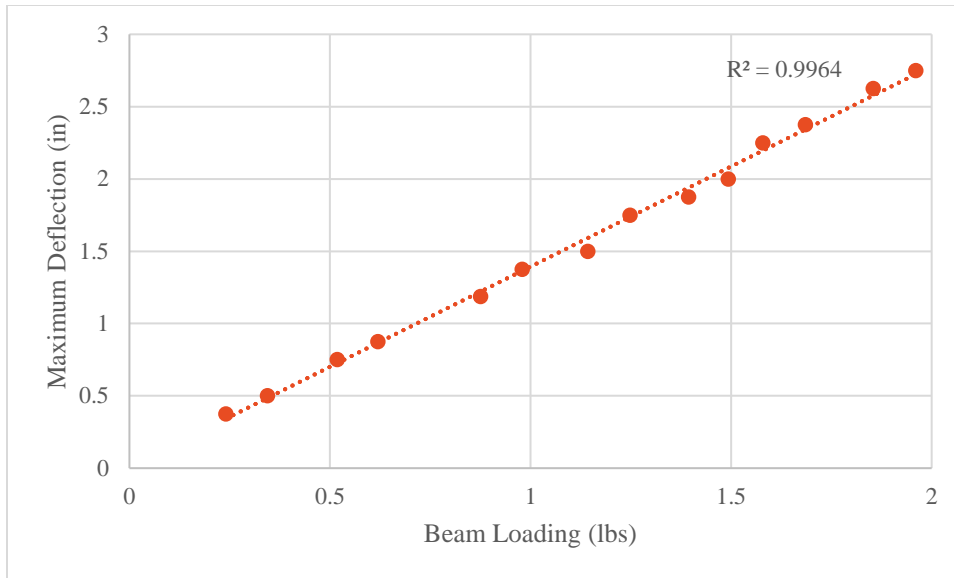
Figure 72: Square Carbon Fiber Rod Cantilever Beam Deflection vs. Loading

With deflection and load data, the estimated Young's Modulus for each data point was calculated and the average taken. Through this testing, it was found that the Young's Modulus was approximately 100,000 MPa. This is a definitive reduction in the published values for the round carbon fiber rods, and what was used for the FEA Analysis in Section 3.5.3. However, for thoroughness, the round carbon fiber rods were tested as well.

As shown in Figure 73, the round rods also follow a linear relationship. While less data points were taken due to the expected outcome of this test being only a verification of the manufacturer's data, the trend still becomes clear. Following the same procedure as the square rods, an average Young's Modulus of 112,000 MPa is found, with an I of 137.4 mm^4 and length L of .55 meters. While the assumption that both rods would have the same performance is mostly correct, this decrease in actual versus theoretical Young's Modulus appears to be the primary cause for the reduction in overall load capacity.
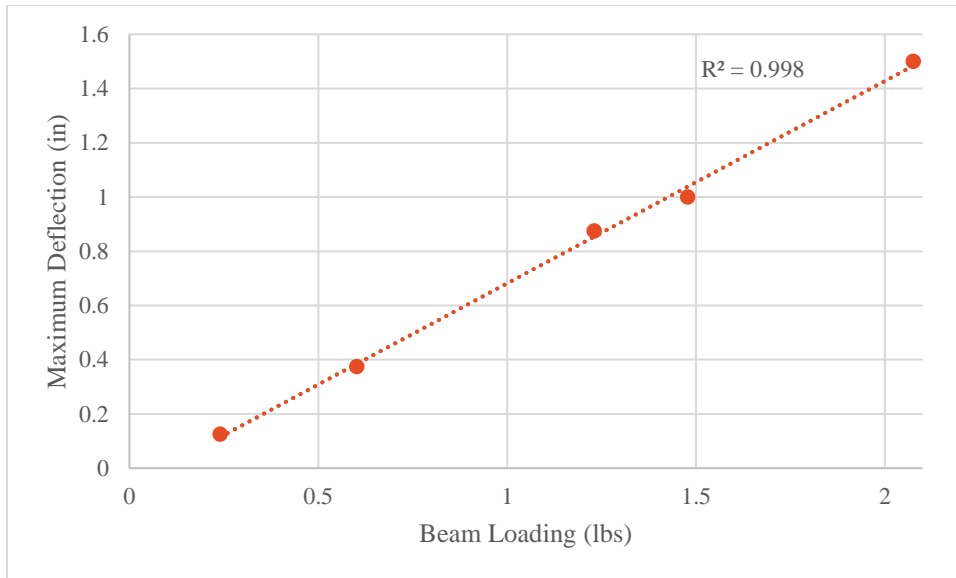
Figure 73: Round Carbon Fiber Rod Cantilever Beam Deflection vs. Loading

Finally, an interesting observation made was the failure mode of each rod. While the definitive ultimate bending stress was not measured, a load of 2.5 kg was applied for a qualitative analysis. While the round carbon fiber rod snapped at its securing point (no picture available), the square carbon fiber rod delaminated (Figure 74).

Figure 74: Square Carbon Fiber Rod Failure

6 Final Design Parameters

6.1 Electronic System Design

The electronics used in the final iteration of the aircraft is discussed previously in the preliminary design section. This includes using the DXF 14.8V 4S 6500mAh 100C LiPo battery as the power source for all the electrical components on the aircraft. The motor that was decided on is the Scorpion SII-4020-630kv motor to maximize the power to weight ratio and obtain higher speeds in missions two and three. The E-flite 100-amp pro switch-mode BEC brushless ESC was selected for its 100-amp rating which is above the amp draw of the motor during normal operation. This always ensures a significant margin of safety. It is also safe guarded by both the heavy-duty toggle switch 20/15A 125/227V and the 100-amp fuse in between the battery and ESC. The servos selected were the Hitec HS-425BB pro ball bearing servos in order to ensure enough torque was applied to the control surfaces in flight. The receiver selected was the LICHFIT fast speed RC receiver for Spektrum AR8000 8CH for its eight channels of control and ease of connectivity with the remote control. Lastly the remote control chosen was the Spektrum DX6i remote control due to its effective controls and ease of programming. The final circuit diagram for this aircraft can be seen below in Figure 75.
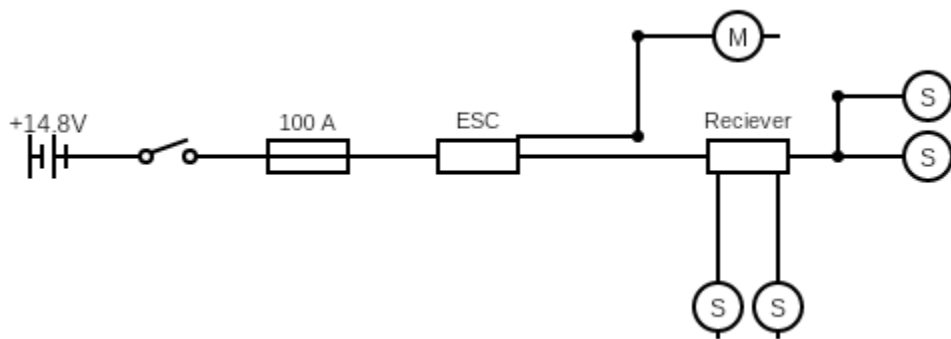
Figure 75: Plane Circuit Diagram

6.2 Aerodynamic and Control Surface Design

Over the course of the design process, while the material and orientation switched occasionally, the overall design for the ailerons, elevator and rudder stayed relatively constant. This is because the surface area percentages remained the same throughout the time working on the aircraft. This 15 to 20 percent surface area of the surface to wing or tail ratio should allow for effective control of the aircraft at high speeds but also ensure there will be enough control of the aircraft as it taxis and accelerates to flight speed. The main changes made throughout the design process were to change the material of the surfaces from wood to a more reliable foam. The only other major change was the tail, which was scaled up to nearly double the initial size due to an underestimation of the impact the tail had to provide. Over the iterations, the control surfaces were optimized to be smoother and better fitted to the aircraft, more specifically constructed to fit at

perfect angles, and had a better hinge mechanism to ensure smooth tuning with minimal gap between the control surface and wing or tail. Overall, the control surfaces have improved greatly from the first iteration while the design and construction of them remained relatively constant with respect to the rest of the aircraft.

6.3 Structural Design

6.3.1 Wings

Table 8: Wing Dimensions

Chord	8 in
Span	33 in
Area	264 in^2
Foil	4415
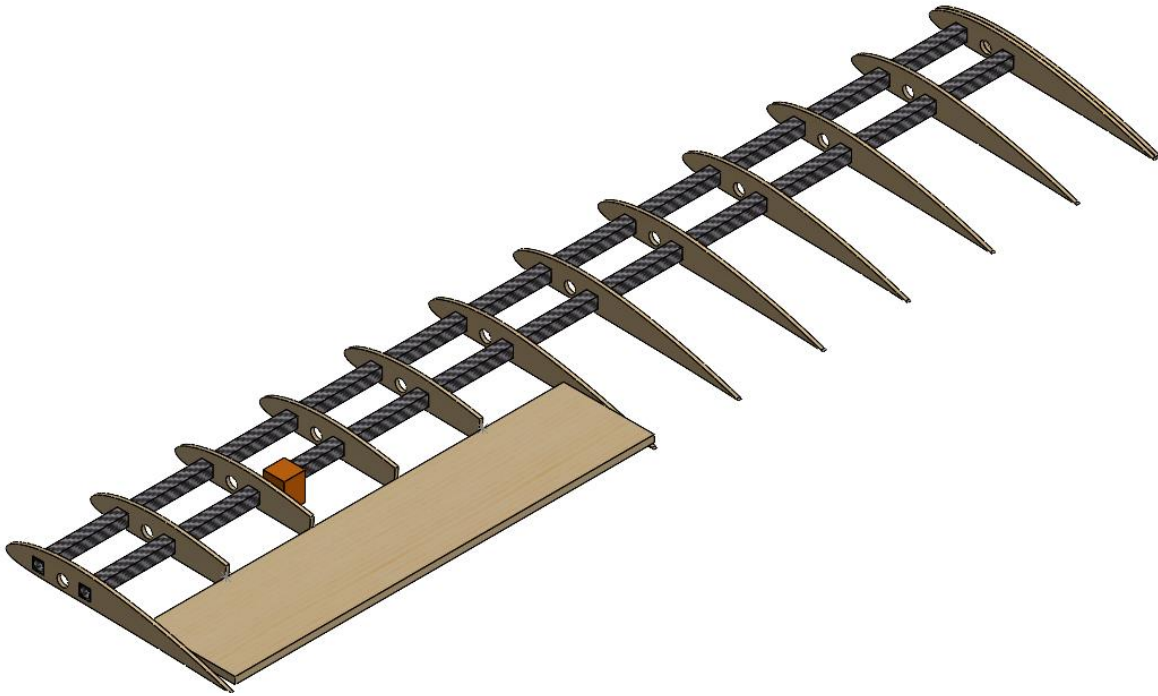
Figure 76: Left Wing Structure

Table 8: Wing Dimensions summarizes the dimensions of each wing. The wing design remained relatively unchanged during the entire project. The only major difference between the first and last set of wings that was constructed was the addition of alerion. The wings were constructed use two main sections, a left and right wing.

The main rigidity of our wings was provided by two 0.394 inch by 0.394-inch square carbon fiber rod that ran the length of each wing. Each rod was cut to a length of 33 inches to conform with the dimensions of our box. Each wing was constructed using 14 ribs pictured in. In the wing there were two types of ribs: full ribs and cut ribs. The cut ribs were implemented in our later designs to allow for the alerion to be placed in each wing. The full ribs were 8 inches long,

while the cut ribs were only 4.77 inches long. All ribs were laser cut from ¼ inch play wood. Full ribs are pictured in Figure 77 and cut ribs are pictured in Figure 78.

Figure 77: Full Rib Side Profile

Figure 78: Cut Rib Side Profile

Each rib featured 3 holes; two 0.394 by 0.394-inch square holes to allow the ribs to be slid on and epoxied to the two carbon fiber rods that ran the length of each wing and one 0.394-inch diameter round hole to allow for wire to be run through the wings so electronics could receive power and signals. The square holes are 1.65 inches apart, which matches the row of holes that run along the top of the airframe side pieces that can be seen Figure 77. The circular hole is centered in th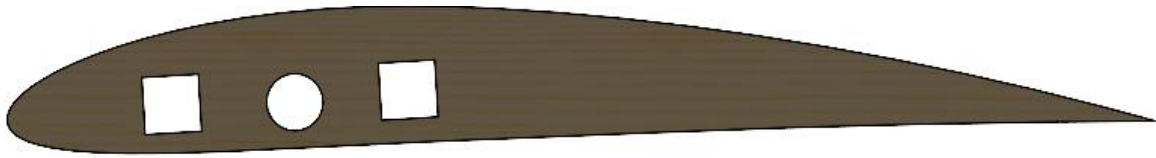e space between the square holes, 0.825 inches between the square holes. The holes for the carbon fiber rods were precisely cut with an offset in height to put the wings at a 3.3 angle of attack when the fuselage was level with the ground. On each edge of our wings, 2 ribs were placed against each other to provide additional structural support to both ends. One side held the wings of the aircraft while the other provided support for an antenna attachment.

6.3.2 Wing Mounting Mechanism Stand

The mounting mechanism for the wings was designed to be simple, to ensure that aircraft assembly time requirements were met. The final inside rib of each wing contained a ¼ in. screw embedded within it, with a length of roughly 2 in. Two small cylindrical carbon fiber rods meant to fit within the rectangular carbon fiber rods were loosely fitted to connect the wing rods together, with the mounting screws sliding into the mounting holes that were located between them on each side. Once slid through, a washed and hex nut were used to bolt the wings tightly in place.

6.3.3 Airframe

Table 9 Airframe Dimensions

Length	22.25 in
Width	3.5 in
Height	4.6 in
Payload area	6 in x 3 in x 3 in
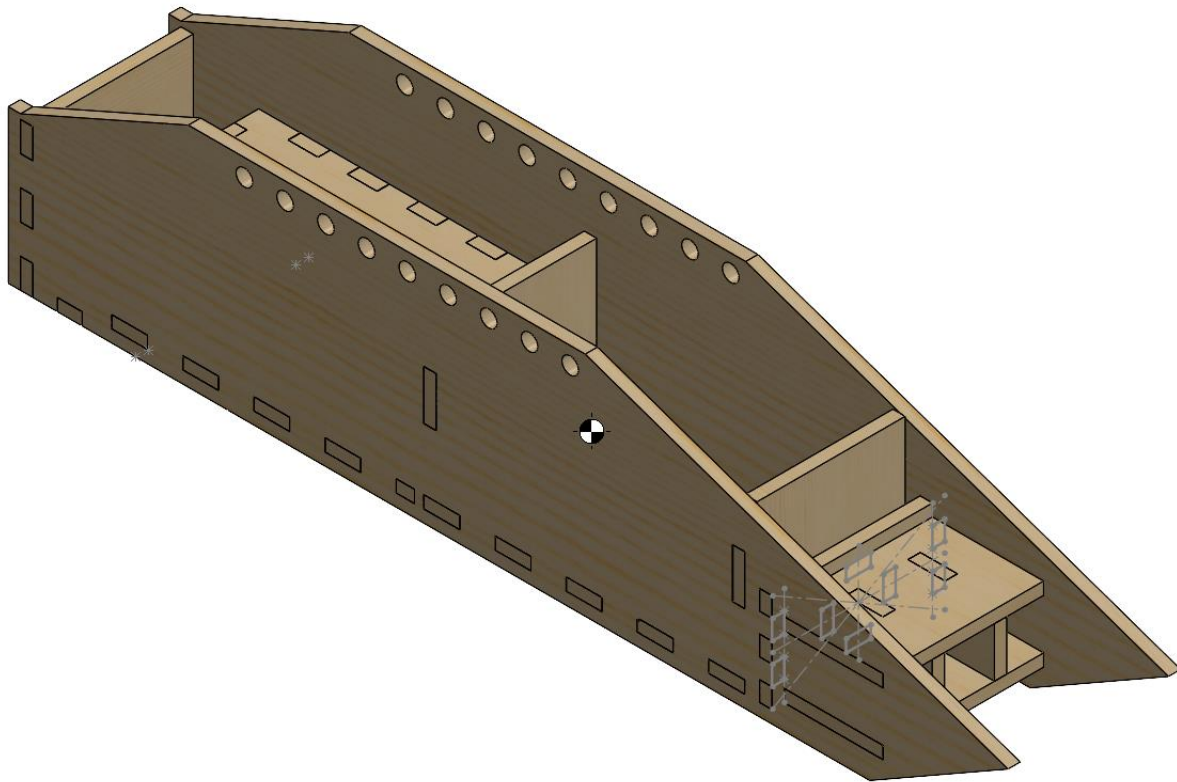
Figure 79: Fuselage

Table 9 Airframe Dimensions summarizes the dimensions of the airframe pictured in Figure 79. The Airframe is constructed using the pieces described in section 4.4.2. Each piece was laser cut is the WPI Maker Space from high quality 1/4-inch plywood. Each sub assembly is slotted into the air frame side pieces. See Figure 79. Each subassembly has tabs at each connection point. To secure the connection points a dot of wood glue is added to each tab then the pieces are slotted together. The airframe sides are then compressed together to ensure they are as close to a square fuselage as the material allows. Due to the design of the Fuselage each sub assembly is glued at the same time to each side of the airframe.

The design of the airframe remained relatively similar through all iteration of its design. In the first iteration of the airframe, which was constructed to do a glide test to test the wing's performance, the payload box was not installed, and each piece was not notch yet. Each piece slid into a hole in the airframe side piece. This presented a challenge during construction and all later iteration included the hole and tab system described in section 4.4.2. The first iteration of the airframe side pieces also featured cutouts to reduce weight. To achieve this ½ inch of material was left around each side of every hole or the edge of the airframe side to provide stability but all other material was removed. See Figure 80 for reference.

Figure 80: First Iteration of Airframe Side
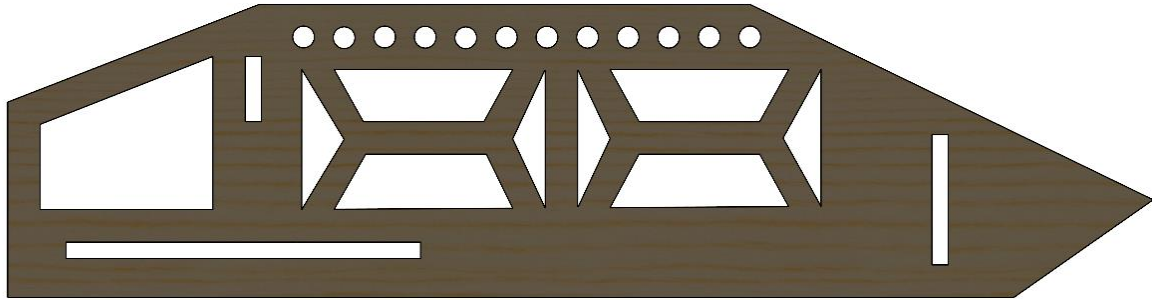
The second iteration included a newly designed payload box and improved manufacturability. The subassemblies were constructed and fixed to the airframe side using hot glue to reduce manufacturing time and decrease repair time. The cut-out sections that make the first iteration distinctive were removed due to decreasing the overall strength of the fuselage for a minimal improvement to weight of the aircraft. During a test the plane pitched downward crashing nose first into the ground and the front part of the airframe side was broken beyond repair leading to the cut idea being dropped entirely. Additionally, the second iteration is where the tab and hole system for attaching the subassemblies was implemented to great effect. Manufacturing became far faster and easier as you did not have to worry about spacing the side exactly 3.5 inches apart the subassembly did that themselves. One extra support beam can be seen just below and in front of the front most round hole in Figure 80. This was removed in future iterations as extra stability was not needed because the subassemblies provided enough lateral strength. See Figure 81 for reference.
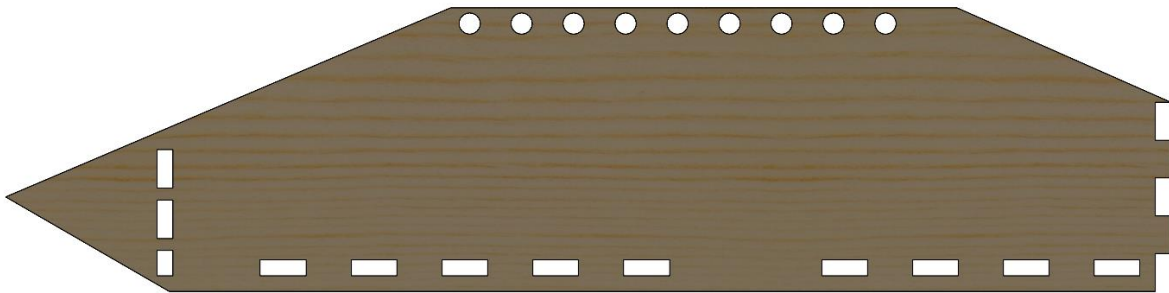
Figure 81: Second Iteration of Airframe Side

The third and final iteration of the airframe included all lessons learned from previous airframe designs. New stronger and higher quality plywood was purchased and used in the construction of the final fuselage. Unfortunately, the second interatom was made with lesser quality plywood and hot glue and the motor plate was ripped off the front of the plane during testing as there was no material holding it in from the front. Airframe side was slightly redesigned to include ¼ inch of plywood in front of the motor plate to prevent failure due to adhesives again. Also, the final design used wood glue and epoxy as its only adhesives, not hot glue. Due to some issue with installing the motor onto the plane, the battery box was moved slightly backwards to

allow for easier access to the back of the motor plate. Tabs were added to each side of the payload box to increase its stiffness. Additionally, the tail attachment was redesigned to be further integrated into the airframe sides between the second and third iteration as during a glide testing the tail box became loose from damage that occurred during a crash. The top and bottom piece of the tail box was extended to span the entire width of the fuselage and to slot into slot cut out of the airframe, after this change no problem with the strength of the tail attachment has been observed. Due to a struggle to attach the landing gear in a structurally sound way a small plate was implemented just behind the motor plate and before the battery box to allow for a bolt system to be used in attaching the landing gear. The airframe side was slightly lengthened between the second and third iteration to allow the addition of the landing gear plate, additional material in front of the motor plate, and moving the battery box back. See Figure 82 for reference.
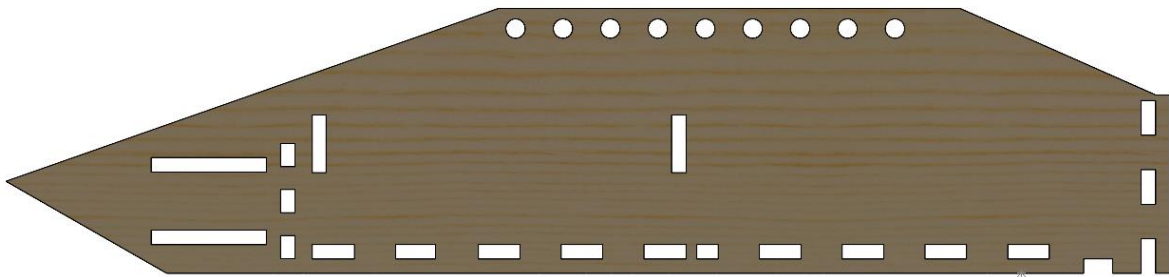
Figure 82: Final Iteration of Airframe Side

6.3.4 Antenna Mount

As shown in Section 3.5.3.3, no changes were necessary in the design of the antenna mount. Therefore, after final assembly as described in Section 4.3.3, the antenna mount was available for attachment to the plane. To accompany the mount, three PVC tubes were created (Table 10), approximately. While a flight mission was not conducted, the antenna mount was able to be successfully installed into the final wing (Figure 83).

Table 10: PVC Tube Data

Length (above mount)	Weight (grams)
3 inches	46
6 inches	67
9.5 inches	99

Figure 83: Antenna Mount on Wing

6.3.5 Ground Test Stand

The ground test stands were constructed using scrap wood. The ground test stand is made up of two free standing structures that are designed to easily slot into the outside end of each wing. The base of each side of the ground test structure was made from ¾ inch plywood hand cut into a 12 inch by 18-inch rectangle. Fastened to the base are 2 structural beams constructed out of standard 2 inch by 4-inch pine lumber. The first piece of lumber is 18 inches tall and straight up and down. It is secured to the base by screws from the bottom. The second piece of lumber is 11.5 inches tall and placed at an angle to support the vertical beam. The support beam is screwed into the base from below and then screwed into the vertical beam from the side. The mechanism contains two screws fixed perpendicularly into the wood, spaced apart to match the spacing of the carbon fiber rods running through the wings. This ensures screws would slot into the holes of the

square carbon fiber rods to make sure the load is distributed through the rods. See Figure 84 for reference.
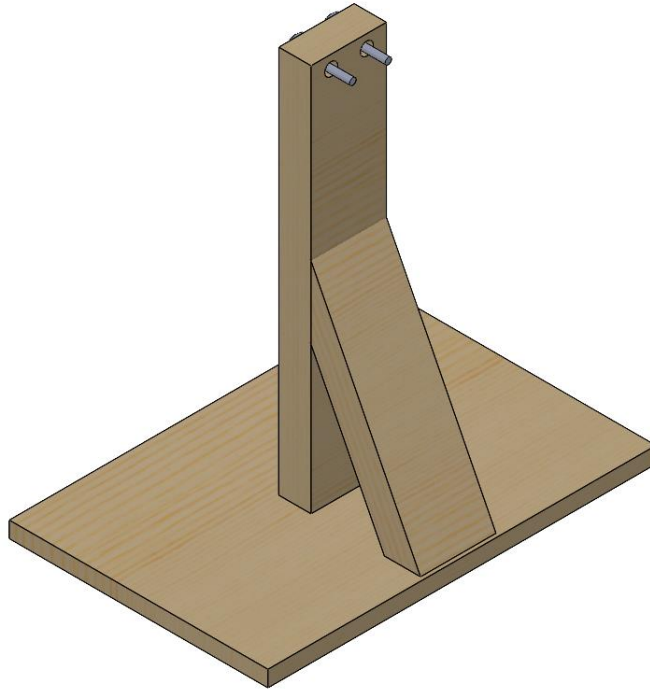

Figure 84: Ground Test Stand

7 Performance Results

7.1 Flight Readiness Checklist

This checklist has been heavily influenced by the Central Massachusetts R/C Modelers 2019 Winter Down-Time Aircraft Checklist and it would be highly recommended to have a printed copy of this checklist at all times of the pre-flight process as another reference. This checklist can be seen in Appendix A – Flight Readiness Checklist [3]**.** The following steps should be completed before any flight tests are attempted:

Before leaving to go to flight location:

- Look over the major structural components to make certain the foam, carbon fiber, plywood and other parts are intact and do not have any cracks.
- Set up the plane for that day's flight configuration.
- Lift the plane to ensure the center of gravity is located in the expected position and then mark this with a pencil, pen or sharpie at the center of the fuselage and on the wing tips so it is clear to whoever is flying it.
- Once over the control surfaces to ensure they are level with the airfoils they are impacting when power is added to the system (the motor will not be plugged in during this test due to safety precautions)
- Check servos to ensure the set screw is tight and that each servo has a free range of motion.
- Ensure that the hinges for the control surfaces are rotating freely and the control horns are securely attached to each surface.
- Unplug the battery and attach the motor and seal the connections with electrical tape to avoid any short circuits.
- Check the Monokote on the fuselage, wing and tail and any other coverings to make sure it is smooth and has minimal wrinkles or holes that would impact performance.
- Landing gear should also be checked to ensure the wheels are installed securely to their brackets.
- Pack all necessary wrenches for wing attachments, extra batteries and chargers, Allen keys for control surfaces and motor mount, screwdriver for landing gear, electrical tape, and duct tape along with any other tools needed to assemble and repair the plane on location.

At the flight location:

- The wings should be added onto the plane and attached snuggly with the bolt and wrench and the aileron wires can then be attached into the split servo wiring port which should already be connected to the receiver.
- The landing gear, tail and any other unconnected components should now be added to the aircraft.
- If the tail was not already pre-connected, ensure the push rods are connected properly between the tail to the servos at the back of the fuselage.

- The propellor should also be attached with the compression washer if it is not already and it should be checked multiple times to make sure it is tightly attached.
- If this is a mission that requires an addition of either a payload weight, antenna, or counterweight or other attachments they should be added at this stage.
- Ensuring the safety switch is in the off position, the battery should be placed in its compartment and plugged into the system and then the wires should be checked to ensure a secure connection.
- The battery compartment should be checked to make sure the battery is secure and will not move during flight and that the container is in good condition.
- After all checks are made and everyone in the vicinity is made aware, the safety switch can now be flipped to the on position.
- Before flight the control surfaces should be tested quickly with the remote control to ensure functionality as well as spinning the motor on very low power to confirm it is functioning and is turning the correct direction.
- After all these checks have been made the plane should be able to taxi itself to the start using the control surfaces to steer and the motor at low power to move it takeoff position
- Once everyone is a safe distance away from the aircraft, the plane should now be safe to take-off and attempt the mission it is directed for.

7.2   Glide Tests

7.2.1   Controls Results

During the glide testing an important note was that the plane was receiving power to onboard components such as the ESC, receiver and servos even though the controller was not being used. This power was applied just to ensure that the servos would stay in their stationary positions after the plane had been tossed to get the smoothest glide possible. However, during this test, since a major part was catching the plane, the motor was completely disconnected from the circuit for the safety of the team members catching the plane with the tarp. During this test, with the control surfaces remaining stationary at their level position, it was proved that the plane could glide straight without power to the motor. From these tests it gave confidence in the control surface design and shape as it proved when the plane would go to fly, the controls should need minimal trimming to keep the plane flying in a straight direction.

When it came to the wiring and electronics on the aircraft itself, one issue found during these tests was the wire extending from the fuselage to the aileron servo could become loose due to its length. To account for this the wire extenders within the wing were reattached and then taped together securely. Apart from this, the electronics functioned as expected with the remote control easily connecting to the receiver and all servos were functional to the expected degrees of motion. This test solidified the wiring diagram within the plane which can be seen in section 6.1 and would be used in every following test of the aircraft.

7.3 Take-Off & Taxi Tests

Prior to take-off, the aircraft was operated at around half throttle to test its maneuverability on the ground during taxi. Initial testing revealed that the aircraft was able to respond well to the rudder controls as the tail wheel configuration was secured directly into the rudder. However, repeated testing on rough surfaces caused significant damage to the landing gear and tail wheel configuration, given that the landing gear was secured to a small, detachable, wooden part through wood glue and the tail wheel parts were rated for aircraft half the size of the one that was built for this project. To fix this issue, a metal mounting plate for the landing gear was secured to the front end of the fuselage to more evenly distribute the forces the landing gear experiences from landing and from the vibrations associated with taxiing. Heavier duty ail wheel components reinforced with carbon fiber and metal mounting plates replaced the weaker, original tail wheel parts.

With the modifications made to the landing gear and tail wheel configuration, there were no further issues going into the official takeoff test. The aircraft was able to takeoff within 10 [yd] or 30 [ft], which was well within the competition specifications.

7.3.1 Controls Results

These tests are the first tests which were conducted with a fully live electronic system, which included the motor which is a significant change from the earlier glide tests. The remote control was also utilized to control the craft and get into the air as opposed to being thrown in the glide tests. One of the biggest takeaways from this set of testing came from just taxiing before take-off. The pilot, using both the rudder which was attached to the swiveling tail wheel and the ailerons, was able to effectively turn the aircraft on the field and use the remote control to taxi straight ahead for take-off attempts. This taxiing is an important test for the stability of the connections between the servos and the control surfaces as the ground generates a significant vibrational impact on these connections that are made to be mobile. After a few iterations of tightening and eventually using super-glue, the effect of the taxiing was no longer able to impact this connection. Another key result obtained from this test is the ability to steer and taxi the plane straight. With a very powerful motor, the ability to taxi in a straight line is incredibly important to a fast and smooth take-off which our plane is capable of.

Take-off also gave good feedback on how the control surfaces should act and be trimmed for the actual flight. One major observation found from our take-offs was a tendency to twist left along its central axis. This can be explained by the fact our motor is very powerful for the size of this plane and the spinning of the motor at full throttle causes a lot of torque. The short hop off the ground makes it hard to detect exactly the extent of the torque and how much to adjust the control surfaces to compensate for this. However, this is very good to know as when full flight occurs it is already known that the ailerons will need to be trimmed to the right to compensate for the torque of the motor. It was also noted that this torque can be accounted for by the pilot as when the aircraft took off, the pilot was successfully able to correct this instability using the ailerons to cause smooth and straight flight for the few seconds it was in the air. Lastly, the electronics wiring system, as

mentioned previously, remained the same as that in the previous glide tests with the addition of the motor and functioned exactly as expected for both the taxiing and take-off tests.

7.4 Flight Test

Upon assembly and completion of control surface tests, engine throttle was set to maximum, and the aircraft took off within the same distance as the take-off test. Video footage shows that there was slight wobbling around the roll axis of the aircraft during its climb up to altitude, which was due to a slight imbalance in the center of gravity across the width of the aircraft. Regardless, the aircraft climbed to an altitude of 50 ft in 8 s, resulting in a climb rate of roughly 6.25 ft/s. During flight, the aircraft was able to traverse the width of a field in 3.5 s at max speed, which was equivalent to roughly 214 ft. Thus, resulting in an estimated max speed of 61.1 ft/s or roughly 42 mph. The aircraft was able to complete a controlled 180 deg. turn in roughly 7 s. Given the real data and utilizing the prediction calculation process in Predicted Mission Performance it is estimated that the aircraft would have completed Mission 1 in roughly 182 s.

The addition of the 2.124 lbs payload results, similar to the predicted results while using the same calculation process, results in little to no change in the top speed and turn rate Using the same method as what was used for calculating the number of predicted laps, the aircraft would have completed 9 full laps of the course while nearly completing 88% of the tenth lap during the ten minute duration of Mission 2.

7.4.1 Controls Observations

The flight test conducted for this aircraft did not last a very long span of time but did deliver very important information for the controls when analyzed. Getting into the air was smooth, like the tests conducted for taxiing and take-off, which was expected as the controls remained consistent since the end of that leg of testing. The major difference in this test was to continue the acceleration and gain altitude and finally maneuver within in air. The elevator was one of the challenges that was found at this stage, as the 15 percent surface area of the tail did not have as great of an impact on the altitude as it was hoped at the speed it reached. This is important to note as it is an issue that can easily be fixed by just creating a new elevator that expands the total tail area and generates more torque when controlled. However, apart from the elevator, the other control surfaces all served their purposes very well, with the ailerons being utilized to perform smooth turning during the time the plane was in the air. All the electronic circuits also functioned just as anticipated with the first real test of a long-distance remote control to receiver connection with no visible signs of any input delay or lack of connection. The servos also functioned well and turned the control surfaces to their expected degrees of rotation in flight.

8 Conclusion and Future Improvements

8.1 Controls Improvements

For the general electrical components implemented into the aircraft the team would generally recommend the components utilized over the course of this project. Both the ESC and receiver were very reliable through all of the testing throughout the project and would highly recommend using them on future aircraft. The receiver allows for great amounts of control and ease of set-up for the many servos that are involved in an aircraft of this scale. The ESC was proven reliable and the only reason to switch it would be if the battery itself was changed to a significantly different rating. The battery used through this project was also good for this aircraft, it was on the heavier side but should remain functional for future DBF competitions as the competition rules for battery selection generally remain constant.

The servos utilized throughout this project worked well and fit within the form of the aircraft. They also applied all the needed torque to ensure that the control surfaces would have their full degrees of motion in testing. One future improvement that could be suggested is using a smaller servo with similar torque properties to the Hitec servos outlined in this paper. This would allow for an easier and more adjustable fit in tight areas such as the ribs of the wings where the servos utilized currently just fit right below the Monokote layer. Decreasing the size of the servos would also create some small benefits for the total weight and allow for other sections to gain some weight if needed in future planes.

Of the control surfaces on this aircraft, the most effective design were the ailerons and similar designs could be scaled and used in future DBF aircraft. However, for the tail the team would recommend future projects expand the surface area ratio or the elevator from 15 percent to 30 percent of the total tail area. A new elevator was made for this ratio but has yet to be tested and this increase should allow for sufficient attitude control of the aircraft. This adjustment is critical as having more control than necessary will always be beneficial when comparing a plane with a lack of control authority. Other than the elevator, the team would recommend keeping the remaining surfaces semi consistent at 20 percent of the total surface area of their respective planes. The ailerons should also be placed close to the wing tips as they are in the current plane design to maximize the amount of torque obtained by the aileron surface area.

8.2 Aerodynamics Improvements

Overall, the aerodynamics of the aircraft were able to produce ample lift to ensure an excellent takeoff distance and top speed. With more time, the team would investigate improving the aerodynamics of the fuselage as well as conduct further analysis and experimentation with wing configurations and dimensions.

The fuselage is already designed similarly to an airfoil, with a flat bottom and curved top side to introduce a pressure gradient and generating lift throughout the body. However, its rough edges, flat nose, and open top introduce drag, thus reducing top speed and causing instabilities during flight. Smoothing these edges out in the design, as well as introducing a smoother front

nose resemblant of a commercial aircraft, will improve laminar flow over the fuselage and reduce overall drag acting on the plane, thereby improving its performance. Sealing the top end of the aircraft will contribute to this and will add further protection to the electrical components found within the fuselage, as long as an air intake is implemented to allow for cooling of these electrical components during operation.

Greater time would be taken into optimizing wing sizing and configurations to see which combination would optimize flight performance. The span of each side of the wing was set to fit the full length of the packaging as a benchmark, which resulted in a relatively large wing surface area that produced large amounts of lift. However, this large surface area also results in increased amounts of friction/drag across the wings. With more time, an iterative analysis that adjusts the chord length and span of the wings would be conducted to find a dimensioning that strikes a balance between obtaining the necessary amount of lift for the aircraft while minimizing drag to achieve higher top speeds. Ease of manufacturing would be put aside to explore the benefits of different wing configurations and shapes, perhaps maintaining the high wing configuration while implementing a trapezoidal shape to explore its potential for inducing lower levels of drag at higher speeds.

8.3   Propulsion Improvements

As shown in the propulsion tests, the motor is able to output large amounts of thrust. However, the Aerodynamics sub team determined that the thrust output of the motor is not entirely necessary for cruise and only aids in getting up to speed in a short amount of time. It would be worth considering downsizing the motor a bit to reduce the weight of the plane while aiding in minimizing the effects of torque. The KV constant of the Scorpion motor is low in comparison to other motors that can output comparable numbers of thrust without the torque associated with it. A higher KV motor would allow for higher RPM's to be run with a slight decrease in getting up to top speed quicker. This may be worth considering since the torque produced by the motor had to be counteracted by the control surfaces upon flight and can potentially throw off the roll of the plane when paired with the antenna mission, or for just general flight.

The next improvement that would hold merit would be to test the dynamic portion of the thrust stand test via the wind tunnel to properly ascertain the amount of thrust capable at varying wind speeds. These tests would have given insight on how the motor performs at varying windspeeds, even if some of the wind tunnel readings prove to be unreliable. The current dynamic tests are simulated outside but the wind speed and direction itself forms uncertainties in the results, especially given the weather conditions of the local area constantly changing on a day-to-day if not hour-to-hour basis. More analysis could be done in areas like amp draw to verify the results and provide accurate battery drain results over time, but due to time constraints these tests had to be forgone.

8.4   Structural Improvements

Overall, the structures that were designed for this plane were successful. The wings were stiff and strong enough to allow for flight and significant loading during ground test missions. The

fuselage was able to contain and support all the needed components to allow for successful missions. Our selection and use of plywood supplemented with carbon fiber and steel plates allowed for successful missions, but the need for extra steel plates increased the weight of our plane.

Plywood was an adequate material for most purposes needed on the airplane on the fuselage but, was not an ideal material for all cases such as the landing gear plate where the wood could not sustain the force required by landing. Use of a heavy steel plate was needed to reinforce the landing gear plate to allow for operation of the plane. Further use of carbon fiber to make a stronger and lighter fuselage is a direction for future design work to increase the speed of the plane.

Plywood was strong enough for most of the wing structure. The carbon fiber rod performed well in the indented role of providing the wings strength and stiffness. However, 14 spares were evenly spaced along the span of the wing cut from ¼ inch plywood, all these spars were really doing is proving shape to the Monokote. Reduction in the number of spares placed along the span or a change in material to a lighter wood or thinner wood would decrease weight of the wings and would most likely not affect the strength of the wings.

9 Broader Impacts

The project was created around being able to create a flyable aircraft that would be able to successfully carry out missions resemblant of surveillance and electronic warfare. With further development, implementing the suggested improvements and, perhaps, significantly better manufacturing quality and materials, the design can serve both military and domestic purposes.

Given the nature of the competition missions this year, the aircraft's success would indicate that it could perform localized surveillance and jamming missions for military applications. Given its limited battery life, it would be more practical as a deployable, remote-controlled drone by ground forces. It would be able to survey a target area for hostiles and jam electrical signals prior to infiltration, ensuring that troops are better prepared with updated field data, which in turn would increase the likelihood of mission success while minimizing risk.

If produced with cheaper materials, and if manufacturability was made easier and more streamlined, our design can be mass produced to serve domestic needs. There may be no need to carry an antenna for electronic warfare, but its surveillance capabilities can be used for a wide range of business, monitoring, and recreational purposes. With creativity and the proper modifications, the ability for the aircraft to carry a payload or wing attachment while flying at high speed can satisfy the needs of many.

10 References

[1] (AIAA), American Institute of Aeronautics and Astronautics, *2022-23 Design, Build, Fly Rules,* AIAA DBF, 2022.

[2] J. Lynch, V. Joshi, V. Peng and E. Ren, "Creating MATLAB simulations to model aircraft dynamics," Vedang Joshi, 2019.

[3] Central Massachusetts R/C Modelers, *Winter Down-Time Aircraft Checklist CMRCM 2019,* Central Massachusetts R/C Modelers, 2019.

[4] D. P. Raymer, Aircraft Design: A Conceptual Approach, Sixth Edition, Amrican Institute of Aeronautics and Astronautics, 2018.

[5] N. Shoer, T. Bugdin, J. Trainor, M. Shriner, D. Teirlinck, S. Henehan and S. Weaver, "Design of a Fixed Wing Micro Aerial Vehicle," Worcester Polytechnic Institute, 2021.

[6] J. Schutes, A. Rosano, M. Kelly, D. Cashman, N. Tosi, A. Andraka, G. Di Christina, C. Sullivan, C. Pugilese and Z. Demers, "Design of a Micro Aerial Vehicle," Worcester Polytechnic Institute, 2015.

[7] Y. Li, C. Samantha, M. Almeida, M. Dimilia, A. Korza, J. Donahue and T. Hlavenka, "Micro Aircraft Design Dbf," Worcester Polytechnic Institute, 2017.

[8] C. Davenport, J. Jonas, J. Martin, H. Mazur, S. Vinson and B. Wirtz, "Aircraft Design for AIAA Design Build Fly Competition," Worcester Polytechnic Institute, 2022.

[9] J. Anderson, "Fundamentals of Aerodynamics 6th Edition," McGraw-Hill, 2016.

[10] R. V. Cowlagi, "Integrated Notes, AE 3713 Introduction to Aerospace Control Systems, AE 4733 Guidance, Navigation, and Communications, AE 4723 Aircraft Dynamics and Control," Worcester Polytechnic Institute.

[11] K. Gao, "Understanding Motor Turns & Kv Rating," ATees.

[12] J. Lynch, V. Joshi, V. Peng and E. Ren, "Creating MATLAB simulations to model aircraft dynamics," Vedang Joshi, 2019.

Appendix A – Flight Readiness Checklist

Winter Down-Time Aircraft Checklist CMRCM 2019

Pilot/Owner _____

AMA# _____ FAA# _____

Aircraft _____ Complete a sheet for each of your aircraft

The Once Over:

Covering:
- [ ] Holes
- [ ] Wrinkles
- [ ] Cracked / Broken Balsa

Landing Gear:
- [ ] Wheels
- [ ] Wheel Collars
- [ ] Wheel Pants
- [ ] Retracts

Stucture:
- [ ] Tail / Rudder Mounting
- [ ] Wing Solid/Straight
- [ ] Wing Bolts/Mounting
- [ ] Rubberband Posts

The Details:

Hinges:
- [ ] Ailerons
- [ ] Rudder
- [ ] Elevator
- [ ] Flaps

Control Horns:
- [ ] Throttle
- [ ] Ailerons
- [ ] Rudder
- [ ] Elevator
- [ ] Flaps

Servos:
- [ ] Mounting
- [ ] Binding
- [ ] Arm Screw
- [ ] Clear of Obstructions
- [ ] Correct Direction

Motor/Batteries:
- [ ] Firewall Screws
- [ ] Engine Mount Screws
- [ ] ESC Wires and Plugs
- [ ] Battery Wires/Connectors
- [ ] Battery Secure
- [ ] Battery Swelling
- [ ] Prop TIGHT

Engine/Tank:
- [ ] Firewall Screws
- [ ] Engine Mounting Screws
- [ ] Fuel Tank Wrapped in Foam
- [ ] Clunk not Binding
- [ ] Carb/Linkage not Binding
- [ ] Fuel Lines OK
- [ ] Kill Switch
- [ ] Exhaust Secure
- [ ] Glow/Spark Plug OK
- [ ] Prop TIGHT

Receiver:
- [ ] Battery Cycled
- [ ] Foam Wrap/Mounting Secure
- [ ] Switch OK
- [ ] Connectors OK
- [ ] Antenna Secure
- [ ] 2.4 Ghz Antennas at 90 degrees to each other
- [ ] Satellite Module installed per recommendations
- [ ] Stabilization Correct
- [ ] Servo plugs tight

Transmitter:
- [ ] Battery Cycled or New
- [ ] Antenna not Bent/Broken/Cracked
- [ ] 2.4 Ghz Antenna wires OK
- [ ] Engine/Motor Kill
- [ ] Safety Cutoff
- [ ] Programming
  - Correct Aircraft ID's
  - Control Surfaces
  - Trim Check
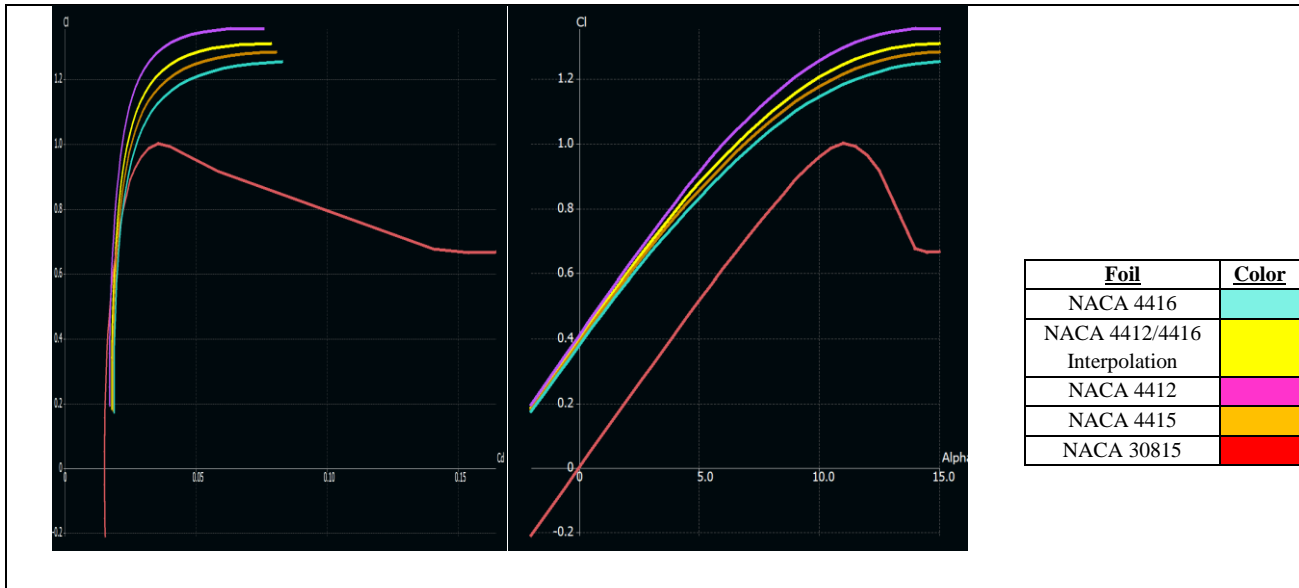 - Mix Functions

Appendix B – Excess Aerodynamic Data

Figure B1: Lift coefficient versus drag coefficient (left) and lift coefficient versus AOA (right) for analyzed airfoils in XFLR5.
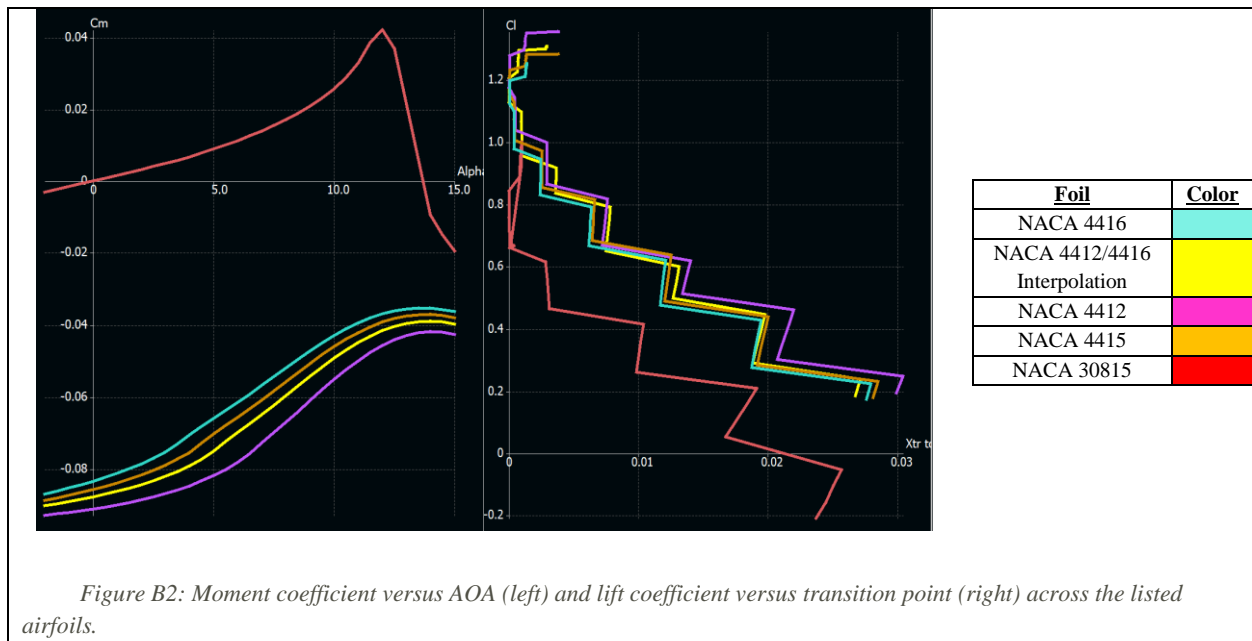
Foil	Color
NACA 4416	
NACA 4412/4416 Interpolation	
NACA 4412	
NACA 4415	
NACA 30815	

Figure B2: Moment coefficient versus AOA (left) and lift coefficient versus transition point (right) across the listed airfoils.
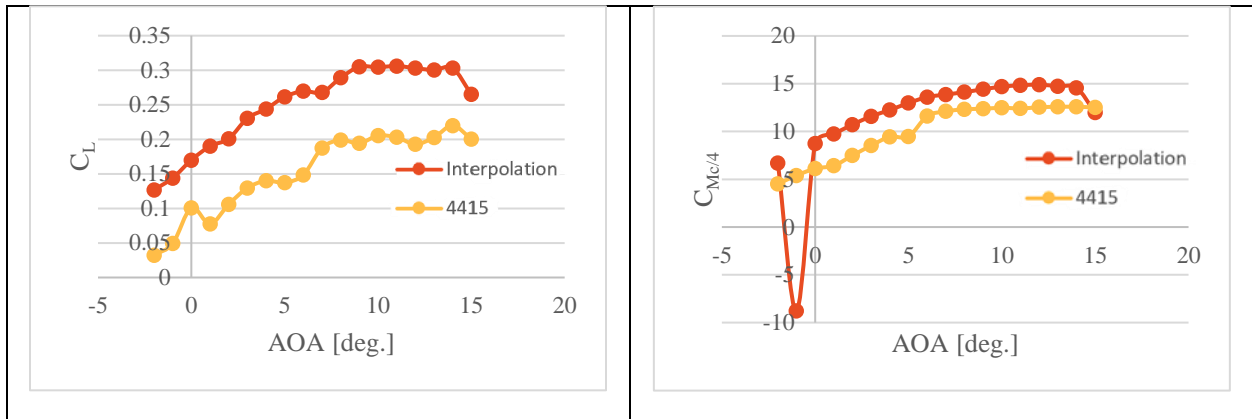
Foil	Color
NACA 4416	
NACA 4412/4416 Interpolation	
NACA 4412	
NACA 4415	
NACA 30815	

Figure B3: Lift coefficient (left) and quarter-chord moment coefficient (right) versus AOA at a wind tunnel testing speed of 60 mph.
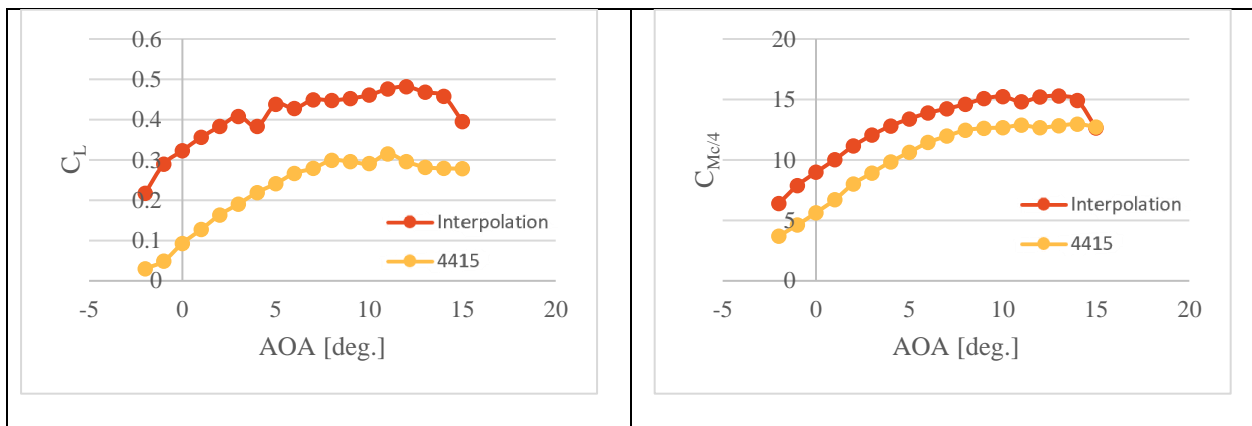
Figure B4: Lift coefficient (left) and quarter-chord moment coefficient (right) versus AOA at a wind tunnel testing speed of 70 mph.
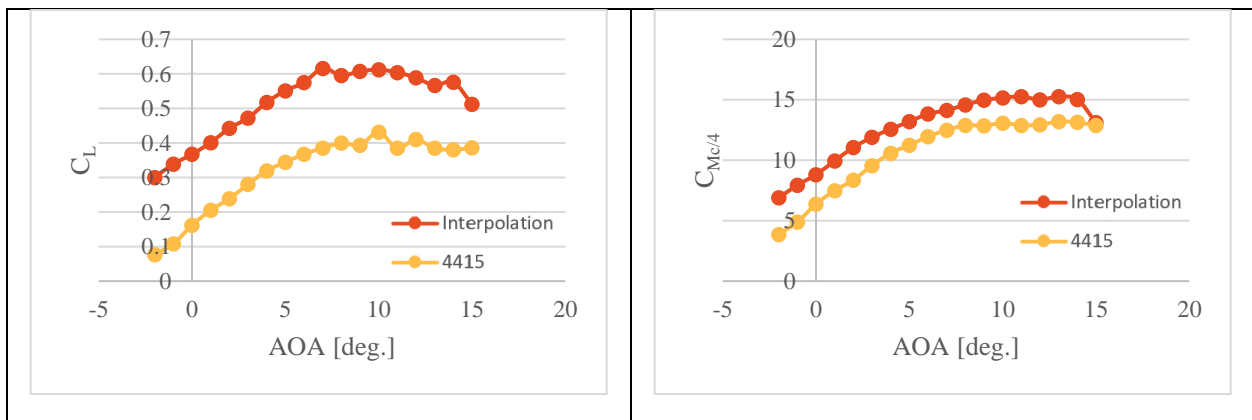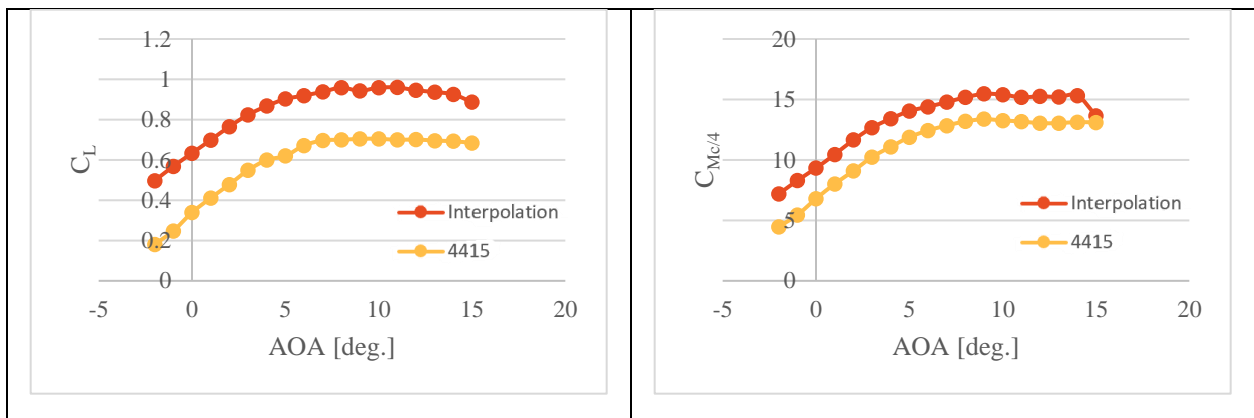

Figure B5: Lift coefficient (left) and quarter-chord moment coefficient (right) versus AOA at a wind tunnel testing speed of 80 mph.
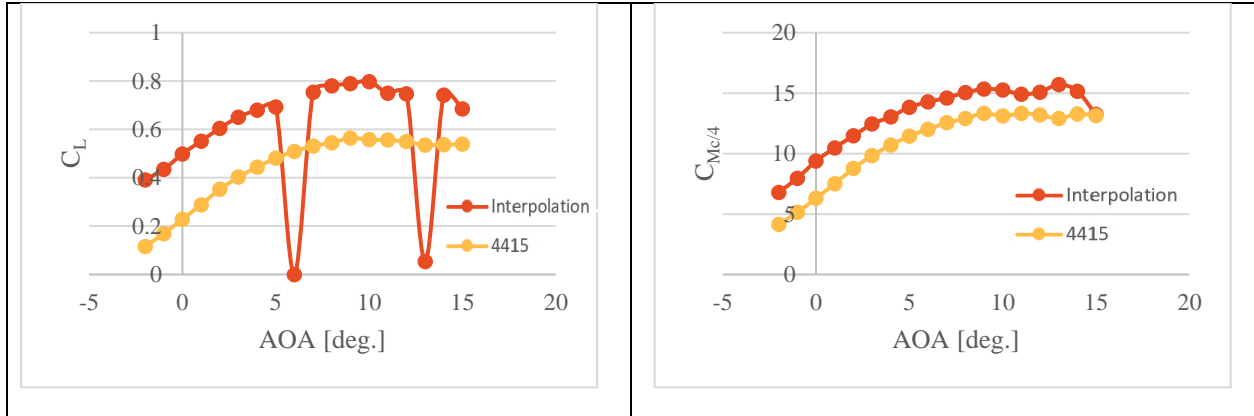
Figure B6: Lift coefficient (left) and quarter-chord moment coefficient (right) versus AOA at a wind tunnel testing speed of 90 mph.
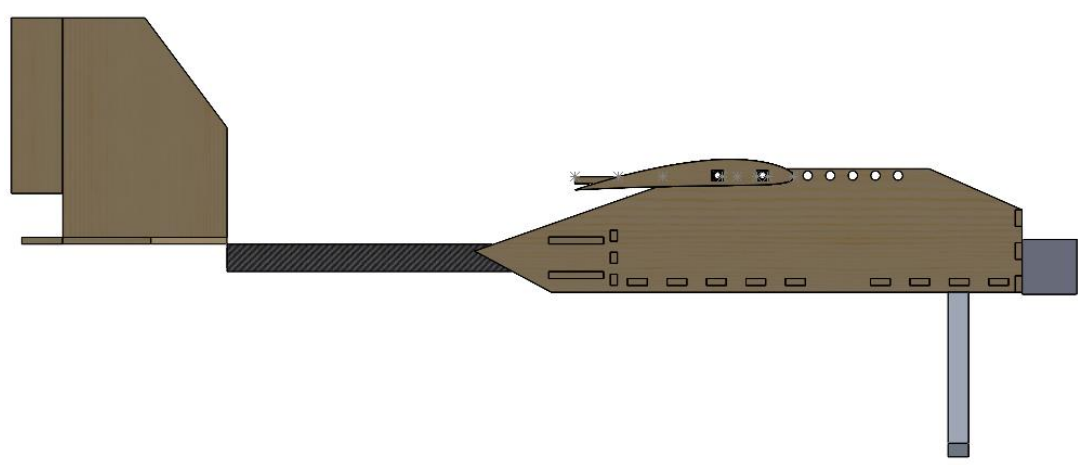

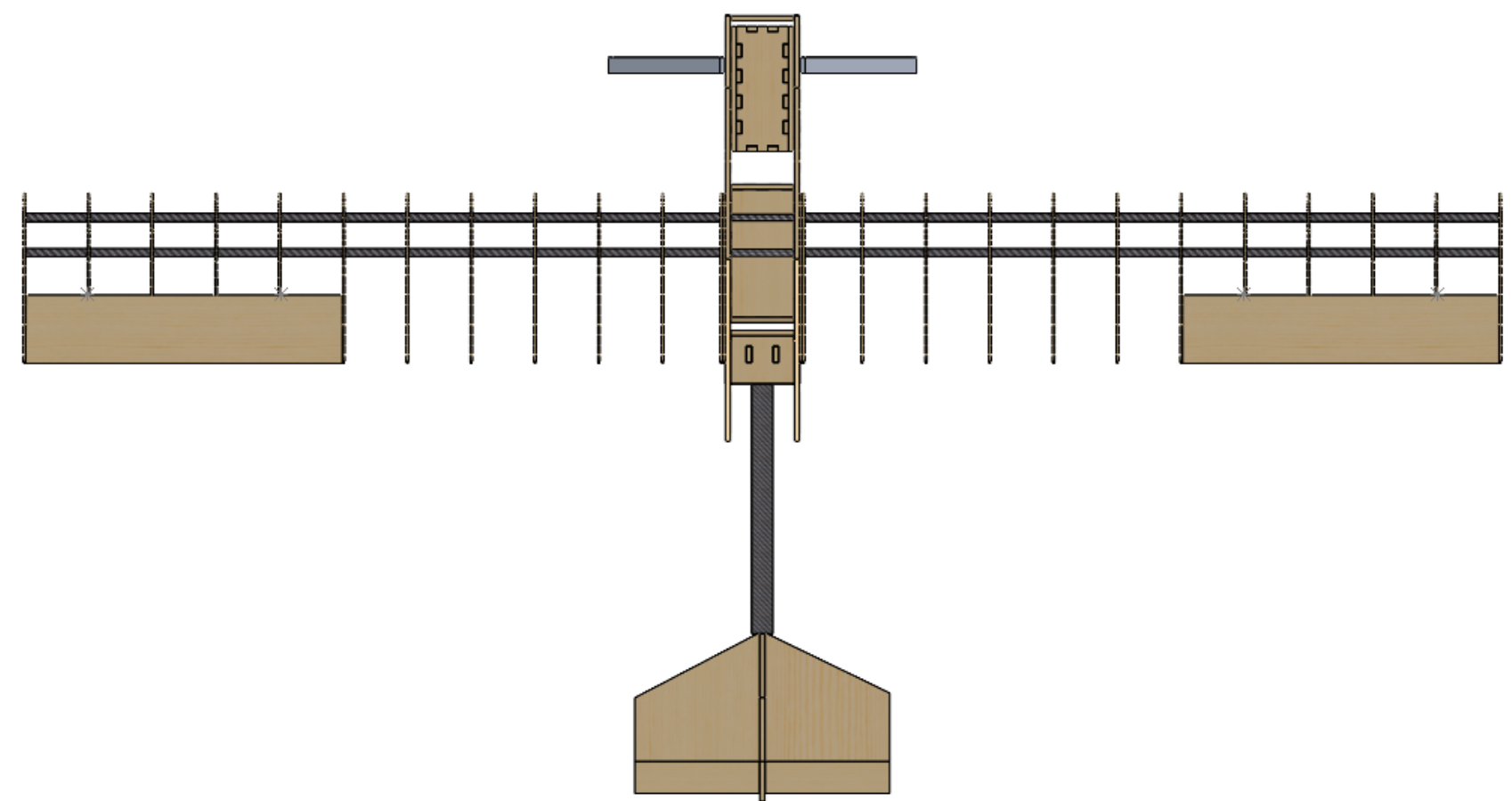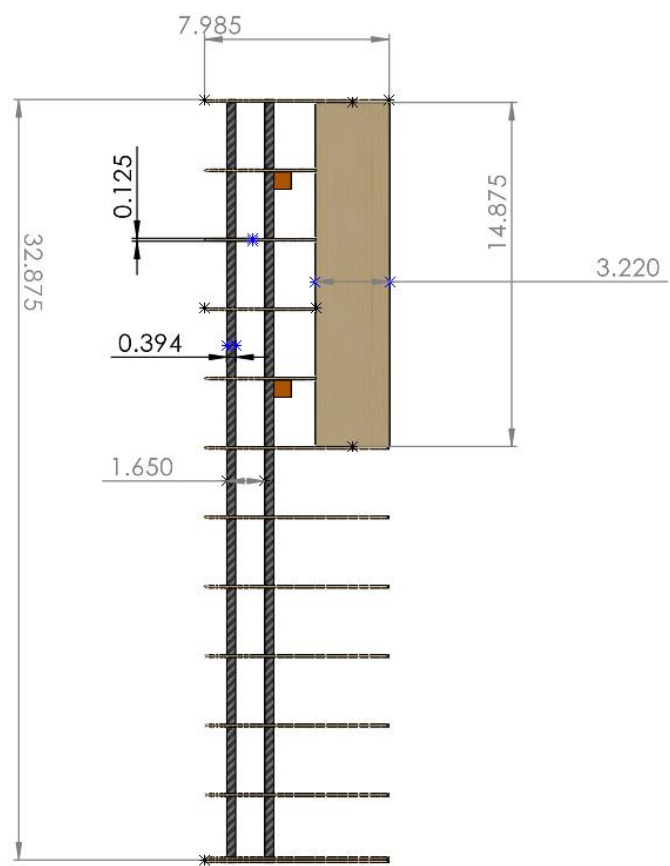*Figure B7: Lift coefficient (left) and quarter-chord moment coefficient (right) versus AOA at a wind tunnel testing speed of 100 mph.*
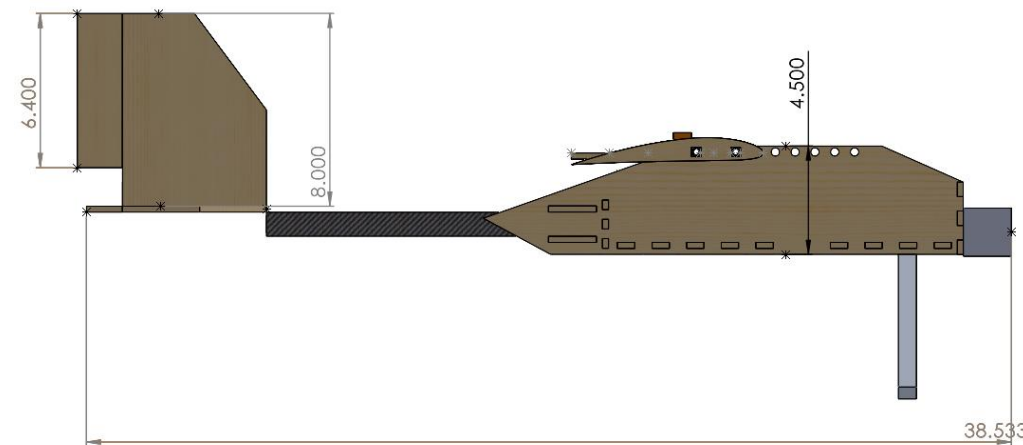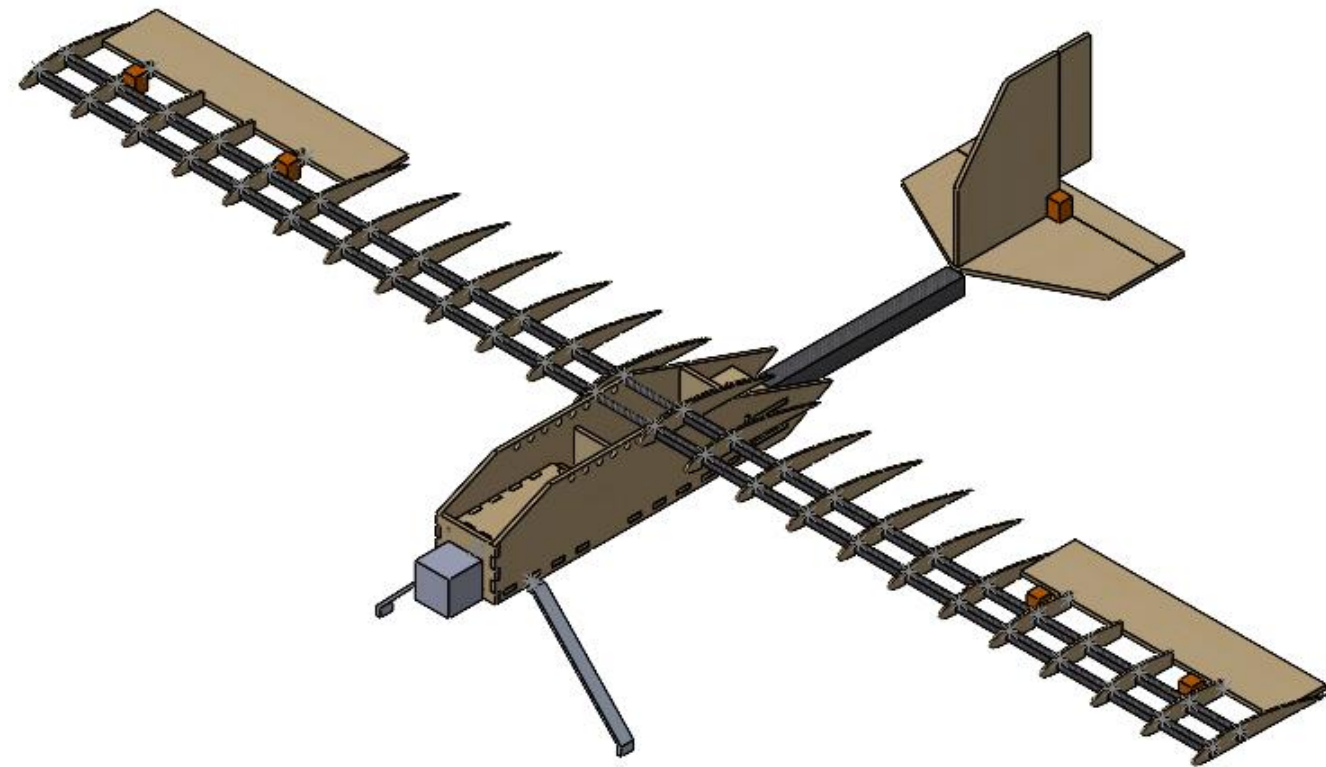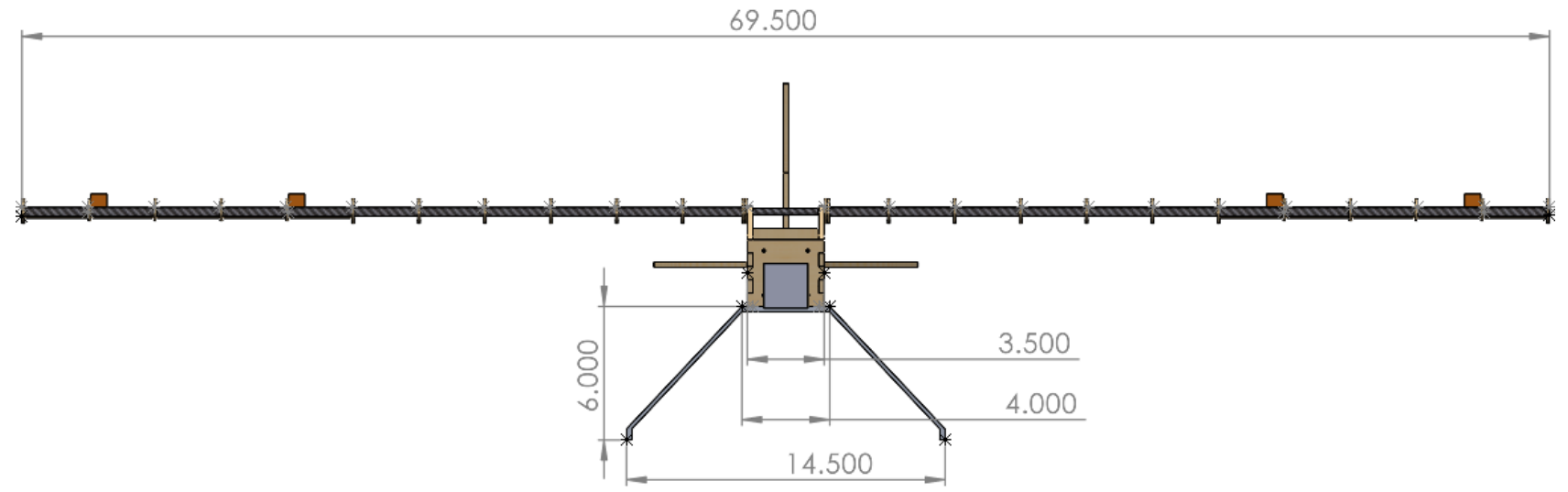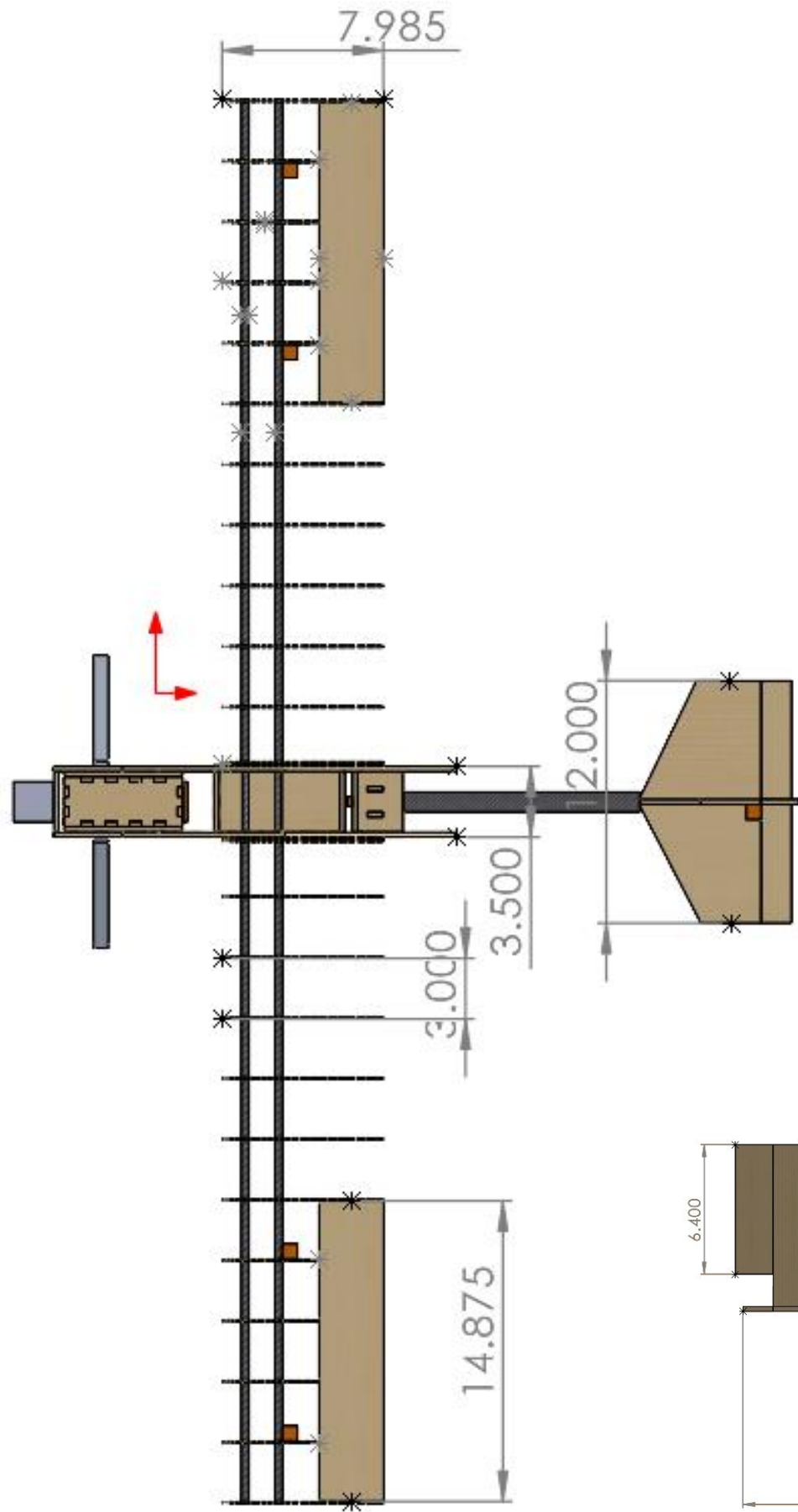
		Name	Date	3 View Drawing	
Drawn		AP	2/13/23		
				Title:	
				Team 1 Plane	
Comments:					
Unit: Inches				Drawing NO. DBF_2023_Team_1_WPI_Drawing 1	REV
Unless otherwise Specified				Scale 1:8	Sheet 1 of 2

	Name	Date		Structural Arrangement	
Drawn	AP	2/13/23			
			Title:		
				Team 1 Plane	
Comments:			Drawing NO.		REV
Unit: Inches			DBF_2023_Team_1_WPI_Drawing 1		
Unless otherwise Specified			Scale 1:8		Sheet 1 of 2